

Probabilistic Methods applied to the Bearing Capacity Problem

Von der Fakultät für Bau- und Umweltingenieurwissenschaften
der Universität Stuttgart
zur Erlangung der Würde eines Doktors der Ingenieurwissenschaften (Dr.-Ing.)
genehmigte Abhandlung,

vorgelegt von
CONSOLATA RUSSELLI
aus Turin (Italien)

Hauptberichter: Prof. Dr.-Ing. P.A. Vermeer

Mitberichter: Prof. Dr.-Ing. A. Bárdossy

Tag der mündlichen Prüfung: 14. Februar 2008

Institut für Geotechnik der Universität Stuttgart

2008

Mitteilung 58
des Instituts für Geotechnik
Universität Stuttgart, Germany, 2008

Editor:

Prof. Dr.-Ing. P. A. Vermeer

© Consolata Russelli
Institut für Geotechnik
Universität Stuttgart
Pfaffenwaldring 35
70569 Stuttgart

All rights reserved. No part of this publication may be reproduced, stored in a retrieval system, or transmitted, in any form or by any means, electronic, mechanical, photocopying, recording, scanning or otherwise, without the permission in writing of the author.

Keywords: probabilistic methods, failure probability, bearing capacity

Printed by e.kurz + co, Stuttgart, Germany, 2008

ISBN 978-3-921837-58-0
(D93-Dissertation, Universität Stuttgart)

Preface

Traditional geotechnical analyses use a single “Factor of Safety”, which implicitly includes all sources of variability and uncertainty inherent in the geotechnical design. In foundation analysis for example, Terzaghi’s bearing capacity equation leads to an estimate of the ultimate soil resistance, which is then divided by a Factor of Safety to give allowable loading levels for design. Meanwhile probabilistic geotechnical analyses have been proposed to include the effects of soil property variability in a more scientific way. For the bearing capacity problem, it implies that the soil properties such as the friction angle and the cohesion are random variables that can be expressed in the form of probability density functions. Meanwhile pioneering experimental studies have been performed providing information on such functions for the random input variables. Now the issue has become one of calculating the probability density function of some outcome, such as the bearing capacity of a foundation. Mrs. Consolata Russelli, focuses exactly on this problem.

On taking the bearing capacity of a footing as a benchmark problem, she considers several stochastic procedures. Besides the well-known Monte-Carlo simulations she uses approximations of first and second order. The main focus of her study is the application of the Point Estimation Method (PEM), as developed by Rosenblueth. She modifies this method by taking sampling points, which suit the characteristics of the problem. On top of that she focuses on the critical part of the curve. This is indeed a promising approach that merits further research. No doubt, this so-called Advanced Point Estimation Method can also be applied to slope stability and other geotechnical problems.

The financial support by the BMBF (Federal Ministry of Education and Research) in the form of an IPSWAT¹ scholarship to Mrs. Russelli is gratefully acknowledged.

Prof. Dr.-Ing. P. A. Vermeer
Stuttgart, March 2008

¹ IPSWAT stands for International Post-graduate Studies in Water Technologies

Acknowledgments

The research presented in this thesis is the result of the work carried out during the years 2003-2007 at the Institute of Geotechnical Engineering (IGS) of Stuttgart University. Behind this work there are important contributions and the significant support of a certain number of persons, whom I would like to thank sincerely.

First of all, I want to thank Prof. Dr.-Ing. Pieter A. Vermeer, Head of the Institute of Geotechnical Engineering at Stuttgart University for providing me with the opportunity to accomplish my doctoral studies under his excellent supervision. No doubt, this doctoral research would not have been possible without his support, patience and constant suggestions.

I would like to thank Prof. Dr. rer. Nat. Dr.-Ing. habil. András Bárdossy, Head of the Department of Hydrology and Geohydrology of the Institute of Hydraulic Engineering at Stuttgart University for his precious advice and constant encouragement. His practical experience and technical knowledge made an invaluable contribution to this thesis.

My sincere gratefulness to Prof. Dr.-Ing. Habil. Hermann Schad, Head of the Geotechnical Department of the Otto-Graf-Institute, at the MPA Stuttgart and to Ao. Univ.-Prof. Dipl.-Ing. Dr. techn. Helmut F. Schweiger, M.Sc., Head of the Computational Geotechnics Group at the Institute for Soil Mechanics and Foundation Engineering at Graz University of Technology for the interesting discussions about important points of this thesis.

I would cordially thank the International Doctoral Program in the field of “Environment Water” (ENWAT) of Stuttgart University and the German Federal Ministry of Education and Research (Bundesministerium für Bildung und Forschung, BMBF) for supporting my doctoral studies scientifically and financially by granting me the IPSWaT (International Postgraduate Studies in Water technology) scholarship for a duration of three years.

I would like to express my gratitude to all my colleagues of the Institute of Geotechnical Engineering at Stuttgart University for their help, both professional and moral, and for the very agreeable and stimulating working atmosphere. I would especially thank my colleagues Dipl.-Ing. A. Möllmann and Dr. Dipl.-Ing. M. Leoni and my friend C. Cimatoribus, Dr. candidate at the

Institute for Sanitary Engineering, Water Quality and Solid Waste Management of Stuttgart University for the time spent with me for several discussions related to my research and for their support in case of difficulties encountered during my work.

Special thanks to Mr. G. Gay for correcting my English.

I also warmly thank my parents and my brother for supporting me throughout my life. Even if hundred kilometers separate us, they have always been present with their affection and love.

Finally I would like to thank Murat for being such a comprehensive and patient husband. I will always remember his encouraging words during the hard times of my doctoral studies.

Consolata Russelli
Stuttgart, April 2008

Contents

1	Introduction	1
1.1	Thesis purpose and motivation	1
1.2	Thesis restrictions	3
1.3	Thesis outline	4
2	Probabilistic concepts for geotechnical engineering	7
2.1	Uncertainty in Geotechnics	7
2.1.1	Sources of uncertainty	8
2.1.2	Types of uncertainty	9
2.2	Random variables	9
2.2.1	Main characteristics of random variables	10
2.2.1.1	The probability distribution and the probability density functions	11
2.2.1.2	The mean value	12
2.2.1.3	The variance and the standard deviation	12
2.2.1.4	The coefficient of variation	13
2.2.1.5	The skewness	14
2.2.1.6	The covariance and the correlation coefficient	16
2.3	Useful continuous probability distributions of random variables	17
2.3.1	The normal and the standard normal distributions	18
2.3.2	The shifted and the standard lognormal distributions	19
2.4	The reliability analysis	21
2.4.1	The factor of safety	21
2.4.2	The safety margin and the failure probability	22
2.4.3	The reliability index	24
3	Probabilistic methods for quantifying uncertainties in Geotechnics	27
3.1	Monte Carlo Simulations (MCS)	27
3.2	The First Order Second Moment method (FOSM)	28

3.2.1 Advantages and limitations of FOSM method	29
3.3 The Second Order Second Moment method (SOSM)	30
3.4 The Hasofer-Lind method (FORM)	31
3.4.1 Advantages and limitations of FORM method	32
3.5 The Two Point Estimate Method (PEM)	33
3.5.1 The procedure for implementing the PEM	34
3.5.2 Advantages and limitations of the PEM	37
4 Probabilistic analysis of the bearing capacity problem	41
4.1 Benchmarks on the bearing capacity of a strip footing	41
4.1.1 Benchmark 1: bearing capacity of a strip footing with effective friction angle as input random variable	41
4.1.2 Benchmark 2: bearing capacity of a strip footing with effective friction angle and cohesion as input random variables	42
4.2 Application of Monte Carlo Simulations	44
4.2.1 Monte Carlo results for benchmark 1	45
4.2.2 Monte Carlo results for benchmark 2 with uncorrelated soil Parameters	47
4.2.3 Monte Carlo results for benchmark 2 with correlated soil parameters	50
4.3 Application of the FOSM method	55
4.3.1 FOSM results for benchmark 1	55
4.3.2 FOSM results for benchmark 2 with uncorrelated soil parameters	58
4.3.3 FOSM results for benchmark 2 with correlated soil parameters	60
4.4 Application of the SOSM method	62
4.4.1 SOSM results for benchmark 1	63
4.4.2 SOSM results for benchmark 2 with uncorrelated soil parameters	64
4.4.3 SOSM results for benchmark 2 with correlated soil parameters	66
4.5 Results comparison and necessity of an alternative method	68
4.5.1 Comparison of MCS, FOSM and SOSM results	68
4.5.2 Necessity of an alternative probabilistic method	72
5 The Two Point Estimate Method applied to the bearing capacity problem	75
5.1 PEM results for benchmark 1	75
5.1.1 Procedure of the PEM	75
5.2 PEM results for benchmark 2 with uncorrelated soil parameters	78
5.2.1 Procedure of the PEM	78

5.3 PEM results for benchmark 2 with correlated soil parameters	81
5.3.1 Procedure of the PEM	82
5.4 Comparison of PEM, MCS, FOSM and SOSM results	88
5.4.1 Comparison of results for benchmark 1	88
5.4.2 Comparison of results for benchmark 2 with uncorrelated soil parameters	91
5.4.3 Comparison of results for benchmark 2 with correlated soil parameters	93
5.5 Discussion of the assumption of the shifted lognormal distribution	94
5.6 Conclusions on the application of the PEM to the bearing capacity problem	102
6 The Advanced Point Estimate Method (APEM) for the reliability analysis	103
6.1 Basic problems concerning the evaluation of failure probabilities	103
6.2 Reliability analysis of the bearing capacity problem	104
6.2.1 Failure probability from Monte Carlo simulations	105
6.2.2 Failure probability from FOSM and SOSM methods	110
6.2.3 Failure probability from FORM	112
6.2.4 Failure probability from PEM	113
6.2.5 Comparison of failure probabilities and necessity of a new approach	115
6.3 Application of the Advanced PEM to the bearing capacity problem	121
6.3.1 Short description of the Advanced PEM methodology	121
6.3.2 The reduced intervals of the input soil parameters	121
6.3.3 Application of the PEM to the reduced intervals of the soil parameters	123
6.3.3.1 Case with $\rho_{c', \tan\phi'} = 0$	123
6.3.3.2 Case with $\rho_{c', \tan\phi'} = -0.6$	126
6.3.4 Shifted lognormal approximation of the bearing capacity results	127
6.3.4.1 Procedure to find the shifted lognormal parameters	128
6.4 Results comparison of MCS, traditional PEM and APEM	130
6.4.1 Case with $\rho_{c', \tan\phi'} = 0$	130
6.4.2 Case with $\rho_{c', \tan\phi'} = -0.6$	133
6.5 Applicability of the estimated failure probability of the bearing capacity	136

7	Conclusions and recommendations for further research	139
7.1	General conclusions	139
7.2	Conclusions with respect to the probabilistic methods applied to the bearing capacity problem	140
7.3	Conclusions with respect to the Two Point Estimate Method	141
7.4	Conclusions with respect to the shifted lognormal distribution	142
7.5	Conclusions with respect to the correlation between the soil parameters c' and $\tan\phi'$	143
7.6	Conclusions with respect to the reliability analysis	144
7.7	Conclusions with respect to the APEM	145
7.8	Recommendations for further research	146
	Appendix	149
A	The Terzaghi's bearing capacity formula	149
B	Derivatives of the bearing capacity for the FOSM and SOSM methods	152
C	Algorithm to evaluate the reduced intervals of the input soil parameters	154
D	Algorithm to evaluate the shifted lognormal parameters and the failure probability of the bearing capacity problem	156
D.1	Main routine for the estimation of the three shifted lognormal parameters	156
D.2	Subroutine for the evaluation of the integrals of the objective function	158
D.3	Subroutines for the definition of the integrals of the objective function	161
D.4	Optimisation results for the bearing capacity problem	162
D.4.1	Case with $\rho_{c'\tan\phi'} = 0$	162
D.4.2	Case with $\rho_{c'\tan\phi'} = -0.6$	163
	Bibliography	165

Abstract

Geotechnical problems are often dominated by uncertainty, such as inherent spatial variability of soil properties or scarcity of representative data. Engineers try to solve these problems using the traditional deterministic approach based on the safety factor, but this cannot explicitly deal with uncertainty, thus affecting the safety of engineering structures. In recent years reliability analyses and probabilistic methods have been applied in order to provide a more rational mathematical framework to incorporate different types of uncertainty into a geotechnical design.

In this thesis probabilistic concepts and methods are described and successively applied to the bearing capacity study of a strip footing. The uncertainties involved in this problem are investigated through a comprehensive literature review.

First of all Monte Carlo simulations are considered. For practical applications this method is too time consuming. Then the approximative First Order Second Moment and Second Order Second Moment methods are applied. Unfortunately these methods do not provide any information about the shape of the probability density function of a performance function, such as the bearing capacity. For this reason another alternative, the Point Estimate Method, is considered. With this approach the skewness coefficient can also be estimated, thus being substantially more accurate than the moments methods, with much less computational effort than the Monte Carlo simulations. Despite the good agreement of the results in terms of mean value and standard deviation, a significant difference is observed between the skewness coefficients provided by the Point Estimate and the Monte Carlo methods.

Another important observation refers to the correlation between the soil parameters cohesion and friction angle. Some authors have based their probabilistic studies considering uncorrelated variables to simplify calculations, thus being more conservative. Other authors found a negative correlation on the basis of experimental data. However in the literature it is hard to find probabilistic studies on the assumption of a negative correlation between soil parameters. In this thesis, the influence of this correlation is accurately investigated. It is found that a negative correlation reduces the variability of the bearing capacity and the uncertainty in the analysis significantly, thus increasing the reliability level.

In addition, the choice of a certain probability density function as approximation of the bearing capacity results is thoroughly discussed. It is found that the shifted lognormal distribution matches all the three moments of the

bearing capacity extremely well, i.e. mean value, standard deviation and skewness, thus being more accurate than other distributions.

The reliability analysis of the bearing capacity problem shows that the results of the Point Estimate method approximated by the shifted lognormal distribution do not match the low failure probabilities evaluated using MCS very well. In order to cope with the shortcoming of the Point Estimate method in assessing small values of the failure probability, a new method is developed, referred to as the advanced Point Estimate method. The proposed method is also applied to the bearing capacity problem and the results are then validated using the Monte Carlo approach.

Zusammenfassung

Geotechnische Probleme, wie zum Beispiel die Tragfähigkeit einer Gründung, unterliegen Unsicherheiten. Gründe dafür sind zum einen geologische Abweichungen und räumliche Veränderlichkeit der Bodeneigenschaften. Zum anderen werden häufig Vereinfachungen und Näherungen bei der Modellierung angenommen. Auch Abweichungen von der Realität, die durch die Modellierung hervorgerufen werden, sind nicht zu vernachlässigen.

Traditionell versuchen Ingenieure, diese Probleme mit Hilfe deterministischer Berechnungen zu lösen. Durch die Anwendung von Sicherheitsbeiwerten und konservativen Annahmen bei der Planung und dem Entwurf kann aber ein technisches System überdimensioniert werden und extrem teuer sein. Außerdem werden sogar erweiterte deterministische Methoden bei sehr hoher Unsicherheit unbrauchbar. Infolgedessen kann das Zuverlässigkeitsniveau einer geotechnischen Struktur nicht quantitativ geschätzt werden.

Die Bewertung von geotechnischen Unsicherheiten ist eine nicht einfache Aufgabe. In der Realität ist eine Unsicherheit aufgrund des Mangels an vollkommenem Wissen oder der unvollständigen Information über vorhandene Daten unvermeidbar. Aus diesem Grund erfordert die Ermittlung der Unsicherheit notwendigerweise die Anwendung der Wahrscheinlichkeitstheorie, welche die Unsicherheit in den Entwurfsprozess durchweg quantitativ bestimmen und eingliedern kann.

Trotz des Nutzens einer Wahrscheinlichkeitsanalyse sind Ingenieure häufig noch skeptisch, wenn sie diese Herangehensweise anwenden, weil sie irrtümlich denken, dass der geforderte Berechnungsaufwand viel größer als für eine deterministische Analyse ist. Dazu können manchmal Schwierigkeiten beim Verständnis und bei der Interpretation der probabilistischen Ergebnisse angetroffen werden. Die Wahrscheinlichkeitsanalyse sollte jedoch nicht als Ersatz für die konventionelle deterministische Berechnung betrachtet werden, da, in der Tat, diese Analyse ein ergänzendes Mittel ist, um mit Unsicherheiten umzugehen.

Ziel und Motivation

Das erste Ziel dieser Arbeit ist, weit verbreitete Wahrscheinlichkeitskonzepte und -methoden zu beschreiben und ihre Anwendung auf geotechnische Probleme mit kleinen Versagenswahrscheinlichkeiten vereinfacht darzustellen. Somit wird ein theoretisch fundiertes Gerüst zur Verfügung gestellt, um relevante Unsicherheiten in der Analyse konsistent einzubeziehen. Unter den

vorhandenen Wahrscheinlichkeitsmethoden werden dann Verfahren für eine weitere Analyse gewählt, die für geotechnische Probleme am besten geeignet sind.

Außerdem wird in vorliegender Arbeit eine neue Wahrscheinlichkeitsmethode entwickelt, welche die Einschränkungen anderer Methoden überwinden kann, besonders für die Auswertung der kleinen Versagenswahrscheinlichkeiten einer geotechnischen Struktur. Um von praktischen Ingenieuren angenommen zu werden, sollte diese neue Methode für Zuverlässigkeit- und Risikoanalysen geotechnischer Probleme leicht anwendbar sein und sowohl Expertenwissen als auch Entscheidungsträger unterstützen.

Zu diesem Zweck wird ein einfaches Beispielproblem betrachtet, die Analyse der Grundbruchtragfähigkeit einer Flachgründung auf einer homogenen Bodenschicht, für die eine analytische Lösung zur Verfügung steht. Aufgrund der natürlichen Streuung der Scherfestigkeitsparameter werden die effektive Bodenkohäsion und der effektive Reibungswinkel als Zufallsvariablen angenommen und durch bekannte Verteilungsfunktionen beschrieben. Andere Bodenparameter, die nicht abhängig von irgendeiner bedeutenden Streuung sind, werden deterministisch behandelt, um die Komplexität des Problems zu verringern.

Zuerst kommen Monte-Carlo Simulationen (MCS) zur Anwendung. Um genaue statistische Werte zu erhalten, werden mindestens zehntausend Realisierungen innerhalb des betrachteten Bereiches der Bodenparameter ausgewertet. Da diese Methode in der Praxis allzu rechenintensiv und zeitaufwändig ist, werden andere Methoden wie die Momentenmethoden FOSM (First Order Second Moment) und SOSM (Second Order Second Moment) angewendet, bei denen um den Mittelwert der Eingangsparameter linearisiert wird. Eine andere Näherungsverfahren ist das Punktab schätzverfahren (PEM) nach ROSENBLUETH (1975, 1981). Bei der PEM wird die Verteilungsfunktion der Scherfestigkeitsparameter diskretisiert, indem man einige Stützpunkte wählt. Danach können der Mittelwert, die Standardabweichung und die Schiefe der Grundbruchtragfähigkeit durch gewichtetes Aufsummieren der diskreten Realisationen (Stützpunkte) ermittelt werden. Die PEM benötigt mehr Berechnungsaufwand als die Methoden FOSM und SOSM. Die Ergebnisse sind jedoch wesentlich genauer, weil diese Annäherung nicht nur Mittelwert und Standardabweichung der Grundbruchtragfähigkeit auswertet, sondern auch deren Schiefekoeffizient.

In dieser Arbeit werden auch die Ergebnisse der Zuverlässigkeitsanalyse des Grundbruchtragfähigkeitsproblems gezeigt, indem die bereits erwähnten Wahrscheinlichkeitsverfahren angewendet werden.

Dabei wird die betroffene Schwierigkeit bei der Auswertung von kleinen Versagenswahrscheinlichkeiten betont. Aus diesem Grund wird eine neue Methode berücksichtigt, die erweiterte PEM oder kurz APEM (Advanced Point Estimation Method), die die Erweiterung der traditionellen PEM darstellt.

Es wird aufgezeigt, dass diese vielversprechende Annäherung ausgezeichnete Einschätzungen der kleinen Versagenswahrscheinlichkeit der Grundbruchtragfähigkeit ergibt, besonders wenn ihre Ergebnisse mit denen des aufwändigen Monte-Carlo Verfahrens verglichen werden.

Einschränkungen

Um die Berechnungen zu vereinfachen, werden die folgenden Annahmen und Einschränkungen in vorliegender Arbeit vorgenommen:

1. In Bodenschichten streuen die Parameter wie die effektive Kohäsion und der Reibungswinkel räumlich in horizontaler und vertikaler Richtung. Die Verteilung dieser Eigenschaften in einer bestimmten Bodenschicht hängt von der zugehörigen Heterogenität, von der geologischen Geschichte der Bodenbildung und von deren fortlaufender natürlicher Veränderung ab. Eine homogene Bodenschicht ist selten. In den meisten Bodenschichten zeigen Eigenschaften eine bedeutende räumliche Streuung. In dieser Studie wird die Bodenschicht als homogen mit einheitlichen aber nicht genau bekannten Bodeneigenschaften behandelt. Der Einfluss der räumlichen Streuung der Bodenparameter, die eine bedeutende Fehlerquelle ist, und deren Korrelationslänge zwischen verteilten Punkten werden ignoriert. Wird die Streuung der Bodeneigenschaften betrachtet, können Unsicherheiten geotechnischer Probleme wesentlich verringert werden. Wegen der extrem hohen Kosten von Baugrunduntersuchungen ist es leider praktisch unmöglich, genügend Daten zu sammeln, um die Streuung einer Bodeneigenschaft genau zu kennen. Folglich ist es notwendig, den Trend der vorhandenen Daten der Bodeneigenschaften innerhalb eines großen Volumens zu interpolieren.

2. Das bedeutende Risiko aufgrund von Messfehlern, der Unsicherheit in der Modellierung und des menschlichen Versagens bei technischen Systemen kann herabgesetzt werden, z.B. indem die Anzahl und die Präzision von Messungen sowie die Genauigkeit des Modells verbessert werden. Wenn diese Fehler in einer Wahrscheinlichkeitsanalyse betrachtet würden, könnte die Unsicherheit eines technischen Entwurfs besser quantitativ bestimmt werden.

3. Trotz der Bemühungen, Unsicherheiten der Bodeneigenschaften in einer Wahrscheinlichkeitsanalyse zu berücksichtigen, besteht immer die Möglichkeit, einige von ihnen zu vernachlässigen. Dieses könnte die Lösung eines bestimmten geotechnischen Problems erheblich beeinflussen. Zusätzlich werden häufig viele Parameter nicht behandelt, um Wahrscheinlichkeitsanalysen zu vereinfachen. Auf diese Weise wird ihr Beitrag nicht betrachtet, wenn man das Zuverlässigkeitsniveau eines technischen Systems auswertet. Deshalb kann die berechnete Versagenswahrscheinlichkeit nur als unterere Grenze zur absoluten Versagenswahrscheinlichkeit angesehen werden. Eine anspruchsvollere Risikoanalyse wäre erforderlich, um das Risiko weiterer nicht berücksichtigter Unsicherheiten miteinzubeziehen.

Überblick

In diesem Zusammenhang werden die folgenden Kapitel berücksichtigt:

Kapitel 2: Dieses Kapitel beginnt mit der Berücksichtigung von wesentlichen Quellen und Arten der Unsicherheit im Bereich der Geotechnik. Die wichtige Rolle der Anwendung von Wahrscheinlichkeitsmethoden als Alternative zur deterministischen Analyse wird betont, um Unsicherheiten quantitativ zu bestimmen. Es folgt nachher eine Beschreibung der wichtigsten Statistik- und Wahrscheinlichkeitskonzepte von Zufallsvariablen, welche für diese Arbeit relevant sind. Eine Definition von Zufallsvariablen wird dann gegeben. Dabei werden ihre Haupteigenschaften und einige nützliche Verteilungsfunktionen beschrieben. Schließlich hebt das Kapitel die Bedeutung des Durchführens einer Zuverlässigkeitsanalyse und des Auswertens der Versagenswahrscheinlichkeit eines technischen Entwurfs hervor. Es wird gezeigt, wie sich der traditionelle Sicherheitsbeiwert zu der Versagenswahrscheinlichkeit, welche ein realistischeres Maß eines Zuverlässigkeitssystems ist, in Beziehung setzt.

Kapitel 3: Ziel dieses Kapitels ist, einige weithin bekannte Wahrscheinlichkeitsmethoden zu erläutern, mit denen vorhandene Unsicherheiten rationaler behandelt und Wahrscheinlichkeitskonzepte in geotechnische Analysen einbezogen werden können. Besondere Aufmerksamkeit wird den Monte-Carlo Simulationen (MCS), dem Punktabwärtungsverfahren (PEM), den Momentenmethoden FORM, FOSM und SOSM gewidmet. Die Vorgehensweise dieser Methoden wird weitgehend veranschaulicht und die entsprechenden Vorteile und Einschränkungen diskutiert.

Kapitel 4: Dieses Kapitel behandelt eine mögliche Anwendung der Methoden MCS, FOSM und SOSM zur Grundbruchtragfähigkeit eines Streifenfundaments auf einer homogenen Bodenschicht. Zwei Fallstudien werden vorgestellt, für welche die effektive Kohäsion und der effektive Reibungswinkel als Zufallsvariablen angenommen werden, da diese die größte Auswirkung auf die Baugrundtragfähigkeit haben. Unterschiedliche Werte des Korrelationskoeffizienten zwischen den Bodenparametern werden betrachtet. Insbesondere wenn die Ergebnisse der oben genannten Methoden verglichen werden, wird aufgezeigt, wie die Korrelation die Wahrscheinlichkeitsanalyse stark beeinflusst, da die Streuung der Grundbruchtragfähigkeit und die Unsicherheit erheblich verringert werden. Schließlich wird der Bedarf einer alternativen Methode angesprochen, welche die Einschränkungen der Methoden MCS, FOSM und SOSM bewältigen kann.

Kapitel 5: In diesem Kapitel wird gezeigt, wie die PEM die Einschränkungen der Methoden MCS, FOSM und SOSM überwinden kann. Daher erweist sich die PEM als eine attraktive und leistungsfähige Alternative zu den anderen Wahrscheinlichkeitsmethoden, da sie weniger Berechnungsaufwand erfordert. Aus diesem Grund wird die PEM auf das Grundbruchtragfähigkeitsproblem angewendet. Ihre Ergebnisse werden dann mit denen der Verfahren MCS, FOSM und SOSM verglichen. Es wird gezeigt, dass die Ergebnisse der PEM genauer als die der Methoden FOSM und SOSM sind; jedoch wird ein bedeutender Unterschied zwischen den Schiefekoeffizienten von PEM und MCS beobachtet. Zusätzlich werden die Bedeutung und der Einfluss der Korrelation zwischen Bodenparametern bei der Anwendung der PEM hervorgehoben.

Kapitel 6: Dieses Kapitel greift die grundlegenden Probleme der Zuverlässigkeitsanalyse auf, die auf der Auswertung einer kleinen Versagenswahrscheinlichkeit fokussiert. Zunächst werden die Ergebnisse der Zuverlässigkeitsanalyse des Grundbruchtragfähigkeitsproblems, welche in Versagenswahrscheinlichkeit und Zuverlässigkeitsindex ausgedrückt werden, dargestellt und verglichen, indem bekannte Wahrscheinlichkeitsmethoden einschließlich MCS und PEM verwendet werden. Um die Einschränkungen der PEM bei der Ermittlung einer kleinen Versagenswahrscheinlichkeit zu überwinden, wird danach eine sogenannte erweiterte PEM (kurz APEM) eingeführt. Diese ist in der Literatur bislang nicht behandelt worden. Die Grundidee dieser Methode ist, Augenmerk auf die verhältnismäßig kleinen Werte der Bodenkohäsion und des Reibungswinkels zu richten, die zum Versagen führen.

Die APEM wird auf verringerte Intervalle der Scherfestigkeitsparameter angewendet, um die Versagenswahrscheinlichkeit der Grundbruchtragfähigkeit genauer abzuschätzen. Dieser Wert wird dann mit der ermittelten Versagenswahrscheinlichkeit der MCS verglichen, um die Genauigkeit der APEM zu bestimmen.

Kapitel 7: Die relevantesten Ergebnisse dieser Arbeit werden im abschließenden Kapitel zusammengefasst. Darüber hinaus werden die wichtigsten Schlussfolgerungen aufgegriffen und Empfehlungen für weiterführende Forschungsprojekte gegeben.

Chapter 1

Introduction

It has long been recognised that uncertainties, such as the inherent spatial variability of soil properties, often dominate many events or problems of interest to geotechnical engineers. Traditionally engineers try to solve these problems by deterministic calculation through the use of safety factors and adopting conservative assumptions in the process of engineering planning and design. In this way an engineering system can be over-designed and extremely expensive. Furthermore, even advanced deterministic methods become useless when the uncertainty is very high. As a result the reliability level of a geotechnical structure cannot be estimated quantitatively.

The assessment of geotechnical uncertainties is not an easy task. As a matter of fact uncertainty is unavoidable, due to the lack of perfect knowledge or to the incomplete information about available data. For this reason the determination of uncertainty necessarily requires the application of probability theory, which quantifies and integrates uncertainty into the design process in a consistent manner.

Despite the benefits gained from a probabilistic analysis, engineers are often still sceptical in adopting this approach, because they think, erroneously, that the calculation effort required is much larger than for a deterministic analysis. In addition, difficulties are sometimes encountered in understanding and interpreting probabilistic results.

Probabilistic analysis should not however be considered as a substitute for the conventional deterministic design, it is in fact a complementary measure to deal with uncertainties.

1.1 Thesis purpose and motivation

The first object of this research is to describe well-known probabilistic concepts and methods and show their application to geotechnical low probability estimation problems in a straightforward way, thus providing a rational framework to incorporate consistently relevant uncertainties in the analysis.

Among the available probabilistic approaches, the ones most suitable for the geotechnical field will be then chosen for a further analysis.

Moreover, in the present thesis a new probabilistic approach will be developed, which should be able to cope with the shortcomings of other methods, especially for the evaluation of low failure probabilities of a geotechnical structure. In order to be accepted by practical engineers, this new method should be easily applicable for reliability and risk analyses of geotechnical problems, supporting both engineering judgement and decision making.

To achieve these aims a simple example problem is analysed: the bearing capacity study of a strip footing on a homogeneous soil layer, for which an analytical solution is available. The soil shear strength parameters, i.e. the effective cohesion and friction angle, are described by specific probabilistic distribution functions. While other soil parameters that are not subject to any significant variation are treated deterministically to reduce the complexity of the problem.

Initially Monte Carlo simulations (MCS) are applied. In order to obtain accurate statistical values at least ten thousand realisations are required within the considered range of soil parameters. Since this method is too complex and time consuming for the practice, other methods are examined, such as the First Order Second Moment (FOSM) and the Second Order Second Moment (SOSM) methods, which produce a linearization around the average values of the input random variables. Another approximation method is the Point Estimate Method (PEM) after ROSENBLUETH (1975, 1981). With the PEM a continuous distribution curve is replaced by particularly specified discrete probabilities and the first three moments of a probability distribution function, i.e. mean value, standard deviation and skewness, can be defined. The determination of these moments is realized through the weighted sum of every discrete realizations, also referred to as sampling points. The PEM requires more computational effort than FOSM and SOSM methods. The results however are substantially more accurate, because this approach evaluates not only mean value and standard deviation of the bearing capacity, but also its skewness coefficient.

In this thesis, the results of the reliability analysis of the bearing capacity problem by applying the already mentioned probabilistic techniques will also be shown, stressing the difficulty encountered in evaluating low failure probabilities. For this reason a new approach is taking into account, the advanced PEM, or shortly APEM, which represents the enhancement of the traditional Point Estimate method.

This promising technique will be shown to give excellent predictions of the failure behaviour of the bearing capacity, especially when its results will be compared with those of Monte Carlo method.

1.2 Thesis restrictions

In order to simplify the calculations, the following assumptions and restrictions are adopted in this research:

1. In soil layers parameters, such as the effective cohesion and the friction angle, vary spatially in both horizontal and vertical directions. The distribution of these properties on a particular soil layer depends on the inherent heterogeneity, the geological history of soil formation and its continuous modification by nature. A homogeneous soil layer is rare. In most soil layers properties show a significant variation over space.

This study is carried out by treating the soil layer as homogeneous with uniform, but not exactly known, soil properties. The influence of the spatial variability of soil parameters, which is a significant source of error, and the correlation length (or scale of fluctuation) between the different points of the random field are ignored. Taking into account the variability in soil properties when predicting geotechnical performance may substantially reduce the uncertainties associated with a design. Unfortunately, because of the extremely high costs of subsurface investigations, it is practically impossible to collect enough data to exactly understand the variation of a soil property. Therefore it is necessary to interpolate the trend of the available data of soil properties within a large volume.

2. The significant risk due to the measurement, model and human errors in engineering systems can be minimized, for example, by improving the quantity and precision of measurements, the accuracy of the model and the quality assurance and control system. When these errors are taken into account in a probabilistic analysis, the uncertainty of an engineering design could be better quantified.

3. Notwithstanding the efforts of including soil properties uncertainties in a probabilistic analysis, there is always the possibility of missing some of them. This could affect the solution of a certain geotechnical problem significantly. Additionally many parameters are not usually taken into account in order to simplify probabilistic analyses. In this way their contribution is not considered

in evaluating the reliability level of an engineering system and the computed failure probability can only be seen as a lower bound to the absolute failure probability. A more sophisticated probabilistic risk analysis would be needed to assess the risk due to all undetected events.

1.3 Thesis outline

In order to achieve the objects of the present research discussed in section 1.1, the following chapters will be considered:

Chapter 2: this chapter starts by considering the primary sources and types of uncertainty in the geotechnical field, underlying the importance of using probabilistic methods as alternative to the deterministic analysis to quantify uncertainties. Hereafter follows a description of the most important statistical and probabilistic concepts of continuous random variables, which are relevant to this research. A definition of random variables is then provided by describing its main characteristics and some useful continuous probability distributions. Finally the chapter will highlight the importance of carrying out a reliability analysis and of evaluating the failure probability of an engineering design. It is shown how the traditional safety factor relates to the probability of failure, the latter representing a more realistic measure of a system reliability.

Chapter 3: the aim of this chapter is to review some well-known probabilistic techniques for dealing with uncertainties and for implementing probabilistic concepts into geotechnical analyses in a more rational way. Particular attention is given to Monte Carlo Simulations (MCS), the Point Estimate method (PEM), the First Order Reliability (FORM) method, the First Order Second Moment (FOSM) and the Second Order Second Moment (SOSM) methods. The methodologies are extensively illustrated and the corresponding advantages and limitations are discussed.

Chapter 4: this chapter presents a possible application of the probabilistic methods MCS, FOSM and SOSM to the bearing capacity study of a strip footing on a homogeneous soil layer characterised by the corresponding effective cohesion and friction angle. Two benchmarks are introduced, for which the effective cohesion and friction angle are considered as random variables, since they have the greatest impact on the soil bearing capacity. Different values of the correlation coefficient between the soil parameters will be taken into account. In particular, when the final results of MCS, FOSM and SOSM

methods are compared, it will be shown how this correlation strongly influences the probabilistic analysis, reducing the variability of the bearing capacity and the uncertainty in the final results significantly. Finally, the necessity of an alternative probabilistic approach, which could cope with the shortcomings of MCS, FOSM and SOSM methods, will be discussed.

Chapter 5: the purpose of this chapter is to show how the PEM can overcome the drawbacks of MCS, FOSM and SOSM methods, thus resulting to be an attractive alternative to the other probabilistic methods in terms of computational effort and mathematical simplicity. For this reason, the PEM is also applied to the bearing capacity benchmarks described in chapter 4 and the results are then compared with those of MCS, FOSM and SOSM methods. It will be shown that the PEM results are more accurate than FOSM and SOSM methods; however a large difference between the skewness coefficients of PEM and MCS will be seen. In addition, it will be stressed that care should be taken in applying the PEM when a correlation between soil parameters is considered.

Chapter 6: this chapter starts with a discussion of the basic problems concerning the reliability analysis of engineering systems, focusing on the evaluation of small values of the failure probability. Next, the results of the reliability analysis of the bearing capacity problem by applying well-known probabilistic approaches, including MCS and PEM, are presented and compared, both in terms of failure probability and reliability index. Afterwards, in order to cope with the shortcomings of the PEM for the assessment of small values of the failure probability, a so called advanced PEM, or shortly APEM, is introduced. This has not been previously mentioned in the literature. The basic idea of this method is to focus on the relatively small values of soil cohesion and friction angle, which would most probably cause bearing capacity failure. The APEM will be applied to the reduced intervals of the soil strength parameters to predict the failure behaviour of the bearing capacity. Finally, the applicability of the estimated failure probabilities of the bearing capacity is discussed using diagrams usually employed in decision-making.

Chapter 7: a summary of the most relevant findings of this research is presented in the final chapter, drawing conclusions and including recommendations for further research.

Chapter 2

Probabilistic concepts for geotechnical engineering

Introduction

The purpose of this chapter is to provide the most important statistical and probabilistic concepts of continuous random variables, which are fundamental for this study, such as the mean value or the standard deviation. For more detailed descriptions about the mathematical background of probability theory the author refers to ANG and TANG (1975).

The chapter begins by considering the primary sources and types of uncertainty in the geotechnical field, underlying the importance of using probabilistic methods as an alternative to the deterministic analysis to quantify uncertainties.

It continues by providing a definition of random variables and by describing their main characteristics and some useful continuous probability distributions.

Finally the chapter will address the reliability analysis, highlighting the importance of evaluating the failure probability of an engineering system.

2.1 Uncertainty in Geotechnics

Many sources of uncertainty exist in the geotechnical field ranging from the variability of soil properties to the sampling and testing technique. Engineers try to cope with these problems using deterministic analyses, which are based on the classical notion of the safety factor.

However practical experience shows that the deterministic approach, relying on conservative designs, which are not always safe against failure, is not suitable for dealing rationally with uncertainty. As a result, the reliability of a system can not be properly assessed. This fact will be better explained in section 2.4.

The authors EINSTEIN and BÄCHER (1982) stated in one of their papers that:

„In thinking about sources of uncertainty in engineering geology, one is left with the fact that uncertainty is inevitable. One attempts to reduce it as much as possible, but it must ultimately be faced. [...]. The question is not whether to deal with uncertainty, but how?“.

In this regard, a rigorous evaluation of the uncertainty involved in geotechnical problems necessarily requires the application of probabilistic theory as a complement to conventional deterministic analyses. In fact probabilistic concepts and methods, associated to the statistical theory, offer a theoretical basis for quantifying uncertainties consistently, rendering them into precise mathematical terms. In this way, a logical framework is provided for reliability and risk analysis.

2.1.1 Sources of uncertainty

Geotechnical variability results from different sources of uncertainties. The three primary sources are inherent variability, measurement error and model uncertainty, as described in Fig. 2.1.

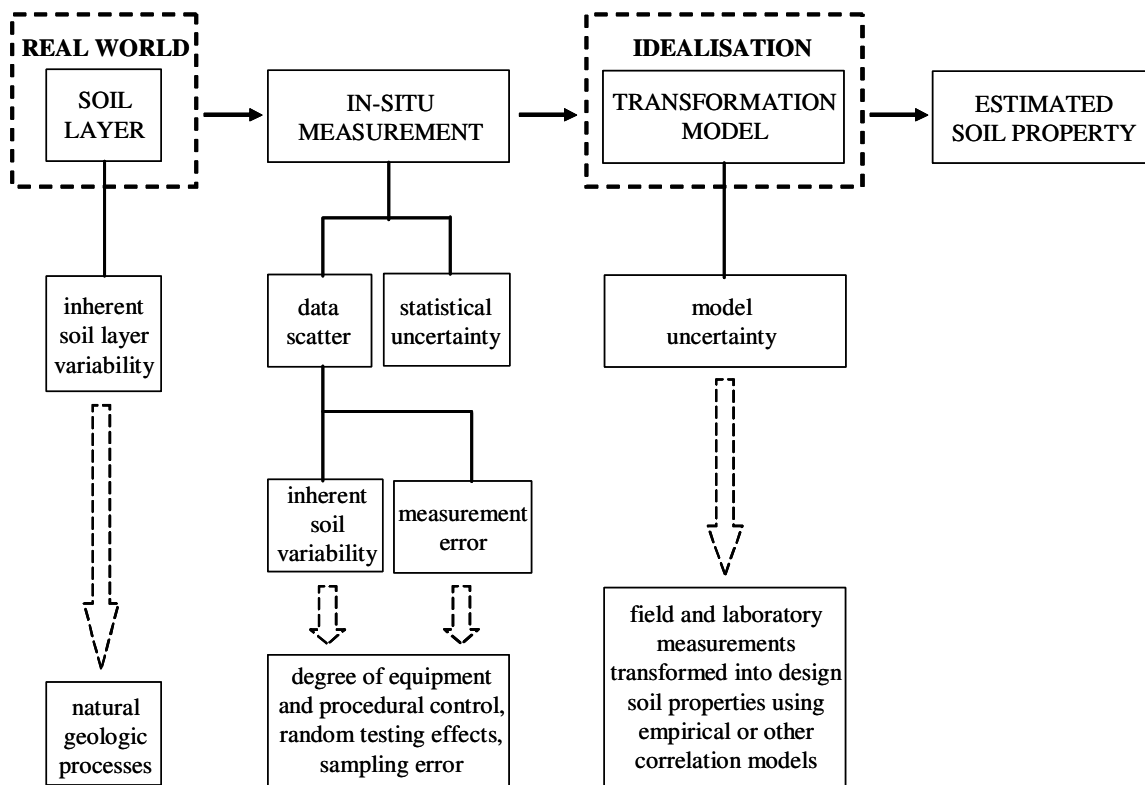


Figure 2.1: Uncertainty in soil property estimates (KULHAWY, 1992)

Inherent variability results primarily from natural geologic processes that created in-situ soil layers. Measurement error is caused by sampling and laboratory testing.

This error is increased by statistical uncertainty that arises from limited amount of information. Finally the model uncertainty is introduced when field or laboratory measurements are transformed into input parameters for design models involving simplifications and idealisations.

2.1.2 Types of uncertainty

Uncertainties associated with geotechnical engineering can be divided into three categories: the inherent or natural uncertainty (aleatory), the uncertainties due to the lack of perfect knowledge (epistemic) and the human error.

The aleatory (from Latin *aleator* meaning “gambler” or *alea* meaning “die”) uncertainty is attributed to the natural variability or randomness of a certain property, such as the spatial variation of the soil layer properties cohesion and friction angle. It could be quantified by measurements and statistical estimations or by expert opinion. This kind of uncertainty is unpredictable and therefore irreducible via collection of more experimental data or use of more refined models. For this type of uncertainty the term probability means the frequency of occurrence of a random event, which is an innate property of nature.

The epistemic (from Greek *επιστημη* meaning “knowledge”) uncertainty arises from the lack of knowledge of a system and it is related to limited or ambiguous data, measurement error, incomplete knowledge, imperfect models and subjective judgement. It can in principle be quantified by experts, but not measured. This kind of uncertainty can be reduced by collecting more experimental data, by improving the measurement and calculation methods and by using more refined models. For this type of uncertainty the term probability means the degree of belief in the occurrence of a random event, which is a subjective interpretation of the individual, e.g. the engineering judgement of an expert.

In Geotechnics aleatory and epistemic uncertainties coexist in most practical applications.

2.2 Random variables

In a probabilistic analysis the geotechnical parameters, which represent the major sources of uncertainties, are treated as random variables.

A random variable is a mathematical function defined on a sample space that assigns a probability to each possible event within the sample space.

In practical terms, it is a variable for which the precise value (or range of values) cannot be predicted with certainty, but only with an associated probability, which describes the possible outcome of a particular experiment in terms of real numbers.

In this study the soil shear strength parameters cohesion and friction angle are considered as random variables for the probabilistic analysis of the bearing capacity problem, as described in chapter 4.

2.2.1 Main characteristics of random variables

The most important statistical parameters related to the soil layer variability are the mean value, the standard deviation, the skewness and the correlation coefficients between the soil properties.

Another important characteristic is the autocorrelation length, or scale of fluctuation, which describes the spatial variability of a soil property in both horizontal and vertical direction. As information on this parameter is rather limited in literature, it is ignored in this study, as is traditionally done. However its consideration may contribute to a reduction in model uncertainty. To define all these parameters we need to collect much experimental data on soil properties using in-situ and laboratory tests.

The variability of these data can then be plotted graphically as histograms, or frequency diagrams, as shown in Fig. 2.2.

Using histograms it is possible to verify the consistency of data of a certain event and to identify trends, biases in measurements, errors in the results and outliers.

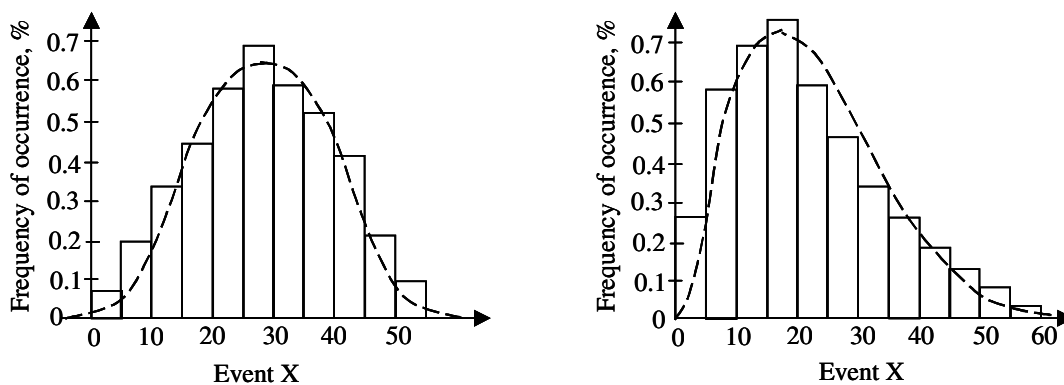


Figure 2.2: Frequency diagram of a certain event and possible probability density functions

2.2.1.1 The probability distribution and the probability density functions

The probability distribution function $F_X(x)$, also called cumulative distribution function or shortly CDF, describes the probability measures that a random variable X takes on a value less than or equal to a number x , for every value x . This function is defined as

$$F_X(x) \equiv P(X \leq x), \quad \text{for } -\infty < x < +\infty \quad (2.1)$$

If the random variable is discrete, the CDF is found by summing up all its probability measures on a given sample space. While, if the random variable is continuous, its probability measures can also be described in terms of a probability density function $f_X(x)$, or shortly PDF. This function can be integrated to obtain the probability that the random variable takes a value in a given interval. Formally, the PDF is the derivative of the CDF, thus the following relationship exists

$$f_X(x) = \frac{dF_X(x)}{dx} \quad (2.2)$$

Considering Eqs. (2.1) and (2.2), the probability of a random variable X being in the interval $[x_1, x_2]$ can be evaluated as follows

$$\int_{x_1}^{x_2} f_X(x) dx = F(x_2) - F(x_1) = P(x_1 < X \leq x_2) \quad (2.3)$$

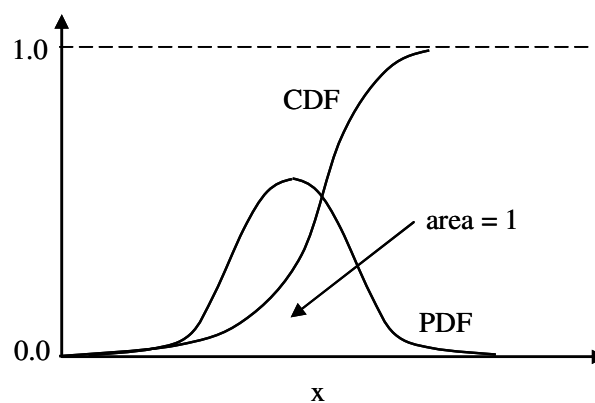


Figure 2.3: CDF and PDF of a continuous random variable

The CDF must be a continuous non-decreasing function with values in the interval [0,1]. As a consequence, the PDF is a non-negative function for all values x and the total area under this function is always unity. Both functions are plotted in Fig. 2.3.

For more detailed descriptions about the probability distribution and the probability density functions the author refers to ANG and TANG (1975).

2.2.1.2 The mean value

The mean value of a random variable, also defined as expected or central value, is the sum of the probability of each possible outcome of an experiment multiplied by its value. Thus it represents the weighted average of all the available experimental data of the variable according to the corresponding frequency of occurrence.

In general, if X is a continuous random variable, such as the effective cohesion of a homogeneous soil, and $f_X(x)$ is its probability density function, then its mean value is given by

$$\mu_x = \int_{-\infty}^{+\infty} x \cdot f_x(x) dx \quad (2.4)$$

The mean value is also referred to as the first central moment, or centre of gravity, of a probability density function, which may be, together with the variance or second central moment, the only practically obtainable information on soil data.

2.2.1.3 The variance and the standard deviation

Besides the mean value, another important characteristic of a random variable is its measure of dispersion or variance, also referred to as the second central moment, or moment of inertia, of the variable. This quantity indicates how widely the values of the variable spread around the mean value. For a continuous random variable X with probability density function $f_X(x)$ and using Eq. (2.4), the variance is given by

$$\text{Var}(X) = \sigma_x^2 = \int_{-\infty}^{+\infty} (x - \mu_x)^2 \cdot f_x(x) \cdot dx \quad (2.5)$$

A more understandable measure of dispersion is the standard deviation σ given by the square root of the variance, that is

$$\sigma_x = \sqrt{\text{Var}(X)} \quad (2.6)$$

As its name indicates, it gives in a standard form an indication of the possible deviations from the mean value. It will be possible to observe in next chapters that the standard deviation is of great importance for the evaluation of the uncertainties of input random variables and their consequences.

2.2.1.4 The coefficient of variation

As it is hard to specify whether the dispersion of a variable is large or small only on the basis of the standard deviation, it is more convenient to use the coefficient of variation, or shortly COV. This non dimensional coefficient describes whether the dispersion relative to the central value of a certain random variable is large or small. It is defined as the ratio of the standard deviation over the mean value of the random variable, i.e.

$$\text{COV}_x = \frac{\sigma_x}{\mu_x} \quad (2.7)$$

Some authors have collected information on the ranges of variation coefficient values for spatial variability of different soil properties, as derived from in-situ soil investigation and for the variability due to measurement errors. A well-known study on the COV values is that of PHOON and KULHAWY (1999), which represents a good indication of the order of magnitude for the COV values of soil variability. In this study PHOON and KULHAWY presented data for a sand and a clay layer and they found COV values between 5-15% for the effective friction angle. This range was also put forward by HARR (1989) and CHERUBINI (1997). Occasionally higher COV values can be found for the friction angle, as in the report of MOORMANN and KATZENBACH (2000), where a value of about 30% is indicated for the Frankfurt clay. But this high COV value of the friction angle is not for a particular site, but for the entire Frankfurt area.

Considering the effective cohesion, HARR suggests in his work a value of about 20%. CHERUBINI presents values between 20-30%, LI and LUMB (1987) report a particular clay layer with a COV of 40% and MOORMANN and KATZENBACH quote 50% for the Frankfurt clay. It can be seen that the available data on the effective cohesion show much more variation than for the effective friction angle.

Considering the effective cohesion, HARR suggests in his work a value of about 20%. CHERUBINI presents values between 20-30%, LI and LUMB (1987) report a particular clay layer with a COV of 40% and MOORMANN and KATZENBACH quote 50% for the Frankfurt clay. It can be seen that the available data on the effective cohesion show much more variation than for the effective friction angle.

Referring to the soil unit weight, CHERUBINI (1998) states that its variability is rather limited (i.e. less than 10%) and for this reason this parameter will be considered as deterministic value in this study.

However, the COV values reported in the literature for the shear strength parameters may be considerably larger than the actual inherent soil variability. FENTON and GRIFFITHS (2004) stated that it is still unknown which value of the coefficient of variation should be used for the characterization of soil parameters. In general representative values of COV are those derived from similar geologic origins and collected over limited spatial extents of the investigation site using good quality of equipment and procedural controls.

For this reason considerable research is needed before defining lower and upper bounds of COV of soil properties for any given situation.

2.2.1.5 The skewness

Another useful descriptor of a random variable is the skewness or third central moment. It is a measure of the degree of asymmetry of the probability density function $f_X(x)$ of a random variable X . It is defined as

$$\text{skew}(X) = \int_{-\infty}^{+\infty} (x - \mu_X)^3 \cdot f_X(x) \cdot dx \quad (2.8)$$

For well-known continuous probability density functions, such as the Gaussian distribution, formulas are available in the literature to evaluate directly the skewness, without solving the integral (2.8).

A more convenient non-dimensional measure of asymmetry of a random variable is the skewness coefficient given by

$$v_X = \int_{-\infty}^{+\infty} \frac{(x - \mu_X)^3}{\sigma_X^3} \cdot f_X(x) \cdot dx \quad (2.9)$$

When the skewness coefficient is nil then a function is symmetric, as in the case of a Gaussian normal distribution. Otherwise it may be positive or negative.

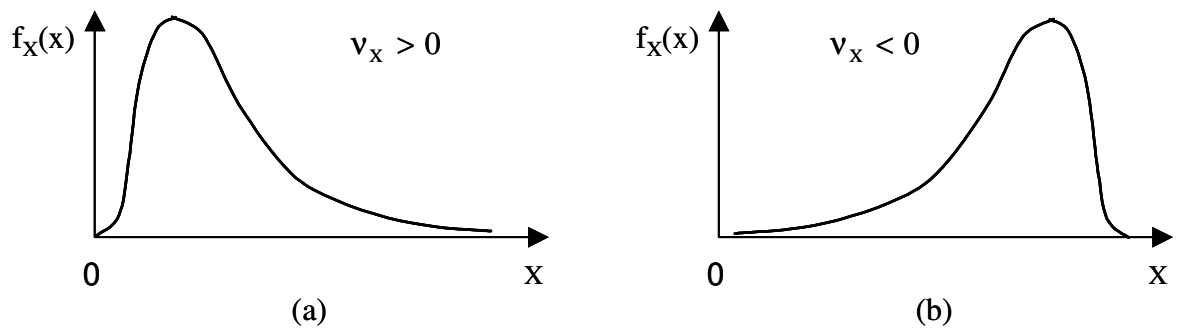


Figure 2.4: Example of positively (a) and negatively (b) skewed distributions

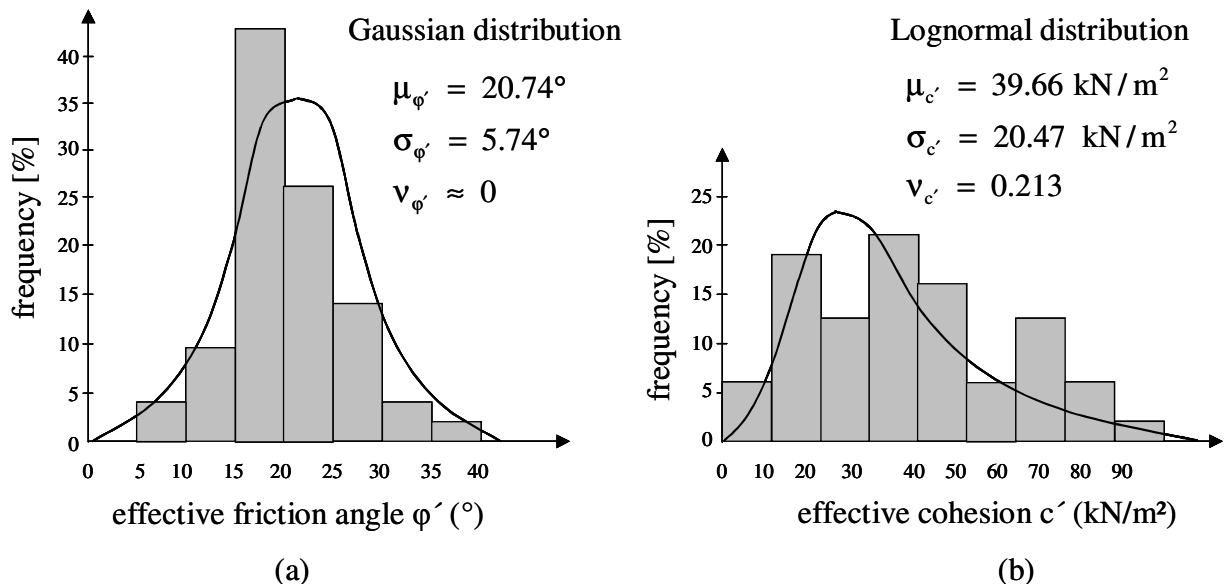


Figure 2.5: Probability density functions of soil strength parameters for the Frankfurt clay (MOORMANN and KATZENBACH, 2000)

Fig. 2.4(a) shows the case of a positively skewed distribution, which is steep for low values of the random variable and flat for large values. A negatively skewed distribution as in Fig. 2.4(b) is flat for low values of the random variable and steep for large values. However negative skewness coefficients would seem to be unrealistic for the distribution of soil parameters.

Considering data as reported by MOORMANN and KATZENBACH and EL RAMLY et al. (2005), it would seem that the skewness coefficient of the effective friction angle could be disregarded and the choice of a Gaussian

distribution would seem suitable, as Fig. 2.5(a) shows. On the other hand, the above authors find skewness of $v_c \approx 1.7$ (MOORMANN and KATZENB) and 4 (EL RAMLY et al.) for the effective cohesion, thus a lognormal distribution would seem to be more appropriate, as plotted in Fig. 2.5(b). In any case, very few data about the skewness coefficient is available in the literature and skewness values need further testing.

2.2.1.6 The covariance and the correlation coefficient

The covariance, also referred to as the joint second moment, is a measure of the degree of linear dependence between two or more random variables. Considering the continuous random variables X and Y, the covariance is defined as

$$\text{Cov}(X, Y) = \int_{-\infty}^{+\infty} \int_{-\infty}^{+\infty} (x - \mu_x)(y - \mu_y) f_{XY}(x, y) dx dy \quad (2.10)$$

When the variables X and Y are statistically independent then the covariance will be equal to zero. Instead of the covariance, the use of the normalized covariance or coefficient of correlation is preferred, which is given by

$$\rho_{XY} = \frac{\text{Cov}(X, Y)}{\sigma_x \cdot \sigma_y}, \quad -1 \leq \rho_{XY} \leq 1 \quad (2.11)$$

When the correlation coefficient is equal to ± 1 there is a perfectly positive, respectively negative, linear relationship between the variables X and Y, as shown in Fig. 2.6(a) and 2.6(b) for the effective cohesion and friction angle. However when it is nil then X and Y are uncorrelated, as in Fig. 2.6(c).

Some authors have based their probabilistic studies on the assumption that soil cohesion and friction angle are uncorrelated. This is often done to simplify calculations. LUMB (1969) was probably the first to study the correlation between soil cohesion and friction angle on the basis of experimental data.

He found a negative correlation between the shear strength parameters in the range $-0.3 < \rho_{c\phi} < -0.7$ for a silty sand, a clayey silty sand and a clayey silt in Hong Kong, implying that low values of the cohesion are associated with high values of the friction angle, and vice versa.

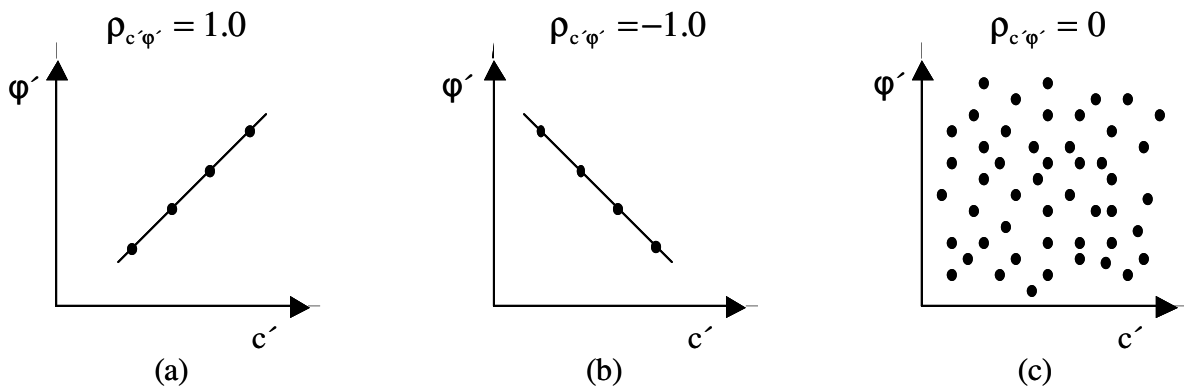


Figure 2.6: Example of perfectly positive correlated (a), perfectly negative correlated (b) and uncorrelated (c) soil properties

However in some cases the correlation was found to be insignificant. LUMB concluded that the assumption of independence of the strength parameters simplifies strength interpretation considerably, and also leads to conservative results if the correlation is in fact negative. Instead the results of CHERUBINI (1998) indicate a significant negative correlation of $\rho_{c'\phi'} = -0.6$ between effective cohesion and friction angle for drained triaxial tests on Blue Matera clays. The same strong value of the correlation coefficient was reported by SCHAD (1985) for a marl in Urbach and confirmed by SPEEDIE (1956). Hence it would seem that a value of about -0.6 is realistic for the soil parameters.

For this reason in this study the effective cohesion and friction angle are assumed to be negatively correlated. It will be shown that negative correlation coefficient decreases the standard deviation of computational results, thus increasing the reliability of the problem considered, or, inversely, decreasing the failure probability.

2.3 Useful continuous probability distributions of random variables

The main characteristics of a random variable can be completely described if the probability density function and its associated parameters are known. In many cases, unfortunately, the form of the distribution function is unknown and often an approximated description is necessary. Several continuous distributions, which play an important role in civil engineering as well as in numerous other engineering fields, can be used as a good approximation for a random variable.

These continuous distributions are applied when the random variables can take any value within some range, such as the normal and the shifted lognormal distributions.

2.3.1 The normal and the standard normal distributions

The normal Gaussian distribution is the probability distribution most frequently used because of its symmetry and mathematical simplicity. It is commonly assumed to characterize many random variables where the coefficient of variation is less than about 30%, as seen in Fig. 2.5(a) for the effective friction angle of the Frankfurt clay.

A random variable X is said to be Gaussian normally distributed with mean μ_x and standard deviation σ_x if its probability density function $f_x(x)$ is given by

$$f_x(x) = N(\mu_x, \sigma_x^2) = \frac{1}{\sqrt{2\pi} \cdot \sigma_x} \cdot \exp\left[-\frac{1}{2} \cdot \left(\frac{x - \mu_x}{\sigma_x}\right)^2\right], \quad -\infty < x < \infty \quad (2.12)$$

In Fig. 2.7(a) the density function of the normal distribution is given for two sets of parameters values. It can be seen that, maintaining the mean value μ_x constant, the standard deviation σ_x governs the spread of the curves.

To simplify calculations using Eq. (2.12), an arbitrary normal distribution can be converted to a standard normal distribution, plotted in Fig. 2.7(b), by transforming the normal variable X into the standard normal variable Z , as below described

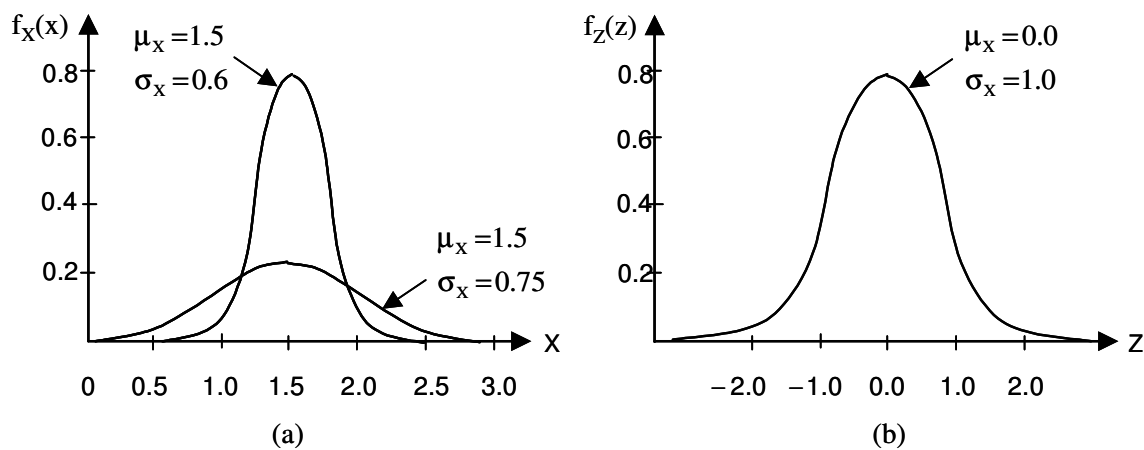


Figure 2.7: Normal (a) and standard normal (b) probability density functions

$$Z = \frac{X - \mu_x}{\sigma_x} \quad (2.13)$$

where Z has mean 0 and standard deviation 1, i.e. $N(0,1)$. Its corresponding probability density function is given by

$$\Phi_Z(z) = \frac{1}{\sqrt{2\pi}} \cdot \exp\left(-\frac{z^2}{2}\right), \quad -\infty < x < \infty \quad (2.14)$$

Probabilities associated with the distribution $\Phi_Z(z)$ are widely tabulated in the literature and are readily available in the software libraries of most computer systems.

From the geotechnical point of view, the Gaussian distribution allows negative soil properties values, which are physically unrealistic. For this reason this distribution could never be more than a rough approximation at best.

2.3.2 The shifted and the standard lognormal distributions

A random variable X has a lognormal distribution if its natural logarithm $Y = \ln(X)$ has a normal distribution. The lognormal distribution for the random variable X may be specified by its mean μ_x , standard deviation σ_x and skewness coefficient v_x . Alternatively, it may be specified by the mean value $\mu_{\ln(X)}$ and standard deviation $\sigma_{\ln(X)}$ of the normal variable $\ln(X)$.

The general formula for the probability density function of the shifted lognormal distribution, also defined as the three parameter lognormal distribution, is given by

$$f_x(x) = \frac{1}{\sqrt{2\pi} \cdot (x - x_0) \cdot \sigma_{\ln(X)}} \cdot \exp\left\{-\frac{1}{2} \left[\frac{\ln(x - x_0) - \mu_{\ln(X)}}{\sigma_{\ln(X)}} \right]^2\right\}, \quad x_0 < x < +\infty \quad (2.15)$$

where x_0 is the location or shifting parameter of the random variable X .

When this parameter is zero then one returns to the standard lognormal distribution, which is then called two parameters lognormal distribution.

Using the shifted lognormal distribution it is possible to match not only the mean value and standard deviation of a certain data population, as the standard lognormal function does, but also the skewness coefficient. This allows a more

realistic data fitting. This is possible using the following closed form equations, which allow the transformation of the lognormal random variable X into the standard normal variable $Y=\ln(X)$:

$$\mu_{\ln(X)} = \ln(\mu_x - x_0) - \frac{1}{2} \cdot \ln \left[1 + \left(\frac{\sigma_x}{\mu_x - x_0} \right)^2 \right] \quad (2.16)$$

$$\sigma_{\ln(X)} = \sqrt{\ln \left[1 + \left(\frac{\sigma_x}{\mu_x - x_0} \right)^2 \right]} \quad (2.17)$$

$$v_x = 3 \cdot \frac{\sigma_x}{\mu_x - x_0} + \left(\frac{\sigma_x}{\mu_x - x_0} \right)^3 \quad (2.18)$$

First of all the Eq. (2.18), which is a third degree polynomial, should be solved numerically to get the required estimate of the location parameter x_0 . When the skewness coefficient v_x is nil, then Eq. (2.18) does not converge to a solution. Once x_0 is known, then the two parameters $\mu_{\ln(X)}$ and $\sigma_{\ln(X)}$ are easily found using Eqs. (2.16) and (2.17). For more detail about the numerical solution of equations (2.16), (2.17) and (2.18) the reader is referred to KOTTEGODA and ROSSO (1997).

Fig. 2.8 shows an example of the shifted lognormal function and its transformation in the standard normal distribution. Practical examples of how matching stochastic values of a certain population using the shifted lognormal distribution will be shown in next chapters.

The lognormal distribution is generally accepted to reasonably model many soil properties, because it is strictly non-negative. It often provides a reasonable shape in cases where the coefficient of variation is larger than 30%, as for the effective cohesion of the Frankfurt clay in Fig. 2.5(b).

Moreover soil properties such as cohesion are often measured as a geometric mean over a certain volume, whose distribution tends to the lognormal distribution by the central limit theorem.

It can be concluded that the lognormal distribution may well represent the natural distribution for many spatially varying soil properties.

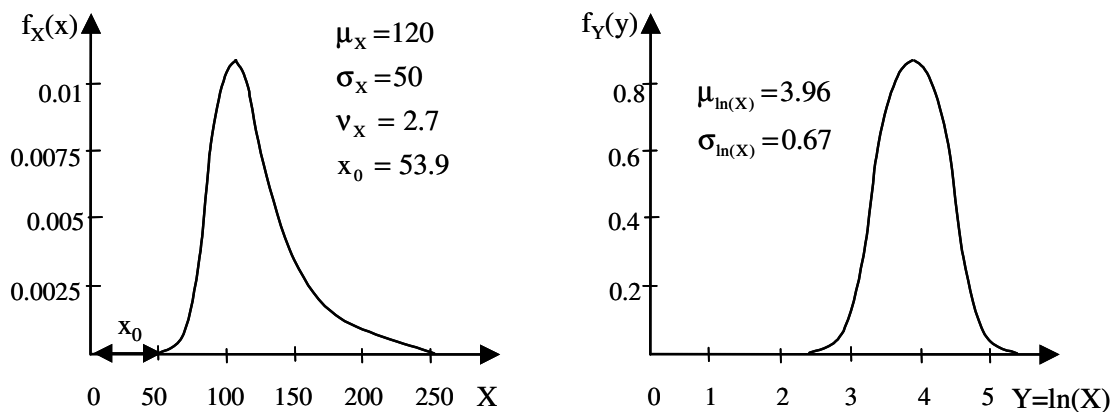


Figure 2.8: Shifted lognormal density function and its transformation in the standard normal distribution

2.4 The reliability analysis

One important challenge for an engineer is the definition of the safety of an engineering project by including the uncertainty components and doing a reliability analysis on which he can base his decisions. In order to achieve consistent levels of reliability, which are subject to important economic and social constraints, proper methods are required.

The object of this section is to show how the traditional safety factor relates to the probability of failure, the latter representing a more realistic measure of a system reliability.

2.4.1 The factor of safety

The traditional deterministic approach is based on the concept of the safety factor FS, which is defined as the ratio between values of available strength or, more generally, the resistance R to failure and the load L soliciting the failure of an engineering system, i.e. $FS = R/L$. Typical values of the safety factor commonly adopted in the geotechnical field are, for example, $FS=2$ for the bearing capacity problem or $FS=1.5$ for the slope stability design of new earth dams.

Unfortunately this conventional analysis leads to conservative designs because uncertainties in analysis parameters are not taken into account during the calculation of the safety factor. In this sense the factor of safety is not a sufficient indicator of safety because the uncertainties in material and load properties can significantly influence the probability of failure.

2.4.2 The safety margin and the failure probability

The traditional safety factor can be replaced by the definition of the safety margin Z , also defined as performance function. This function could indicate the collapse of a structure or, in a very general way, its loss of serviceability.

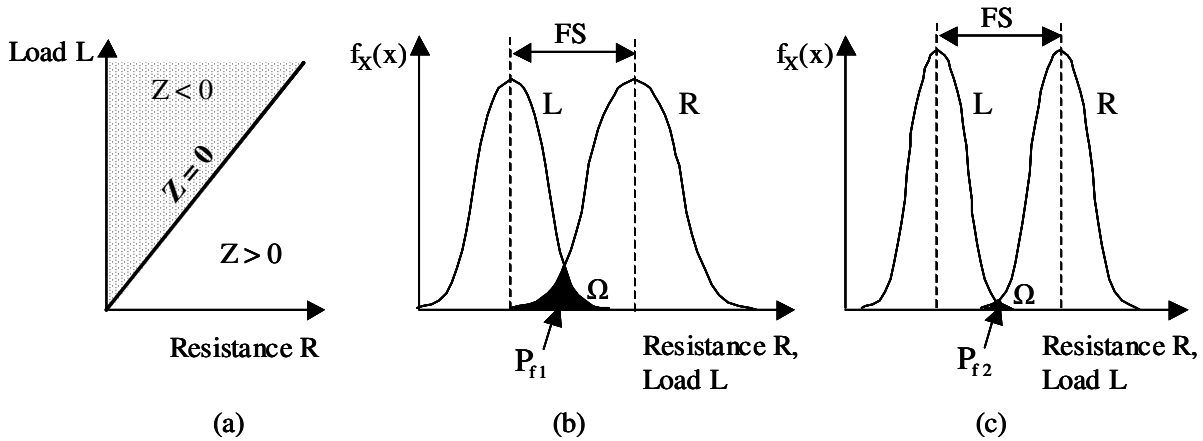


Figure 2.9: (a) Safety margin. (b) and (c) Safety factor versus failure probability

It is defined as the difference between the resistance R and the load L of an engineering system. If X_i represents a collection of input random variables, then the safety margin is given by

$$Z(X_i) = R(X_i) - L(X_i) \tag{2.19}$$

In Fig. 2.9(a) the safety margin is plotted and the failure space is indicated in the Resistance-Load-plane. When $Z < 0$ then failure occurs, while when $Z > 0$ then the system is safe. The boundary defined by $Z=0$ separating the safe and unsafe state is called the limit state function.

The goal of the reliability analysis is the assurance of safety and this is possible only in terms of probability, i.e.

$$P_s = P(Z(X_i) > 0) = P(R(X_i) > L(X_i)) \tag{2.20}$$

where $P(R(X_i) > L(X_i))$ is the probability that the resistance is greater than the load. On the other hand the probability of unsafe conditions or failure probability is given by

$$P_f = 1 - P_s = P(Z(X_i) < 0) = P(R(X_i) < L(X_i)) \quad (2.21)$$

Considering the resistance and the load as random variables with their corresponding probability density function, then the probability of failure P_f is given roughly by the size of the intersecting area Ω , or failure region, for which the load L is greater than the resistance R , i.e. $L > R$, as shown in Fig. 2.9(b) and 2.9(c). More precisely the failure probability is calculated from the convolution integral of the joint probability density function of resistance and load $f_{R,L}(r,l)$ over the failure region Ω , as follows

$$P_f = \iint_{\Omega} f_{R,L}(r,l) \cdot dr \cdot dl \quad (2.22)$$

Figs. 2.9(b) and 2.9(c) are also useful to show how the probability of failure represents a more rational indicator of unsafe conditions than the safety factor. In fact for the two cases of load and resistance in this figure, the safety factor FS is the same, but the probability of failure is very different. Then the same conventional safety factor FS can be associated with a large range of reliability levels, thus showing to be an inconsistent measure of safety.

To help engineers to appreciate the benefits of considering failure probability for reliability analysis, another example is shown in Fig. 2.10(a). Two cases are presented: the first case has a safety factor of 1.4 and lower uncertainty due to the lower standard deviation; the second case has a safety factor of 1.8 but higher uncertainty.

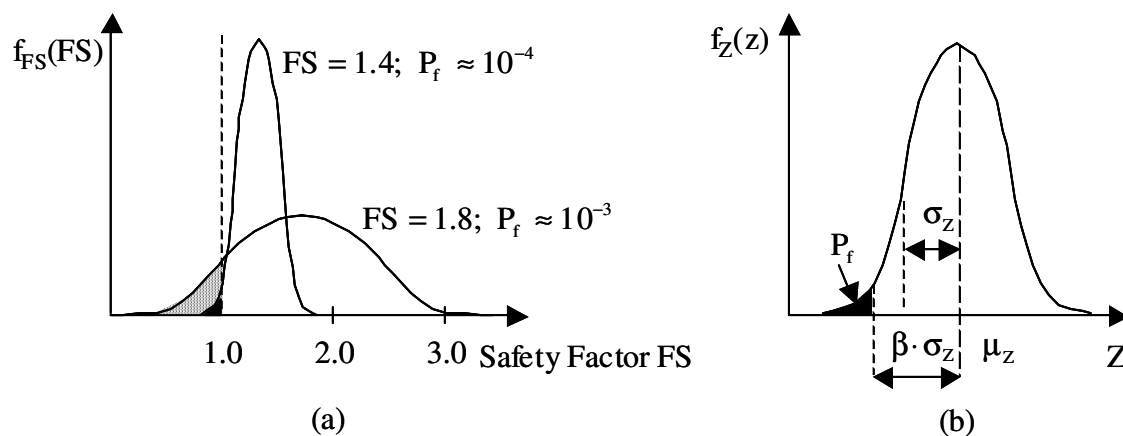


Figure 2.10: (a) Factor of safety and failure probability. (b) Reliability index approach

From a deterministic point of view it would seem that the case with FS=1.8 is safer. However when one compares the failure probability values, then the apparently safer case has a higher probability of failure, thus demonstrating that the deterministic analysis is not always safe against failure.

It can be concluded that, while one does not precisely know what a safety factor of 1.5 means, a failure probability, for example, of 10^{-3} is very clear.

2.4.3 The reliability index

If resistance and load follow normal distributions then the convolution integral (2.22) may be evaluated as

$$P_f = 1 - \Phi(\beta) = \Phi(-\beta) \quad (2.23)$$

where Φ denotes the standard normal distribution function and β is a very useful parameter for characterizing the degree of safety, commonly called the reliability index. This index was first defined by CORNELL (1969) and is given by

$$\beta(\text{normal}) = \frac{\mu_R - \mu_L}{\sqrt{\sigma_R^2 + \sigma_L^2 \pm 2 \cdot \rho_{RL} \cdot \sigma_R \cdot \sigma_L}} = \frac{\mu_Z}{\sigma_Z} \quad (2.24)$$

where μ_R , μ_L and μ_Z , respectively σ_R , σ_L and σ_Z are the mean values, respectively the standard deviations of resistance, load and safety margin. While ρ_{RL} is the correlation coefficient between resistance and load. In the case of uncorrelated input variables the term with the correlation coefficient drops out.

As Fig. 2.10(b) shows, the reliability index represents the number of standard deviations of the safety margin Z by which the mean value μ_Z exceeds the limit state.

Figure 2.11 shows the relation between failure probability and reliability index for a performance function with a normal distribution. It is clear how the reliability index is monotonically related to the failure probability, so that higher values of β imply lower values of P_f . Other distributions give similar curves for $\beta < 2.5$, but the curves differ substantially for higher values of the reliability index.

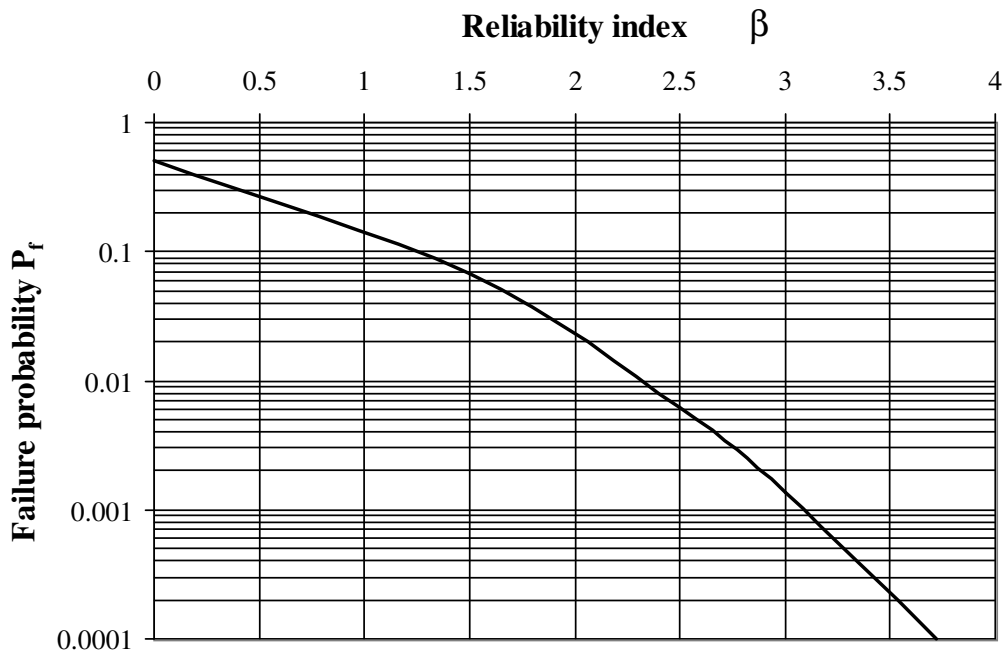


Figure 2.11: Failure probability P_f versus reliability index β for a normal distribution

If resistance and load are uncorrelated and both lognormal then the reliability index is

$$\beta(\text{log normal}) = \frac{\ln\left(\frac{\mu_R}{\mu_L} \cdot \sqrt{\frac{1 + \text{COV}_L^2}{1 + \text{COV}_R^2}}\right)}{\sqrt{\ln[(1 + \text{COV}_R^2) \cdot (1 + \text{COV}_L^2)]}} = \frac{\mu_{\ln Z}}{\sigma_{\ln Z}} \quad (2.25)$$

where COV_R , COV_L are the variation coefficients of resistance and load, while $\mu_{\ln Z}$ and $\sigma_{\ln Z}$ are the mean value and standard deviation of the normal variable $\ln(Z)$.

When COV_R and COV_L are lower than 0.3 and provided that $\beta < 2.5$, it is possible to obtain a very good estimate of the failure probability for lognormal variables using Eq. (2.24) and the relation of Fig. 2.11 (WHITMAN, 1984; FENTON, 2006). For larger values of β , the failure probability is quite sensitive to the shape of the distribution.

Chapter 3

Probabilistic methods for quantifying uncertainties in Geotechnics

Introduction

The quantification and analysis of uncertainty are central issues in the evaluation of reliability and the development of associated reliability based-design.

The purpose of this chapter is to review some well-known probabilistic techniques, such as the Monte Carlo and the Point Estimate methods, for dealing with uncertainties and for implementing probabilistic concepts into geotechnical analyses in a more rational way. Actually, assuming soil parameters, such as the friction angle and the cohesion, as random variables described by a certain probability density function, then probabilistic methods are applied to assess the probability density function and the statistical values of a limit state function (e.g. the bearing capacity) which depends on the input variables. Thus, failure probabilities and reliability indices can be estimated from the output results, leading to a more meaningful evaluation of safety design.

In this chapter the methodology of probabilistic approaches are illustrated and their corresponding advantages and limitations discussed.

3.1 Monte Carlo Simulations (MCS)

The word “simulation” refers to any numerical method meant to imitate a real-life system, especially when other analyses are mathematically too complex or too difficult to reproduce. Without the aid of simulation, a spreadsheet model will only reveal a single deterministic outcome, generally the most likely or average value. One type of simulation technique is the Monte Carlo method, which can be used in every field, from economics to nuclear physics. Of course the way this method is applied varies widely from field to field. In the MCS assumptions are only made on the input random variables, whose values are generated consistently with the corresponding probability

density function. Then the safety margin, for which no assumption on the probability density function is required, is calculated for each realization. The process is repeated numerous times, typically thousands, and the mean value, standard deviation, skewness coefficient and probability distribution of the safety margin are evaluated. Thus Monte Carlo procedure consists of solving a deterministic problem many times to build up a statistical distribution of the output.

This method is close to the real answer and is therefore used as reference for comparison with other probabilistic methods results, as will be shown in the following chapters for the probabilistic analysis of the bearing capacity problem.

However, for certain geotechnical problems, such as slope stability analyses, additional special programming for the MCS would be needed. Moreover, to obtain any real confidence, the model would need a large number of simulations. In practice, it is too time consuming for daily computer calculations, especially for Finite Elements codes. The idea is, therefore, to replace MCS by other probabilistic approaches requiring only a limited amount of calculations.

For more detail about MCS and the way of generating random numbers, the author refers to ANG and TANG (1984), ROSS (1995) and the publication CUR190 of the Delft University of Technology (CUR-Publicatie 190, 1997).

3.2 The First Order Second Moment method (FOSM)

The first relatively simple alternative to MCS is the well-known First Order Second Moment method, or shortly FOSM, which produces a linearisation around the mean value of the input random variables of a probabilistic problem. This method uses a Taylor's series expansion of the performance function to be evaluated to determine the values of its first two central moments, mean value and standard deviation, depending on the input variables. This expansion is truncated after the linear term and, for this reason, the method is called "First Order".

Considering a performance function Z of n random variables X_i , as for example the bearing capacity as function of the cohesion and the friction angle, its Taylor's series expansion about the mean value of the random variables $\mu_{X_1}, \dots, \mu_{X_n}$, truncated after first order terms, gives

$$Z(X_1, \dots, X_n) = Z(\mu_{X_1}, \dots, \mu_{X_n}) + \sum_{i=1}^n (X_i - \mu_{X_i}) \cdot \frac{\partial Z}{\partial X_i} \quad (3.1)$$

The derivatives are evaluated at $\mu_{X_1}, \dots, \mu_{X_n}$, considered as linearisation points. The mean value and the variance of the performance function are given approximately by the following equations

$$\mu_{Z(X_1, \dots, X_n)} \approx Z(\mu_{X_1}, \dots, \mu_{X_n}) \quad (3.2)$$

$$\text{Var}[Z(X_1, \dots, X_n)] \approx \sum_{i=1}^n \left(\frac{\partial Z}{\partial X_i} \right)^2 \cdot \text{Var}(X_i) + 2 \cdot \sum_{i=1}^n \sum_{j=1}^n \left(\frac{\partial Z}{\partial X_i} \cdot \frac{\partial Z}{\partial X_j} \right) \cdot \text{Cov}(X_i, X_j) \quad (3.3)$$

If the random variables are uncorrelated, then the term with the covariance drops out. In general, for n random variables $2n+1$ calculations are involved.

In practice it is sometimes complicated to evaluate derivatives of non-linear functions. For this reason the required derivatives can be estimated numerically using the finite difference approach, described in detail by EL-RAMLY, MORGENSTERN and CRUDEN (2001).

The usual output of FOSM method is the reliability index given by Eq. (2.24) for normally distributed variables. For non-normal probability density functions the reliability index evaluated by FOSM method is only an approximation. Very refined methods have been developed to convert general probability density functions into standard normal distributions (ANG and TANG, 1984).

3.2.1 Advantages and limitations of the FOSM method

The most important advantages of the FOSM method include the following:

- The FOSM method is exact for linear performance functions.
- The summation terms of Eqs. 3.1 and 3.3 provide an explicit indication of the relative contribution of uncertainty of each random variable.
- Experts (EL RAMLY, MORGENSTERN and CRUDEN, 2003) state that, in comparison to MCS, the FOSM method shows an error in its estimates between 5%-15%, which is a reasonable value for geotechnical field. This will be shown in next chapters.

To avoid the misuse of FOSM method in probabilistic analyses, one should be referred of its limitations, which are listed below:

- Due to the Taylor's series truncation after first order terms, the accuracy of the method deteriorates if second and higher derivatives of the

performance function are significant. Thus the accuracy of the FOSM method diminishes as the non-linearity of a function increases. Unfortunately, retaining second and higher order terms of the Taylor's series expansion of a complex function with more than one input variable is mathematically complex.

- The skewness of the output probability density function is not provided.
- As the level of uncertainty in the input variables increases and their probability density functions become more skewed the accuracy of the FOSM method decreases.
- Additional assumptions on the output probability density function must be made to estimate any probability of failure; moreover the reliability index is not uniquely defined, because it depends on the safety format considered (e.g. $R-L=0$, where R = resistance and L = load).
- The shape of the probability density function of the input variables is not taken into account, the random variables are described using only their mean and standard deviation. In this way no information about the shape of the probability density function of the output is provided, but it has to be assumed. This assumption introduces a source of inaccuracy.
- Finally, the FOSM method is applied primarily to problems without spatial correlation among input variables. With extra calculation effort, the method can be applied for two correlated random variables, but this can be very cumbersome.

3.3 The Second Order Second Moment method (SOSM)

The Second Order Second Moment method, or shortly SOSM, represents a slight extension of FOSM method. Actually with SOSM method it is possible to include second order terms of the Taylor's series expansion in the evaluation of the mean value of a performance function.

Considering the variances, or standard deviations, of two random variables X , Y as known, the mean value of $Z(X,Y)$ is given by

$$\mu_{Z(X,Y)} \approx Z(\mu_x, \mu_y) + (x - \mu_x) \cdot \frac{\partial Z}{\partial x} + (y - \mu_y) \cdot \frac{\partial Z}{\partial y} + \frac{1}{2} \cdot \text{Var}(X) \cdot \frac{\partial^2 Z}{\partial x^2} + \frac{1}{2} \cdot \text{Var}(Y) \cdot \frac{\partial^2 Z}{\partial y^2} + \text{Cov}(X, Y) \cdot \frac{\partial^2 Z}{\partial x \cdot \partial y} \quad (3.4)$$

where all derivatives are evaluated at the mean value of the input variables. The term including the covariance drops out if the variables are uncorrelated.

When compared with FOSM method, the obvious advantage of SOSM method is that the calculated mean value is more accurate because second order terms are considered in the analysis.

Important references for FOSM and SOSM methods and their applications to engineering problems are: GRIFFITHS, FENTON and TVETEN (2002), CHRISTIAN and BÄCHER (1992, 1994), MOSTYN and LI (1993), WOLFF (1994), DUNCAN (2000).

3.4 The Hasofer-Lind method (FORM)

A drawback of the FOSM method is that the results depend on the mean value of the input variables at which the partial derivatives of the safety margin are evaluated (invariance problem). Moreover the FOSM method is exact only for linear functions, while for non-linear functions errors are introduced in the analysis.

The Hasofer-Lind method, also well-known as the First Order Reliability Method, or shortly FORM, can overcome this difficulty by calculating the derivatives of the safety margin at a critical point on the failure surface, also called design point. An iterative solution is usually required to find this point, but the process tends to converge very rapidly.

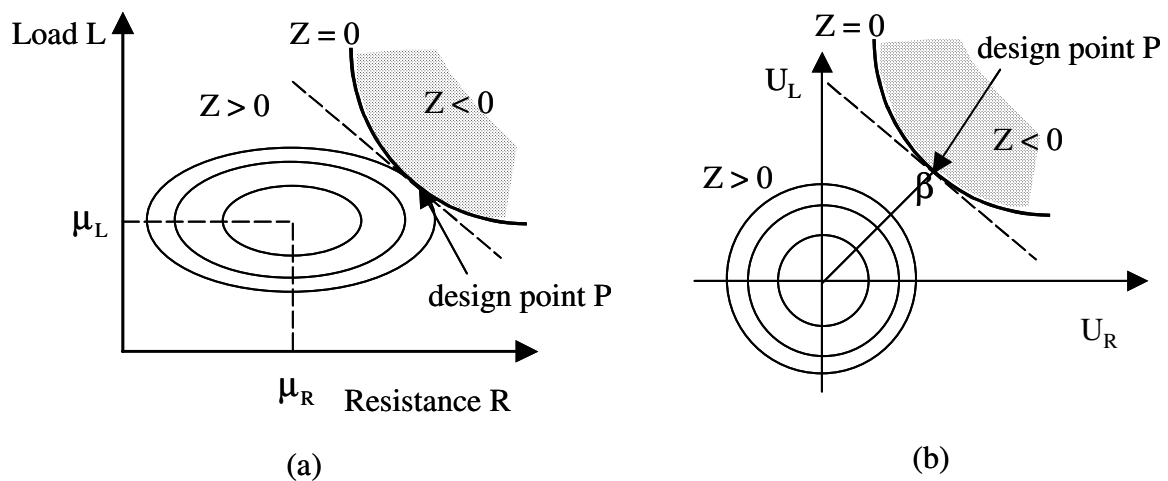


Figure 3.1: Linearisation of the safety margin in the design point in the RL-plane (a) and definition of the reliability index for normalized random variables (b)

In Fig. 3.1(a) the joint probability density function of the random variables R and L is linearised in the design point P. When the variables are non-normally distributed, then they can be transformed into standard normal variables with zero mean value and standard deviation equal to unity, as described by ANG and TANG (1984) and plotted in the standard normalised space as in Fig. 3.1(b).

The shortest distance between the failure point P and the origin of the normalized space is the reliability index β , i.e.

$$\beta = \min_{Z=0} \left(\sqrt{U_R^2 + U_L^2} \right) \quad (3.5)$$

To find the design point many known analytical and numerical optimisation routines can be used, such as those described in VRIJLING (1997).

Other important references for FORM theory and its application are: NADIM (2006), PULA (2006), CHRISTIAN and BÄCHER (1992, 1994).

3.4.1 Advantages and limitations of the FORM method

The most important advantages of the FORM method are the following:

- The reliability index and the failure probability are independent of the safety format used and they can be evaluated also for non-linear functions.
- It is a more efficient method for estimating low probability of failure when compared with other approaches, as will be shown in chapter 6.
- The sensitivity factors give additional information on the influence of the input random variables on the performance function.

As with the FOSM and SOSM methods, the FORM method does not provide the shape of the probability density function and the skewness coefficient of the performance function. In addition this method requires special software or very good programming skill for the iteration procedure, such as the current VaP (Variables Processor) program, developed by the Austrian company “Petschacher Software und Projektentwicklungs GmbH” and the test version of the program ProBox, developed by the TNO Building and Construction Research Institute of Delft.

3.5 The Two Point Estimate Method (PEM)

Another alternative method to evaluate statistical moments of a performance function is the Point Estimate Method, or shortly PEM. The Point Estimate method was first developed by ROSENBLUETH (1975, 1981) and then further developed by other authors such as CHRISTIAN and BÄCHER (1999), EVANS et al. (1993), LIND (1983), ZHOU and NOWAK (1988), HARR (1989), LI (1992), HONG (1998). The method used in this study is the “Two Point Estimate Method” after ROSENBLUETH.

The Two Point Estimate method is a computationally straightforward technique for uncertainty analysis, capable of estimating statistical moments of a model output involving several stochastic variables, correlated or uncorrelated, symmetric or asymmetric. It is fundamentally a weighted average method similar to numerical integration formulas involving sampling points and weighting parameters.

The PEM can be seen as a special case of the orthogonal polynomial approximation procedures leading to the Gaussian quadrature formulas, which are well known in numerical analyses and in Finite Elements methods (CHRISTIAN and BÄCHER, 1999).

The basic idea of this method is to replace the probability distributions of continuous random variables by discrete equivalent distributions having the same first three central moments, to calculate then the mean value, standard deviation and skewness of a performance function, which depends on the input variables.

To do this, two point estimates are considered at one standard deviation on either side of the mean value from each distribution representing the random variables. Then the performance function is calculated for every possible combination of the point estimates, producing 2^n solutions, where n is the number of the random variables involved. Then the mean value, standard deviation and skewness of the performance function can be found from these 2^n solutions.

While the PEM does not provide a full distribution of the output variable, as Monte Carlo does, it requires little knowledge of probability concepts and could be applied for any probability distribution. In future it might be widely used for reliability analysis and for the evaluation of failure probability of engineering systems.

The procedure for implementing the PEM is clearly described in the next section. For a simple introduction, the reader should refer to GRIFFITHS, FENTON and TVETEN (2002).

3.5.1 The procedure for implementing the PEM

The procedure for implementing the PEM is described below step by step.

1. First of all a performance function $Z(X_i)$ depending on n random variables X_i should be considered.
2. Then the locations of the sampling points for every random variables should be estimated. To do this one should first evaluate the so-called standard deviation units $\xi_{X_{i+}}$ and $\xi_{X_{i-}}$, which depend on the skewness coefficient v_{x_i} of the input variables and given by

$$\xi_{x_{i+}} = \frac{v_{x_i}}{2} + \left(1 + \left(\frac{v_{x_i}}{2} \right)^2 \right)^{1/2} \quad \xi_{x_{i-}} = \xi_{x_{i+}} - v_{x_i} \quad (3.6)$$

If the input variables are symmetrically distributed, the standard deviation units will be both equal to unity. Knowing the mean value μ_{x_i} and the standard deviation σ_{x_i} of the input variables, the corresponding sampling point locations x_{i-} and x_{i+} can be calculated using the following formulas

$$x_{i+} = \mu_{x_i} + \xi_{x_{i+}} \cdot \sigma_{x_i} \quad x_{i-} = \mu_{x_i} - \xi_{x_{i-}} \cdot \sigma_{x_i} \quad (3.7)$$

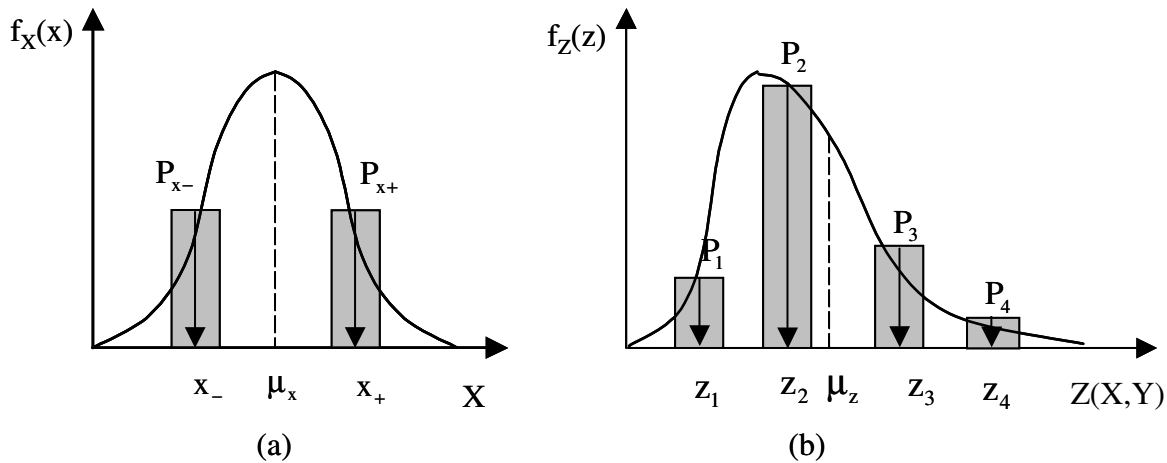


Figure 3.2: Sampling point locations and weights for a single random variable (a) and for a function depending on two random variables (b)

In Fig. 3.2(a) and 3.2(b) the sampling point locations for a single random variable and for a function Z depending on two random variables X and Y are shown.

3. The weights P_i , also called probability concentrations, can now be determined to obtain all the point estimates. As a probability density function encloses an area of unity, then the weights must also sum to unity and they have to be positive. The weights of the random variables are given by different expressions depending on the number of the input variables and on their correlation. An example of weights distribution is shown in Fig. 3.2(a) and 3.2(b).

For a single random variable (ROSENBLUETH, 1975) the weights are easily calculated using the standard deviation units as

$$P_{x+} = \frac{\xi_{x-}}{\xi_{x+} + \xi_{x-}} \quad P_{x-} = 1 - P_{x+} \quad (3.8)$$

When the random variable is symmetric then the weights are both equal to 0.5, as shown in Fig. 3.2(a).

For two correlated random variables (ROSENBLUETH, 1981) the weights are given as follows

$$P_{s_1 s_2} = P_{x_{s_1}} \cdot P_{x_{s_2}} + s_1 \cdot s_2 \cdot \left(\rho_{x_1 x_2} / \left(\left(1 + \left(\frac{v_{x_1}}{2} \right)^3 \right) \cdot \left(1 + \left(\frac{v_{x_2}}{2} \right)^3 \right) \right)^{1/2} \right) \quad (3.9)$$

where $P_{x_{s_1}} \cdot P_{x_{s_2}}$ are the associated weights, with $P_{x_{s_1}}$ and $P_{x_{s_2}}$ being the weights for the input variables evaluated as single variables. $\rho_{x_1 x_2}$ is the correlation coefficient between the variables X_1 and X_2 , s_1 and s_2 take positive sign for points greater than the mean value of the variables and negative sign for points smaller than the mean value.

The sign product $s_1 \cdot s_2$ determines the sign of the correlation coefficient and the subscripts of the weight P indicate the location of the point that is being weighted. For example, considering the point evaluated at $(x_{1+}, x_{2-}) = (\mu_{x_1} + \xi_{x_{1+}} \cdot \sigma_{x_1}, \mu_{x_2} - \xi_{x_{2-}} \cdot \sigma_{x_2})$ then $s_1 = +$ and $s_2 = -$, resulting in a negative product with a weight denoted by P_{+-} .

When the variables are uncorrelated then $\rho_{x_1x_2}$ will be zero and the formula (3.9) will give the associated weights of two uncorrelated random variables.

Unfortunately Eq. (3.9) has some evident drawbacks. First of all, if the skewness coefficient of the input variables has different sign then the radicand under the square root can be negative, which is mathematically impossible. This can happen for example if one input variable has a negatively skewed distribution and the other a symmetrically or positively skewed distribution. Secondly if the skewness coefficient of the input variables is equal to -2 then the denominator of the second term of Eq. (3.9) tends to infinity, giving then infinite weights. Moreover this formula can sometimes give negative values. This fact is unacceptable, because the weights are described as probability values, which are always positive by definition. For example, negative values of the weights can occur when the random variables are symmetric and perfectly correlated (i.e. $\rho_{x_1x_2} = \pm 1$).

The problem of obtaining negative weights could be solved, for example, by applying the Three Points Estimate Method instead of the Two PEM.

Considering all the drawbacks of Eq. (3.9), it is necessary to establish some conditions for its use, i.e.

$$1) \quad P_{x_{s1}} \cdot P_{x_{s2}} > s_1 \cdot s_2 \cdot \left(\rho_{x_1x_2} / \left(\left(1 + \left(\frac{v_{x_1}}{2} \right)^3 \right) \cdot \left(1 + \left(\frac{v_{x_2}}{2} \right)^3 \right) \right)^{1/2} \right) \quad (3.10)$$

$$2) \quad \left(1 + \left(\frac{v_{x_1}}{2} \right)^3 \right) \cdot \left(1 + \left(\frac{v_{x_2}}{2} \right)^3 \right) > 0 \quad (3.11)$$

$$3) \quad v_{x_1} \neq -2 \quad \text{and/or} \quad v_{x_2} \neq -2 \quad (3.12)$$

The first condition assures that the weights are positive. The third condition is actually already implied in the second one.

To overcome the problem in ROSENBLUETH's formula (3.9), a better definition for two correlated random variables, being symmetrically distributed, is given by CHRISTIAN et al. (1999), where the weights can be evaluated as

$$P_{+-} = P_{-+} = P_{x_1\pm} \cdot P_{x_2\mp} \cdot (1 - \rho_{x_1x_2}) \quad P_{--} = P_{++} = P_{x_1\pm} \cdot P_{x_2\pm} \cdot (1 + \rho_{x_1x_2}) \quad (3.13)$$

For n symmetrically distributed and correlated random variables, CHRISTIAN et al. (1999) define the weights as

$$P_{s_1 s_2 \dots s_n} = \frac{1}{2^n} \cdot \left(1 + \sum_{i=1}^{n-1} \sum_{j=i+1}^n (s_i \cdot s_j \cdot \rho_{ij}) \right) \quad (3.14)$$

In equation (3.14) the notation is the same as for equation (3.9).

4. Now it is possible to determine the performance function $Z(X_i)$ at each sampling point located at x_{i+} and x_{i-} . To do this, it is sufficient to introduce the sampling point estimates found using Eqs. (3.7) in the formula of the performance function. For n random variables, the performance function is evaluated at 2^n points.

5. Finally the first three moments of the performance function, respectively the mean value, the variance and the skewness coefficient, can be determined using the following equations

$$\mu_{Z(X_i)} = \sum_{i=1}^{2^n} P_i \cdot Z(X_i = x_i) \quad (3.15)$$

$$\sigma^2_{Z(X_i)} = \sum_{i=1}^{2^n} P_i \cdot \left(Z(X_i = x_i) - \mu_{Z(X_i)} \right)^2 \quad (3.16)$$

$$\nu_{Z(X_i)} = \frac{1}{\sigma^3_{Z(X_i)}} \sum_{i=1}^{2^n} P_i \cdot \left(Z(X_i = x_i) - \mu_{Z(X_i)} \right)^3 \quad (3.17)$$

The standard deviation of the performance function is easily obtained as

$$\sigma_{Z(X_i)} = \sqrt{\sum_{i=1}^{2^n} P_i \cdot \left(Z(X_i = x_i) - \mu_{Z(X_i)} \right)^2} \quad (3.18)$$

ROSENBLUETH (1981) notes that for the multiple random variables case, skewness coefficients can only be reliably calculated using Eq. (3.17) if the variables are uncorrelated. This fact will be shown in chapter 5.

3.5.2 Advantages and limitations of the PEM

The most important advantages of PEM in comparison to FOSM, SOSM and FORM methods are:

- As with the FOSM, SOSM and FORM methods, the PEM does not require the knowledge of the particular shape of the probability density function of the input random variables. Moreover the PEM furnishes the exact solution for linear performance functions.
- It provides not only the mean value and the standard deviation, but also the skewness coefficient of a performance function, giving then more accurate results than FOSM, SOSM and FORM methods, with little or no increase in computational effort.
- The PEM may better capture the behaviour of non-linear functions.
- To evaluate the statistical values of a performance function there is no need to compute the derivatives, nor even their continuity let alone their existence.
- As a non-iterative procedure, the PEM overcomes the convergence problems of the FORM, thus being less time consuming.
- It can be also applied to problems with spatial correlation among multiple input variables, even if more computational effort is required.

When compared with Monte Carlo method, the PEM results in terms of mean value and standard deviation are in good agreement with those of MCS, with smaller computational effort for a comparable degree of accuracy.

Limitations of the PEM as described above:

- No information about the shape of the probability density function of the output is provided, but it has to be assumed, introducing uncertainty in the final results.
- The skewness provided by PEM presents a significant difference to the skewness value derived from MCS, as it will be shown in chapter 5.
- If more accuracy is required, then a larger number of input variables is necessary and higher moments have to be considered, thus increasing the number of calculations.
- Results are poor and less accurate for discontinuous functions or functions having discontinuous first derivatives (CHRISTIAN and BÄCHER, 1999).
- The implementation of PEM into Finite Element codes requires additional out of house software.
- CHRISTIAN and BÄCHER (1999) suggest that the PEM should not be applied for evaluating moments higher than the second (i.e. variance) for non-linear functions. Additionally they observe that the larger the

variation coefficient of the input variables, the larger is the error in the estimates. Finally these authors affirm that caution should be used in applying PEM to cases in which the transformation of input variables changes the distributional form, because the final results can be in error losing important information on the variables main characteristics. This fact will be seen in chapter 5, where the lognormal variable cohesion, with a high COV-value, is transformed into the corresponding normal variable $\ln c'$ for solving probabilistically the bearing capacity problem of a shallow foundation.

Chapter 4

Probabilistic analysis of the bearing capacity problem

Introduction

This chapter presents an application of probabilistic methods to the study of the bearing capacity of a strip footing on a homogeneous soil layer characterised by the effective cohesion c' and friction angle ϕ' . These parameters are selected to be represented as random variables since they have the greatest impact on the soil bearing capacity.

Different values of the correlation coefficient between soil parameters are taken into account in the analysis. The influence of the spatial variability of soil parameters (i.e. the scale of fluctuation), which is a significant source of error, is ignored here.

For a comparison of the failure probabilities from the MCS, FOSM and SOSM methods the author refers to chapter 6.

4.1 Benchmarks on the bearing capacity of a strip footing

4.1.1 Benchmark 1: bearing capacity of a strip footing with effective friction angle as the input random variable

The first benchmark deals with the study of the bearing capacity of a strip footing with a width of 2m on top of a cohesionless homogeneous soil layer, as shown in Fig. 4.1(a). More specifically, the soil type is what can be called a grossly uniform soil, in which the whole mass is all of the same consistency and whose properties show no marked trend with depth or distance.

For this study soil layering is ignored, assuming that in the soil mass no discontinuities or sudden changes exist. The unit soil weight is 15 kN/m^3 and a surcharge $q_0=10 \text{ kN/m}^2$ is considered. The effective soil cohesion c' is taken as a uniform fixed property with a value of 4 kN/m^2 , while the effective friction angle ϕ' is taken into account as a normal random variable with its corresponding statistical values given in Fig. 4.1(b).

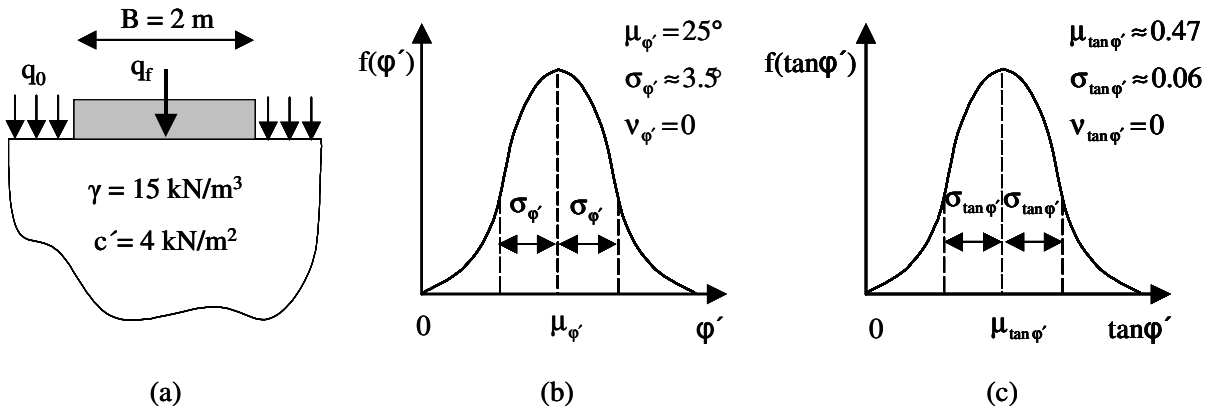


Figure 4.1: (a) Strip footing on a homogeneous soil layer. Normal distribution and statistical values of ϕ' (b) and $\tan\phi'$ (c)

To simplify calculations, the tangent of the friction angle $\tan\phi'$ will be considered as random variable instead of ϕ' . The mean value and standard deviation of $\tan\phi'$ are listed in Fig. 4.1(c).

A coefficient of variation of 13% is considered for $\tan\phi'$, which is a realistic value for the range of COV values found in the literature (PHOON and KULHAWY, 1999; MOORMANN and KATZENBACH, 2000; HARR, 1987; CHERUBINI, 1997), as already discussed in chapter 2. Knowing the mean value and the coefficient of variation of $\tan\phi'$, it is possible to define the standard deviation.

The shape of the probability density function of the bearing capacity, denoted as q_f , has to be found. Its statistical values are evaluated using the probabilistic methods MCS, FOSM and SOSM, already described in chapter 3.

The classical formula (A.4) in Appendix A of TERZAGHI (1943) for the bearing capacity is applied, considering the bearing capacity factor N_γ after BRINCH-HANSEN (1961). For more detail on the ultimate bearing capacity formula the author refers to appendix A. This formula gives a deterministic value of 287.6 kN/m^2 for the bearing capacity.

4.1.2 Benchmark 2: bearing capacity of a strip footing with effective friction angle and cohesion as input random variables

The second benchmark is similar to the bearing capacity problem of the first benchmark, but here the effective soil cohesion is also considered as random variable with a standard lognormal distribution and mean value $\mu_{c'} = 4\text{ kN/m}^2$, as described in Fig. 4.2(a).

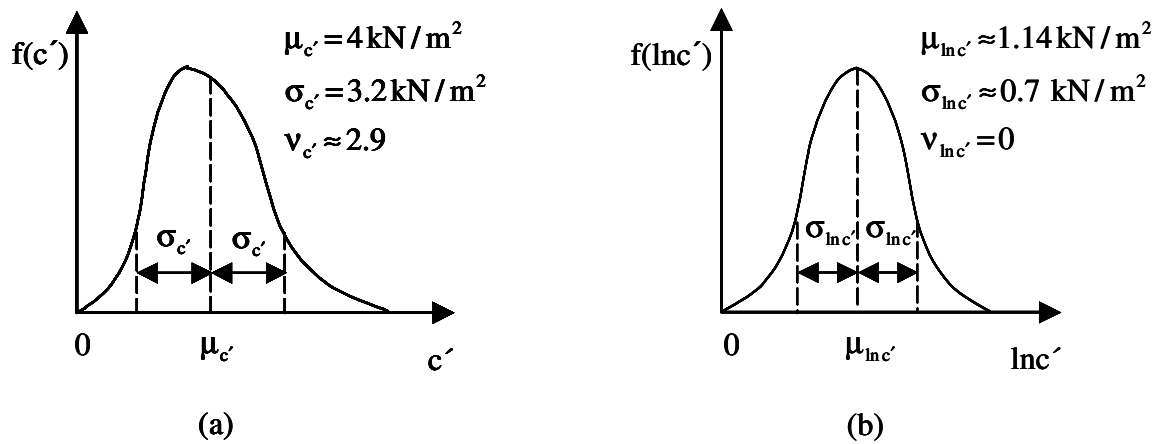


Figure 4.2: Probability distribution and statistical values of the variables c' (a) and $\ln c'$ (b)

A coefficient of variation of 80% is assumed for the cohesion, which is a value somewhat higher than the COV values generally reported in the literature (LI and LUMB, 1987; MOORMANN and KATZENBACH, 2000; HARR, 1987; CHERUBINI, 1997). The standard deviation of the cohesion is also determined from its mean value and coefficient of variation.

The skewness coefficient of the cohesion can be evaluated knowing the $\text{COV}_{c'}$ with the well known formula of BENJAMIN and CORNELL (1970), valid for a standard lognormal distribution

$$v_x = 3 \cdot \text{COV}_x + \text{COV}_x^3 \quad (4.1)$$

which gives a value $v_{c'} = 2.94$. Formula (4.1) can be rewritten considering the standard deviation of the transformed lognormal variable x into the corresponding normal variable $\ln x$, instead of its variation coefficient, thus giving

$$v_x = \sqrt{e^{\sigma_{\ln x}^2} - 1} \cdot (2 + e^{\sigma_{\ln x}^2}) \quad (4.1\text{bis})$$

where $\text{COV}_x = \sqrt{e^{\sigma_{\ln x}^2} - 1}$. For more detail about formulas (4.1) and (4.1bis) the author suggests to refer to BENJAMIN and CORNELL (1970) and to look up well-known probabilistic literature available worldwide.

Considering the property of the lognormal distribution, the cohesion can be transformed into the normal variable $\ln c'$, as shown in Fig. 4.2(b). The mean value and standard deviation of $\ln c'$ are also shown in this figure. These values are useful for simplifying calculations in the probabilistic analysis, as it will be seen in next sections and in chapter 5.

As with benchmark 1, the shape of the bearing capacity and its statistical values should be found by applying the probabilistic methods already mentioned. For the second benchmark different correlation coefficients between the effective soil properties will be taken into account in the analysis.

4.2 Application of Monte Carlo Simulations

For the probabilistic bearing capacity analysis of the benchmarks described in section 4.1, Monte Carlo Simulations are initially performed using a spreadsheet method, more specifically by using the familiar Microsoft Excel software.

The accuracy of MCS results depends on the number of calculations carried out for the input parameters considered. Hence improving the accuracy requires an increase of the simulations number (KOTTEGODA and ROSSO, 1997).

Different numbers of calculations are executed for the bearing capacity problem, respectively 1000, 10000 and 100000. Comparing the results of each case, the mean value and the standard deviation seem to be already stable for 1000 simulations. On the other hand, the skewness coefficient requires 100000 simulations to converge to a constant value, as it will be seen in next sections.

First of all the soil properties are generated as uniformly distributed variables between 0 and 1. They are then transformed into variables with the corresponding mean value, standard deviation and probability distributions, i.e. normal distribution for $\tan\phi'$ and standard lognormal distribution for c' .

The goodness of the generator is judged by subjecting the generated random numbers to the “periodicity test”. This is a useful test to verify the periodicity of the random numbers generated, by testing their uniform distribution and the statistical independency. In fact it can happen in the Microsoft Excel software that these variables start repeating themselves after a while. The periodicity test has shown that the thousand input variables generated are not periodic, so that they can be properly used to perform Monte Carlo Simulations. Successively thousands of successive deterministic bearing capacity calculations are carried out to assess its statistical values and the shape of the distribution function. Because of the many simulations, Monte Carlo method leads to the most accurate and reliable estimation of statistical and probability values.

In next sections the MCS results for both benchmarks are presented and compared. The importance of assuming negatively correlated soil parameters for uncertainty analysis is stressed.

4.2.1 Monte Carlo results for benchmark 1

In the first benchmark the only input variable is $\tan\phi'$, which is normally distributed. Thousands of $\tan\phi'$ -values are generated and thousands of bearing capacity values are estimated, thus obtaining the results shown in Tables 4.1, 4.2 and 4.3 for a different number of Monte Carlo simulations, respectively 1000, 10000 and 100000. For all the three cases the mean value of the bearing capacity is about 6% higher than the deterministic value.

When comparing the statistical values of Tables 4.1, 4.2 and 4.3, one sees that generally mean value, standard deviation and skewness coefficient change slightly as the number of simulations increases, converging to more stable values for 100000 simulations, especially the skewness coefficient.

μ_{q_f}	σ_{q_f}	COV_{q_f}	v_{q_f}
306.713 kN/m ²	101.022 kN/m ²	0.329	0.93

Table 4.1: Statistical values of q_f predicted by 1000 MCS

μ_{q_f}	σ_{q_f}	COV_{q_f}	v_{q_f}
306.562 kN/m ²	102.242 kN/m ²	0.333	1.008

Table 4.2: Statistical values of q_f predicted by 10000 MCS

μ_{q_f}	σ_{q_f}	COV_{q_f}	v_{q_f}
306.924 kN/m ²	103.142 kN/m ²	0.336	1.04

Table 4.3: Statistical values of q_f predicted by 100000 MCS

Referring to the values of the variation coefficient, one knows from the literature (PHOON & KULHAWY, 1999; POPESCU, 2004) that a good range of COV_{q_f} values for the bearing capacity is 0.1-1.0. In Tables 4.1, 4.2 and 4.3 the COV_{q_f} ranges between 0.329 and 0.336, thus the order of magnitude complies with those suggested in the literature.

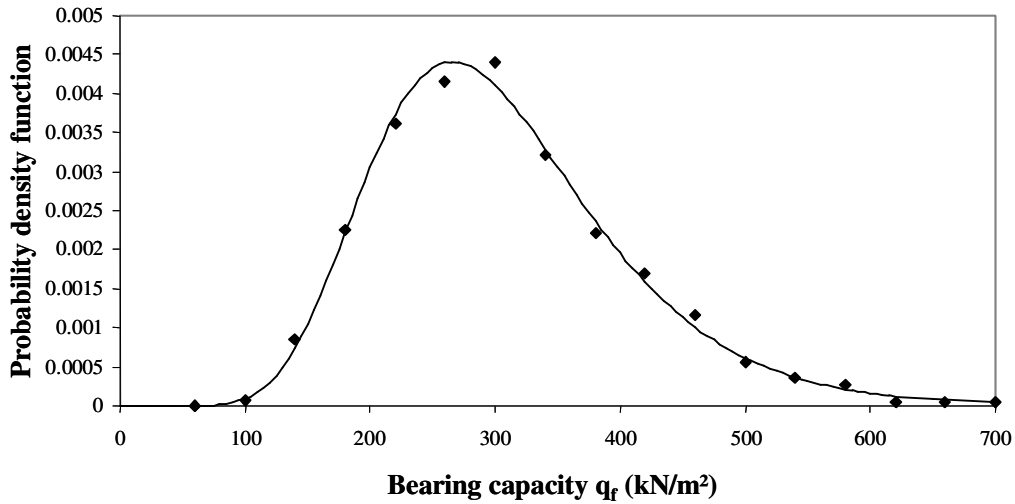


Figure 4.3: Shifted lognormal fit and relative frequency (pointwise) of q_f for 1000 MCS

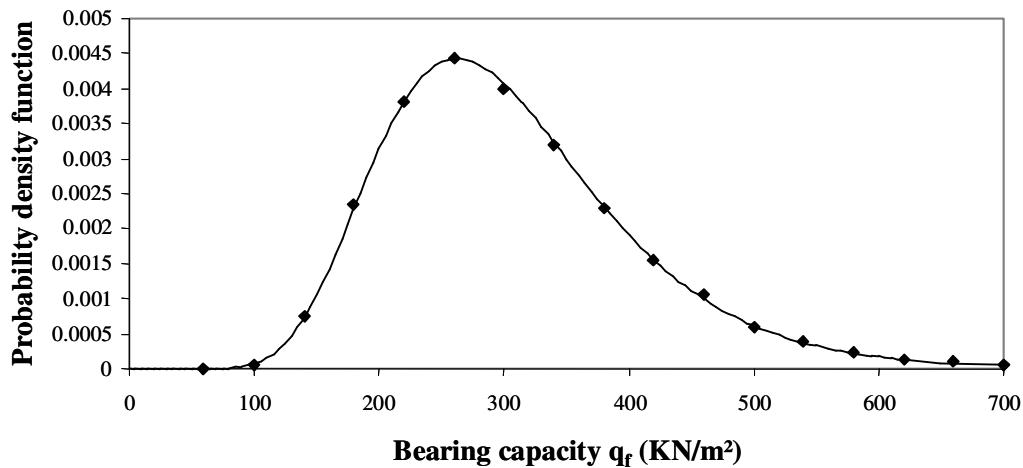


Figure 4.4: Shifted lognormal fit and relative frequency (pointwise) of q_f for 10000 MCS

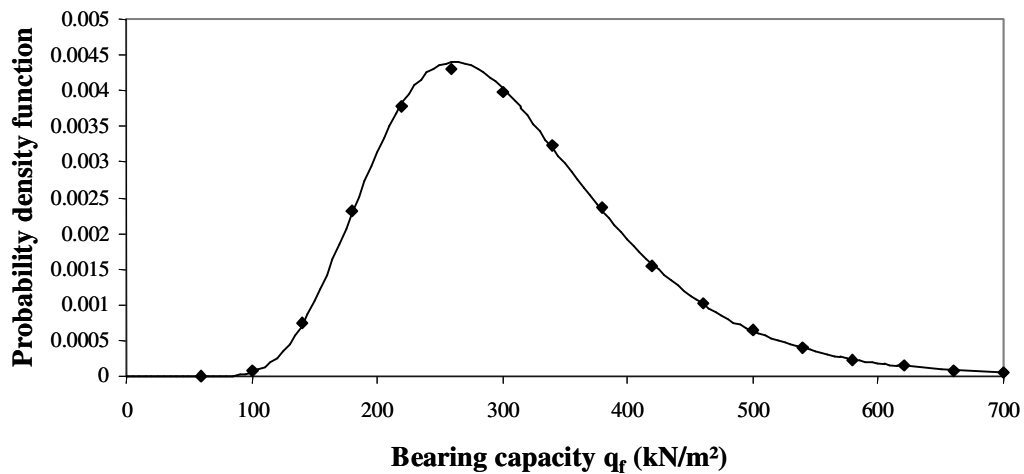


Figure 4.5: Shifted lognormal fit and relative frequency (pointwise) of q_f for 100000 MCS

In Figs. 4.3, 4.4 and 4.5 the probability density function of the bearing capacity is drawn by considering the relative frequency of q_f pointwise together with the corresponding best fit curve using the shifted lognormal distribution.

This distribution seems to match the results of MCS well for all the three cases, becoming smoother and thus being more accurate for a higher number of simulations.

The chi-square test for the goodness of fit shows that the assumed theoretical distribution, i.e. the shifted lognormal distribution, for approximating MCS-results is a suitable model at around 5% significance level.

4.2.2 Monte Carlo results for benchmark 2 with uncorrelated soil parameters

In the second benchmark the effective cohesion is also considered as input variable together with $\tan\phi'$, but no correlation is taken into account between them. Initially the cohesion is transformed into the corresponding normal variable $\ln c'$ to be generated by MCS, then it is transformed back to the lognormal variable c' .

Again thousands of input variables are generated and thousands of bearing capacity values are evaluated, thus obtaining the results shown in Tables 4.4, 4.5 and 4.6. In this case the results of Table 4.4 for mean value, standard deviation and variation coefficient derived from 1000 MCS are slightly higher than those from 10000 and 100000 simulations.

If the statistical values of Tables 4.1, 4.2 and 4.3 are compared to those of Tables 4.4, 4.5 and 4.6, one sees that the mean value generally remains constant and around 6% higher than the deterministic value, while the standard deviation and the skewness coefficient increase. This is due to the consideration of the cohesion as input variable, which introduces more uncertainty in the analysis.

The increase of the standard deviations results in higher COV values of the bearing capacity than those of benchmark 1. However the values are similar to those found in the literature.

In Figs. 4.6, 4.7 and 4.8 the relative frequency of the bearing capacity is again plotted pointwise together with the probability density function by assuming a shifted lognormal distribution as approximation.

μ_{q_f}	σ_{q_f}	COV_{q_f}	v_{q_f}
310.807 kN/m ²	130.135 kN/m ²	0.419	1.255

Table 4.4: Statistical values of q_f predicted by 1000 MCS with uncorrelated soil variables

μ_{q_f}	σ_{q_f}	COV_{q_f}	v_{q_f}
306.805 kN/m ²	123.367 kN/m ²	0.402	1.387

Table 4.5: Statistical values of q_f predicted by 10000 MCS with uncorrelated soil variables

μ_{q_f}	σ_{q_f}	COV_{q_f}	v_{q_f}
306.451 kN/m ²	122.807 kN/m ²	0.401	1.393

Table 4.6: Statistical values of q_f predicted by 100000 MCS with uncorrelated soil variables

Also for benchmark 2 this distribution matches the MCS results well for all the three cases and the chi-square test for the goodness of fit shows that the shifted lognormal distribution is accurate at around 5% significance level.

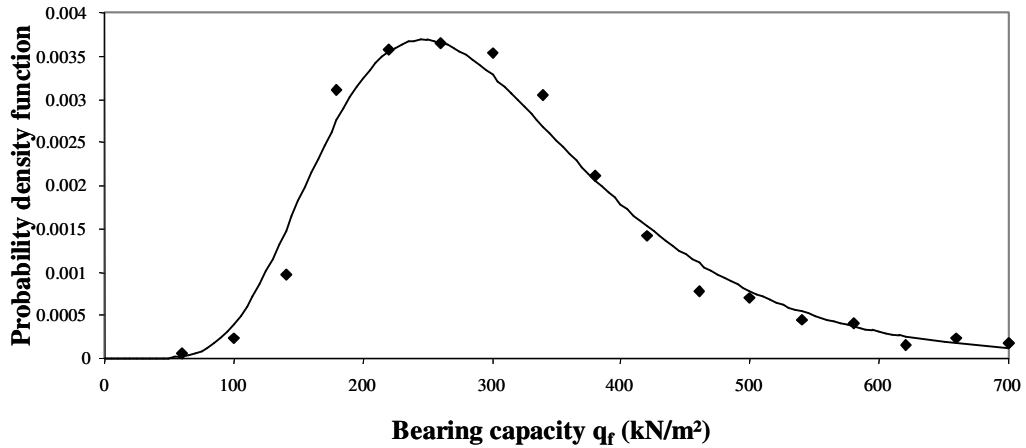


Figure 4.6: Shifted lognormal fit and relative frequency (pointwise) of q_f for 1000 MCS with uncorrelated soil variables

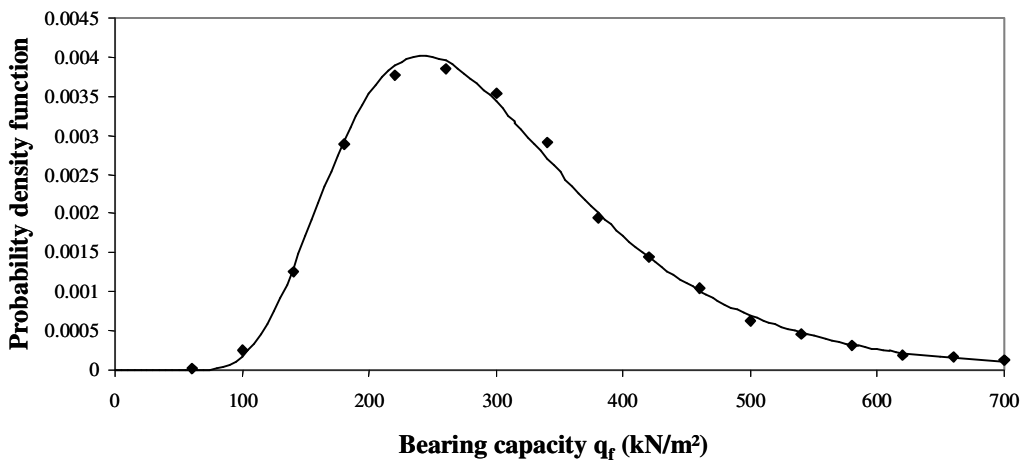


Figure 4.7: Shifted lognormal fit and relative frequency (pointwise) of q_f for 10000 MCS with uncorrelated soil variables

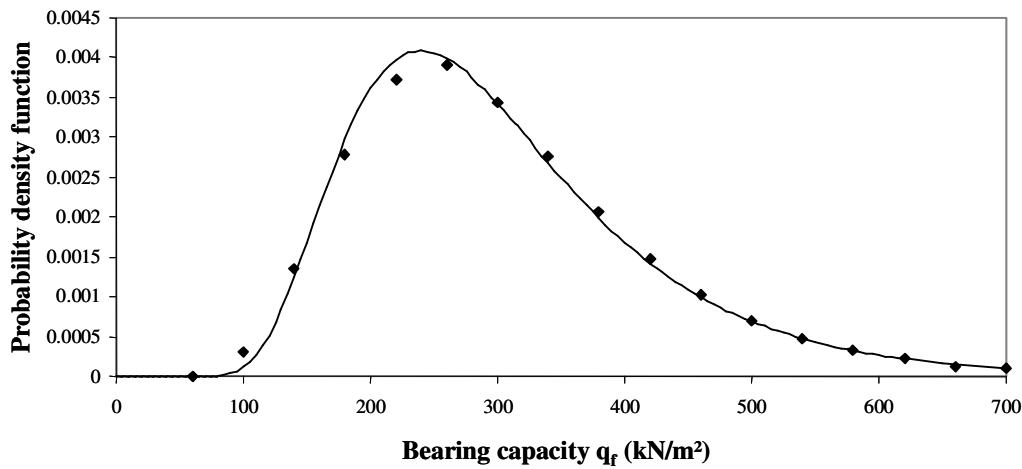


Figure 4.8: Shifted lognormal fit and relative frequency (pointwise) of q_f for 100000 MCS with uncorrelated soil variable

4.2.3 Monte Carlo results for benchmark 2 with correlated soil parameters

Soil properties are generally modelled as spatially perfectly correlated random variables and the results could be therefore uncertain. To perform a proper analysis involving spatially correlated random variables, it is necessary to generate random numbers which will simulate the correlation structure of soil properties. For this reason the effective soil parameters will now be considered as correlated variables. The results in Tables 4.7, 4.8 and 4.9 refer to a correlation coefficient $\rho_{c \tan \varphi} = -0.6$, because this is a most realistic value, as suggested in the literature and as discussed in chapter 2.

The formula of KENNEY and KEEPING (1951, p. 202) for the correlation coefficient is applied to generate thousands of correlated input variables for MCS.

The MCS results are reported in Tables 4.7, 4.8 and 4.9. For this case the statistical values derived from 1000 MCS are slightly lower than those from 10000 and 100000 simulations.

Comparing the statistical values of Tables 4.7, 4.8 and 4.9 to those of Tables 4.4, 4.5 and 4.6, one sees that all the statistical values decrease when a negative correlation of -0.6 is considered. More specifically the mean value changes slightly and is around 3.5% higher than the deterministic value, but the standard deviation decreases significantly, being around 35% lower than the value found considering uncorrelated parameters.

As a consequence the skewness and the variation coefficients also decrease. Thus the variability of the bearing capacity and the uncertainty in the analysis decrease considerably.

The frequency diagrams of Figs. 4.9, 4.10, 4.11 and the shifted lognormal fits show that these plots become narrower and the corresponding peak values consequently higher than those of the case with uncorrelated soil parameters. This difference can be seen better in Fig. 4.12, where the probability density function of q_f from 10000 MCS for soil parameters having no correlation and a value of $\rho_{c', \tan\phi'} = -0.6$ are plotted together. For uncorrelated variables the density function is wider and the peak value is 0.0043, whereas for negatively correlated variables the curve is narrower reaching a peak value of 0.0062.

μ_{q_f}	σ_{q_f}	COV_{q_f}	v_{q_f}
294.288 kN/m ²	72.011 kN/m ²	0.245	1.115

Table 4.7: Statistical values of q_f predicted by 1000 MCS with negatively correlated variables

μ_{q_f}	σ_{q_f}	COV_{q_f}	v_{q_f}
297.848 kN/m ²	73.372 kN/m ²	0.246	0.911

Table 4.8: Statistical values of q_f predicted by 10000 MCS with negatively correlated variables

μ_{q_f}	σ_{q_f}	COV_{q_f}	v_{q_f}
297.327 kN/m ²	73.795 kN/m ²	0.248	0.952

Table 4.9: Statistical values of q_f predicted by 100000 MCS with negatively correlated variables

It is also clear that the variability of the bearing capacity considering correlated soil parameters decreases, starting from a value of around 120 kN/m² for non-zero probabilities compared to a value of around 80 kN/m², for the case with uncorrelated variables.

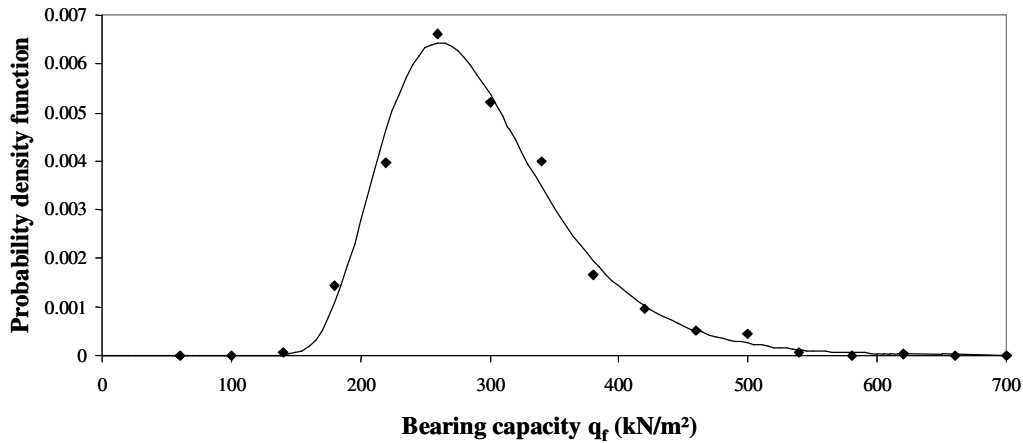


Figure 4.9: Shifted lognormal fit and relative frequency (pointwise) of q_f for 1000 MCS with negatively correlated variables

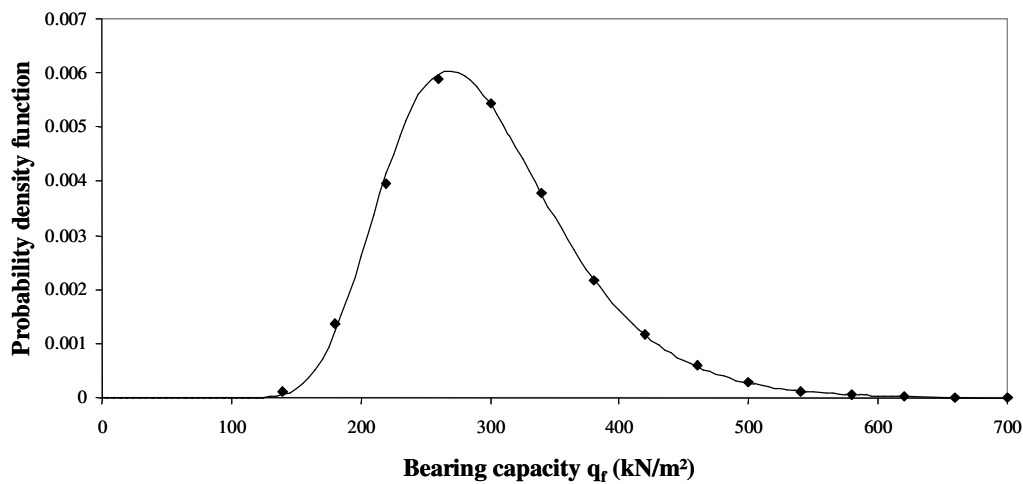


Figure 4.10: Shifted lognormal fit and relative frequency (pointwise) of q_f for 10000 MCS with negatively correlated variables

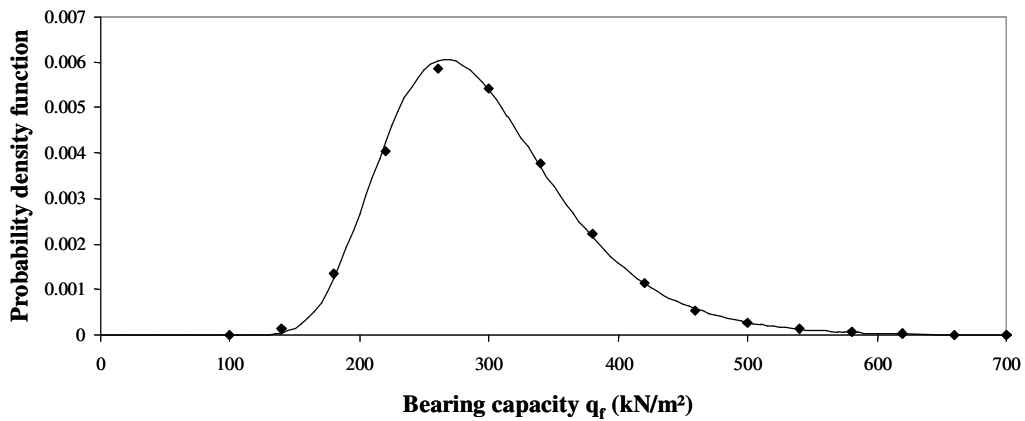


Figure 4.11: Shifted lognormal fit and relative frequency (pointwise) of q_f for 100000 MCS with negatively correlated variables

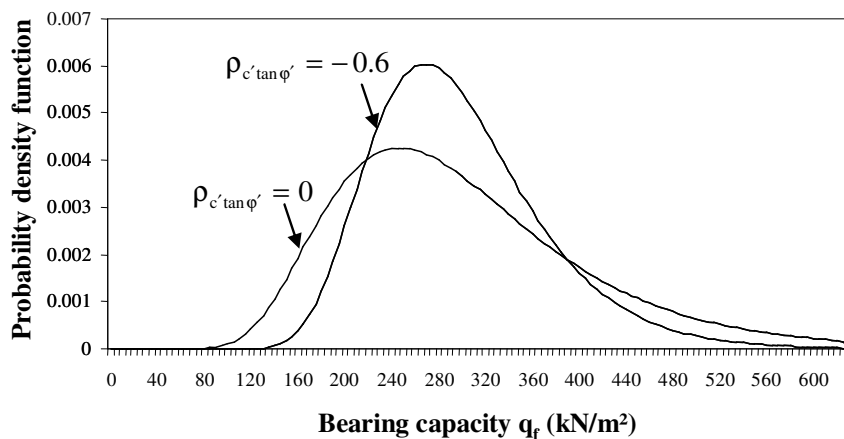


Figure 4.12: Comparison of shifted lognormal fits of q_f from 10000 MCS for uncorrelated and negatively correlated soil variables

In Table 4.10 the statistical values of the bearing capacity are listed for different correlation coefficients from -0.9 to 0.0 . Because of some limitations in the KENNEY and KEEPING's formula, the value $\rho_{c'tan\phi'} = -1.0$ can not be taken into account.

By decreasing the correlation coefficient, the mean value changes slightly. Whereas the standard deviation decreases significantly, from around 123.4 kN/m^2 when there is no correlation between soil parameters down to around 50.3 kN/m^2 , when $\rho_{c'tan\phi'} = -0.9$.

The skewness coefficient has a strange behaviour. In fact, when the correlation decreases from $\rho_{c'\tan\phi'} = 0$ down to the value $\rho_{c'\tan\phi'} = -0.5$, the skewness coefficient decreases too. If one proceed to reduce the correlation down to $\rho_{c'\tan\phi'} = -0.9$, then the skewness coefficient increases, reaching a maximum value of 2.244.

Fig. 4.13 shows the influence of the correlation coefficient variation on the shape of the shifted lognormal fit of the bearing capacity. As already pointed out in Fig. 4.12, the curves become narrower for lower correlation coefficients, thus decreasing the variability of the bearing capacity and increasing the peak of the fit. It is also clear how the skewness coefficient changes the shape of the curves from the least skewed curve for $\rho_{c'\tan\phi'} = -0.5$ to the most skewed one for $\rho_{c'\tan\phi'} = -0.9$.

Recapitulating all these observations, it is then possible to conclude that the choice of a negative correlation for the soil parameters is reasonable, because the uncertainty in the problem decreases considerably.

Notwithstanding the accuracy of MCS results, this method is too time consuming for practical computations, therefore alternative methods need to be considered. In next sections the FOSM and SOSM methods are applied to the same bearing capacity benchmark.

$\rho_{c'\tan\phi'}$	μ_{q_f} (kN/m ²)	σ_{q_f} (kN/m ²)	v_{q_f}
-0.9	294.635	50.321	2.244
-0.8	295.616	57.661	1.462
-0.7	296.734	65.774	1.057
-0.6	297.848	73.372	0.911
-0.5	299.071	81.274	0.877
-0.4	300.305	88.902	0.932
-0.3	301.448	95.729	1.004
-0.2	302.709	103.054	1.100
-0.1	303.986	110.295	1.206
0.0	306.805	123.367	1.387

Table 4.10: Influence of $\rho_{c'\tan\phi'}$ on the statistical values of q_f from MCS

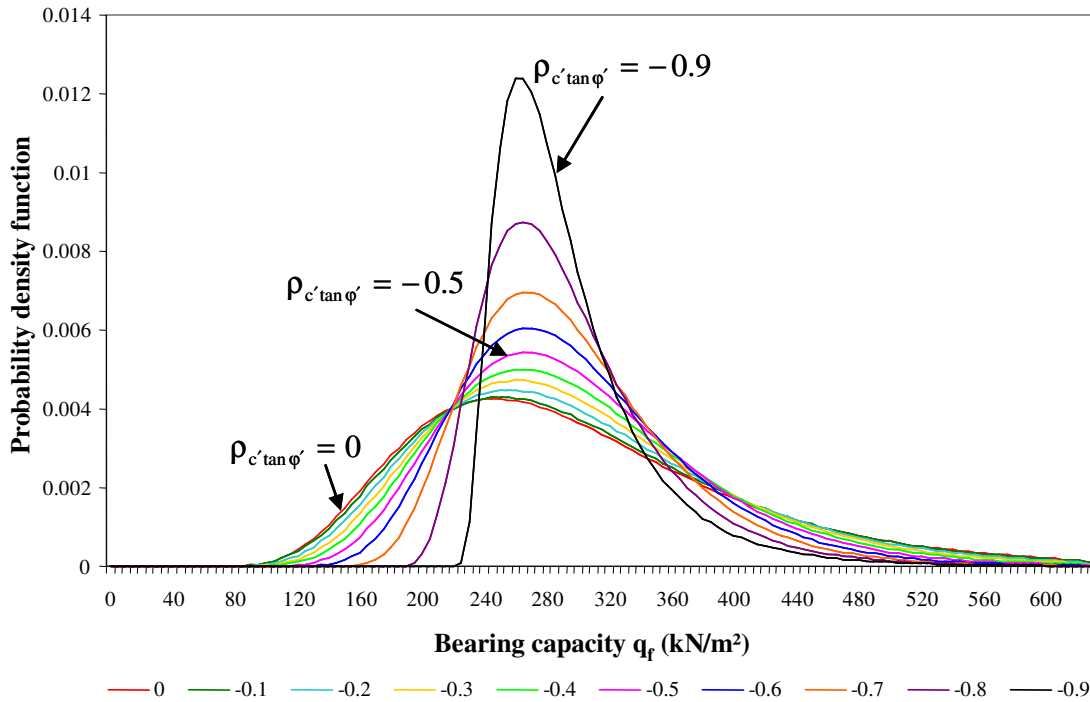


Figure 4.13: Influence of the correlation coefficient variation on the shifted lognormal fit of q_f for 10000 MCS

4.3 Application of the FOSM method

It was highlighted in chapter 2 that the simplest alternative to MCS is the FOSM method, which produces a linearisation around the mean value of the input soil variables. The next sections will show the results of FOSM application to the benchmarks already considered.

4.3.1 FOSM results for benchmark 1

Considering Terzaghi's bearing capacity formula (A.4) in appendix A as a function of $\tan\phi'$, the Taylor's series expansion for the bearing capacity about the mean value $\mu_{\tan\phi'}$ truncated after the first order terms is given by

$$q_f \approx q_f(\mu_{\tan\phi'}) + (\tan\phi' - \mu_{\tan\phi'}) \cdot \frac{\partial q_f}{\partial \tan\phi'} \quad (4.2)$$

where the first term is determined by substituting the mean value of $\tan\phi'$, while the derivative of the second term is evaluated at $\mu_{\tan\phi'}$. The mean value and the variance of the bearing capacity are obtained using formulas (4.3) and (4.4)

$$\mu_{q_f(\tan\phi')} = q_f(\tan\phi' = \mu_{\tan\phi'}) \quad (4.3)$$

$$\text{Var}(q_f) = \text{Var}(\tan\phi') \cdot \left(\frac{\partial q_f}{\partial \tan\phi'} \right)^2. \quad (4.4)$$

Now considering Eqs. (A.5) for the bearing capacity factors N_q , N_c , N_γ in appendix A, together with the following trigonometric relation

$$\tan\left(\frac{\pi}{4} + \frac{\phi'}{2}\right) = \left[\tan\phi' + (1 + \tan^2\phi')^{1/2} \right] \quad (4.5)$$

and substituting them in Eq. (A.4), the bearing capacity formula is then given as

$$q_f = \frac{c'}{\tan\phi'} \cdot \left\{ e^{\pi \cdot \tan\phi'} \cdot \left[\tan\phi' + (1 + \tan^2\phi')^{1/2} \right]^2 - 1 \right\} + q_0 \cdot e^{\pi \cdot \tan\phi'} \cdot \left[\tan\phi' + (1 + \tan^2\phi')^{1/2} \right]^2 + 1.5 \cdot \gamma \cdot \tan\phi' \cdot \left\{ e^{\pi \cdot \tan\phi'} \cdot \left[\tan\phi' + (1 + \tan^2\phi')^{1/2} \right]^2 - 1 \right\} \quad (4.6)$$

Substituting the deterministic value of the unit weight 15 kN/m^3 , the surcharge 10 kN/m^2 , the cohesion 4 kN/m^2 and $\mu_{\tan\phi'} = 0.466$ into Eq. (4.3), it is possible to estimate the bearing capacity mean value, which is $\mu_{q_f} = 290.878 \text{ kN/m}^2$.

The first derivative of the bearing capacity computed analytically with respect to $\tan\phi'$ is given by Eq. (B.2) in appendix B. Substituting again the numerical values of the unit weight, surcharge, cohesion and mean value of $\tan\phi'$ one obtains

$$\frac{\partial q_f}{\partial \tan\phi'} = 1548.592 \text{ kN/m}^2.$$

It is now possible to evaluate the variance and the standard deviation of the bearing capacity using Eq. (4.4), hence

$$\text{Var}(q_f) = 8812.638 \text{ (kN/m}^2\text{)}^2$$

$$\sigma_{q_f} = 93.876 \text{ kN/m}^2.$$

In Table 4.11 the results of the bearing capacity predicted using FOSM method are presented. The estimated mean value is in good agreement with the deterministic one. As for MCS, the coefficient of variation is within the range found in the literature for the bearing capacity (PHOON and KULHAWY, 1999; POPESCU, 2004), being $\text{COV}_{q_f} = 0.323$.

It is important to remember that FOSM method does not provide any skewness coefficient. For this reason no information about the shape of the probability density function of the bearing capacity is given. Thus, in order to estimate any probability, a standard lognormal distribution is assumed as an approximation, which leads to the probability density function shown in Fig. 4.14. A shifted lognormal distribution can not be assumed because the skewness coefficient is unknown and Eq. (2.18) can not be solved.

Using formula (4.1) valid for a standard lognormal distribution, the skewness coefficient of the bearing capacity can be determined, thus leading to

$$v_{q_f} = 1.003.$$

It should be pointed out that the bearing capacity does not vary linearly, but exponentially with $\tan\phi'$. The FOSM procedure only considers linear functions, then uncertainty is introduced in the bearing capacity calculations, giving less accurate results than MCS. This fact will be seen in section 4.5.

μ_{q_f}	σ_{q_f}	COV_{q_f}
290.878 kN/m ²	93.876 kN/m ²	0.323

Table 4.11: Statistical values of q_f predicted by FOSM method for benchmark 1

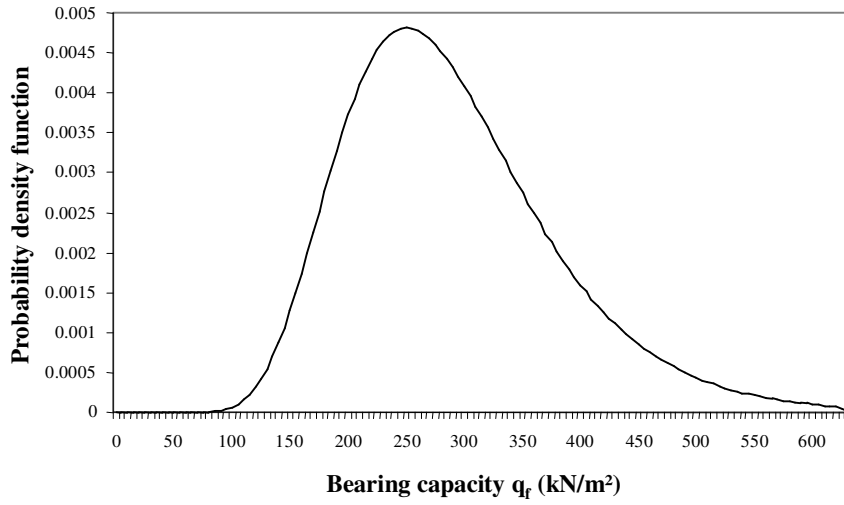


Figure 4.14: Standard lognormal distribution of q_f from FOSM method for benchmark 1

4.3.2 FOSM results for benchmark 2 with uncorrelated soil parameters

Considering now the bearing capacity as a function of both soil parameters $\tan\phi'$ and cohesion, the Taylor's series expansion for the bearing capacity about the mean values $\mu_{\tan\phi'}$ and $\mu_{c'}$, truncated after the first order terms, is given by

$$q_f = q_f(\mu_{\tan\phi'}, \mu_{c'}) + (\tan\phi' - \mu_{\tan\phi'}) \cdot \frac{\partial q_f}{\partial \tan\phi'} + (c' - \mu_{c'}) \cdot \frac{\partial q_f}{\partial c'} \quad (4.7)$$

where the derivatives are evaluated at the mean values $\mu_{\tan\phi'}$ and $\mu_{c'}$. The mean value and variance of the bearing capacity are obtained using formulas (4.8) and (4.9)

$$\mu_{q_f(\tan\phi', c')} = q_f(\tan\phi' = \mu_{\tan\phi'}, c' = \mu_{c'}) \quad (4.8)$$

$$\text{Var}(q_f) = \text{Var}(\tan\phi') \cdot \left(\frac{\partial q_f}{\partial \tan\phi'} \right)^2 + \text{Var}(c') \cdot \left(\frac{\partial q_f}{\partial c'} \right)^2 \quad (4.9)$$

Considering again the trigonometric relation (4.5) and Eq. (A.4) and substituting the mean value of cohesion and $\tan\phi'$, the expected bearing capacity value is $\mu_{q_f} = 290.878 \text{ kN/m}^2$.

The first derivatives of the bearing capacity computed analytically with respect to the soil parameters are given by Eqs. (B.1) and (B.2) of appendix B. Substituting the numerical values for the mean value of the cohesion and friction angle, one obtains

$$\frac{\partial q_f}{\partial c'} = 20.720 \text{ kN/m}^2$$

$$\frac{\partial q_f}{\partial \tan \phi'} = 1548.592 \text{ kN/m}^2.$$

Hence the variance and the standard deviation estimated using Eq. (4.4) will be

$$\text{Var}(q_f) = 13209.084 \text{ (kN/m}^2\text{)}^2$$

$$\sigma_{q_f} = 114.931 \text{ kN/m}^2.$$

Table 4.12 shows the statistical values of the bearing capacity for uncorrelated soil parameters. The mean value is exactly the same of benchmark 1 because in both cases the numerical value of the soil parameters are unchanged. The standard deviation and, consequently, the COV_{q_f} are increased.

μ_{q_f}	σ_{q_f}	COV_{q_f}
290.878 kN/m ²	114.931 kN/m ²	0.395

Table 4.12: Statistical values of q_f from FOSM method for benchmark 2 with uncorrelated soil variables

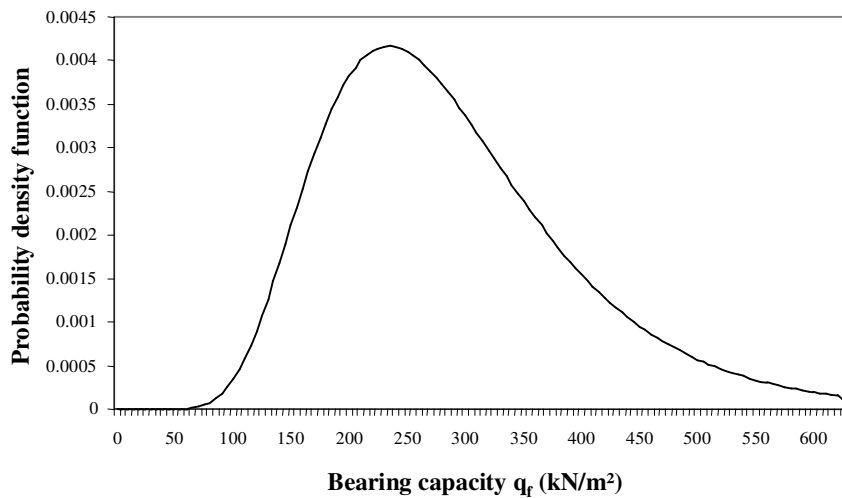


Figure 4.15: Standard lognormal distribution of q_f from FOSM method for benchmark 2 with uncorrelated soil variables

This is because the consideration of the cohesion as an additional input variable introduces more uncertainty in the analysis. Again the value of COV_{q_f} is within the range of values reported in the literature for the bearing capacity.

In Fig. 4.15 the assumed standard lognormal distribution is plotted for the bearing capacity results of Table 4.12. Due to the higher standard deviation, the curve presents a slightly lower peak when compared to the first benchmark (from 0.0048 down to 0.0043), and a slightly higher bearing capacity variability.

Using formula (4.1), one can evaluate the skewness coefficient corresponding to the results in Table 4.12, thus finding $v_{q_f} \approx 1.247$. This value is higher than that found for benchmark 1, because of the increase of the variation coefficient.

4.3.3 FOSM results for benchmark 2 with correlated soil parameters

If the input soil variables $\tan\phi'$ and c' are correlated, then the variance formula (3.3) will be applied taking into account also the last term, which includes the covariance.

Considering a correlation coefficient of $\rho_{c'\tan\phi'} = -0.6$, then the resulting statistical values of the bearing capacity will be those presented in Table 4.13. When compared to benchmark 1, the mean value does not change, instead the standard deviation decreases significantly, thus reducing also the COV_{q_f} .

μ_{q_f}	σ_{q_f}	COV_{q_f}
290.878 kN/m ²	75.761 kN/m ²	0.26

Table 4.13: Statistical values of q_f from FOSM method for benchmark 2 with correlated soil variables

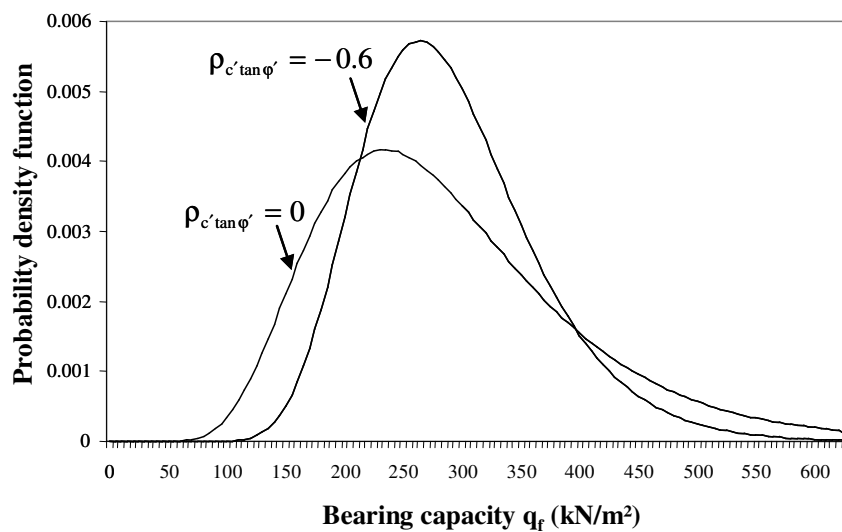


Figure 4.16: Comparison of probability density functions of q_f from FOSM method for benchmark 2 with $\rho_{c'tan\phi'} = 0$ and $\rho_{c'tan\phi'} = -0.6$

Assuming a standard lognormal distribution for approximating the FOSM results, as previously done, it is possible to plot the probability density function of q_f considering both uncorrelated and negatively correlated soil parameters. Benjamin and Cornell's formula (4.1) estimates a value of 0.798 for the skewness coefficient when $\rho_{c'tan\phi'} = -0.6$, which is significantly lower than the uncorrelated case.

In Fig. 4.16 the curve obtained by considering uncorrelated soil variables is wider, having a lower probability peak of ca. 0.0042. Whereas the curve for the case with $\rho_{c'tan\phi'} = -0.6$ has a peak of ca. 0.0057 and a narrower shape, thus giving lower bearing capacity variability and decreasing the uncertainty.

Varying the correlation coefficient from 0 to -1.0 , the standard deviation of q_f decreases down to around 76% for $\rho_{c', \tan\phi'} = -1.0$, as shown in Table 4.14, while the mean value is always constant and equal to 290.878 kN/m².

If the standard lognormal distribution would be assumed to draw the probability density curves of the bearing capacity results of Table 4.14, then the same conclusions of Fig. 4.13 about the shape of the curves and the variability of the bearing capacity with the correlation between the input soil parameters would come out.

Summarizing all these observations it seems to be very important for probabilistic analysis to include a negative correlation between cohesion and friction angle in order to have less uncertainty in the final results.

$\rho_{c', \tan\phi'}$	σ_{q_f} (kN/m ²)
-1.0	27.570
-0.9	44.777
-0.8	57.008
-0.7	67.043
-0.6	75.761
-0.5	83.574
-0.4	90.717
-0.3	97.336
-0.2	103.534
-0.1	109.381
0.0	114.931

Table 4.14: Influence of $\rho_{c', \tan\phi'}$ on the standard deviation of q_f from FOSM method for benchmark 2 with uncorrelated and negatively correlated soil variables

4.4 Application of the SOSM method

FOSM method can be slightly extended for a better prediction of the bearing capacity mean value through the SOSM method. Results of this approach will be illustrated in the next section and compared to those of Monte Carlo and FOSM methods.

4.4.1 SOSM results for benchmark 1

Second order terms of Taylor's series expansion of the bearing capacity will be now added to Eq. (4.3). In this way it is possible to refine the estimate of the bearing capacity mean value, leading to

$$\mu_{q_f} = q_f(\mu_{\tan\phi'}) + (\tan\phi' - \mu_{\tan\phi'}) \cdot \frac{\partial q_f}{\partial \tan\phi'} + \frac{1}{2} \cdot \text{Var}(\tan\phi') \cdot \frac{\partial^2 q_f}{\partial \tan^2 \phi'} \quad (4.10)$$

where the derivatives, given by Eqs. (B.1) and (B.4) of appendix B, are evaluated at $\mu_{\tan\phi'}$. Substituting the numerical values for unit weight, surcharge, cohesion and the mean value of $\tan\phi'$, the first derivative of the bearing capacity is the same as for FOSM method in section 4.3.1, while the second derivative is given by

$$\frac{\partial^2 q_f}{\partial \tan^2 \phi'} = 7060.685 \text{ kN/m}^2.$$

Then the bearing capacity mean value, given by Eq. (4.10), will be $\mu_{q_f} = 303.851 \text{ kN/m}^2$.

The statistical values of the bearing capacity derived from SOSM application are shown in Table 4.15. The mean value is around 5% higher than the deterministic value. Comparing these results to those of Table 4.11 for FOSM method, one sees that the second order terms have increased the mean value of the bearing capacity μ_{q_f} and thus reduced the COV_{q_f} value, while the standard deviation remains constant.

Assuming a standard lognormal distribution, the probability density function of the bearing capacity is plotted in Fig. 4.17. In this case the skewness coefficient, evaluated with formula (4.1), will be $v_{q_f} \approx 0.956$, which is slightly lower than the value found with FOSM method.

μ_{q_f}	σ_{q_f}	COV_{q_f}
303.851 kN/m ²	93.876 kN/m ²	0.309

Table 4.15: Statistical values of q_f from SOSM method for benchmark 1

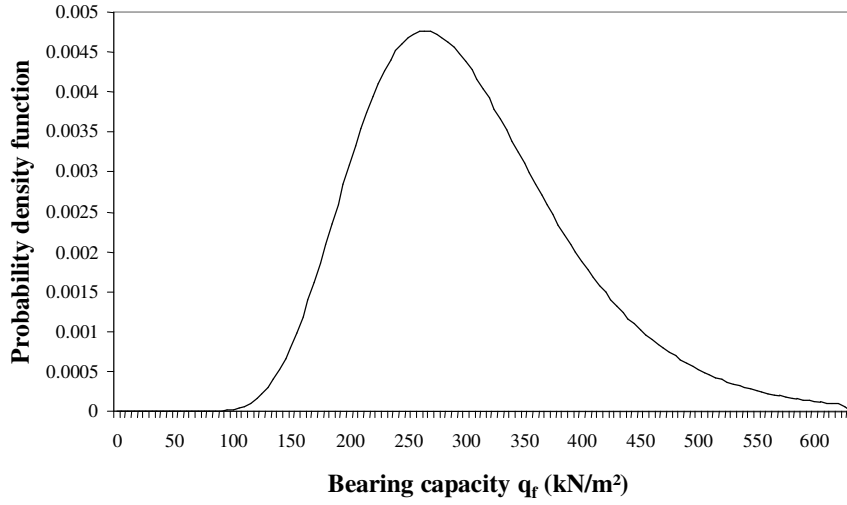


Figure 4.17: Standard lognormal distribution of q_f from SOSM method for benchmark 1

4.4.2 SOSM results for benchmark 2 with uncorrelated soil parameters

By considering the cohesion as input random variable, the mean value formula (4.3) of the bearing capacity will include second order terms of the Taylor's series expansion also for this soil parameter, thus leading to

$$\mu_{q_f} = q_f(\mu_{\tan\phi'}, \mu_{c'}) + (\tan\phi' - \mu_{\tan\phi'}) \cdot \frac{\partial q_f}{\partial \tan\phi'} + (c' - \mu_{c'}) \cdot \frac{\partial q_f}{\partial c'} + \frac{1}{2} \cdot \text{Var}(\tan\phi') \cdot \frac{\partial^2 q_f}{\partial \tan^2 \phi'} + \frac{1}{2} \cdot \text{Var}(c') \cdot \frac{\partial^2 q_f}{\partial c'^2} \quad (4.11)$$

where derivatives are evaluated at the mean values $\mu_{\tan\phi'}$ and $\mu_{c'}$. The first derivatives of the bearing capacity have the same values found for the FOSM method in section 4.3. While the second derivatives with respect to cohesion and $\tan\phi'$ are given by Eqs. (B.3) and (B.4). Substituting the mean values of cohesion and $\tan\phi'$, one obtains

$$\frac{\partial^2 q_f}{\partial \tan^2 \phi'} = 7060.685 \text{ kN/m}^2$$

$$\frac{\partial^2 q_f}{\partial c'^2} = 0 \text{ kN/m}^2.$$

Then the bearing capacity mean value, given by Eq. (4.11), will be $\mu_{q_f} = 303.851 \text{ kN/m}^2$. The corresponding statistical estimates of the bearing capacity are shown in Table 4.16.

Comparing these results to those of Table 4.12, one notes that the second order terms have increased the mean value μ_{q_f} , thus reducing COV_{q_f} value, while the standard deviation is still the same. These results are shown in Fig. 4.18 assuming a standard lognormal distribution as approximation. Using Benjamin and Cornell's formula (4.1), the skewness coefficient value is $v_{q_f} \approx 1.188$, which is slightly lower than the value found by FOSM method for uncorrelated input variables.

μ_{q_f}	σ_{q_f}	COV_{q_f}
303.851 kN/m ²	114.931 kN/m ²	0.378

Table 4.16: Statistical values of q_f from SOSM method for benchmark 2 with uncorrelated soil variables

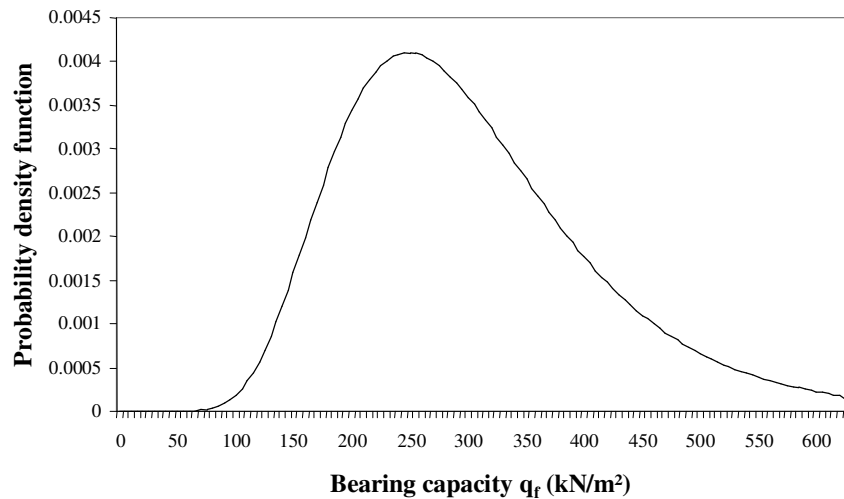


Figure 4.18: Standard lognormal distribution of q_f from SOSM method for benchmark 2 with uncorrelated soil variables

4.4.3 SOSM results for benchmark 2 with correlated soil parameters

Taking into account c' and $\tan\phi'$ as negatively correlated variables with $\rho_{c'\tan\phi'} = -0.6$, the mean value formula (3.4) for the bearing capacity will be applied considering also the last term which includes the covariance, leading to $\mu_{q_f} = 296.067 \text{ kN/m}^2$.

The standard deviation remains constant, as obtained by FOSM. The statistical values of the bearing capacity are presented in Table 4.17. Because of the lower mean value, the variation coefficient also decreases.

When a standard lognormal distribution is assumed to plot the results of Table 4.17, it is possible to evaluate the skewness coefficient by using Benjamin and Cornell's formula (4.1), thus obtaining a value of 0.785. This value is very similar to the estimate of FOSM method for the same benchmark, even if slightly lower.

Fig. 4.19 shows the comparison between probability density functions for uncorrelated and negatively correlated soil parameters. As for FOSM method, the curve for uncorrelated variables is wider having a lower probability peak, while the curve for the case with a negative correlation of -0.6 has a higher peak and a narrower shape with lower bearing capacity variability.

Varying the correlation coefficient from 0 to -1.0, the mean value of the bearing capacity will vary as shown in Table 4.18. On the other hand, the standard deviation values are the same of those presented in Table 4.14 from FOSM method. When compared with the FOSM results, a decrease of the correlation coefficient results in a reduction of both mean value and standard deviation of the bearing capacity. Additionally, as already seen for the FOSM application, a perfect negative correlation between cohesion and $\tan\phi'$ strongly influences the bearing capacity variability.

If again the standard lognormal distribution would be assumed to draw the probability density curves of the bearing capacity results of Table 4.18, then the same conclusions of Fig. 4.13 about the shape of the curves and the variability of the bearing capacity with the correlation between the soil variables would result.

μ_{q_f}	σ_{q_f}	COV_{q_f}
296.067 kN/m ²	75.761 kN/m ²	0.256

Table 4.17: Statistical values of q_f from SOSM method for benchmark 2 with correlated soil variables

Summing up all these observations, it would seem that SOSM method can refine the estimate of the bearing capacity mean value. However results show that the improvement is small and hardly worthwhile for the proposed benchmarks.

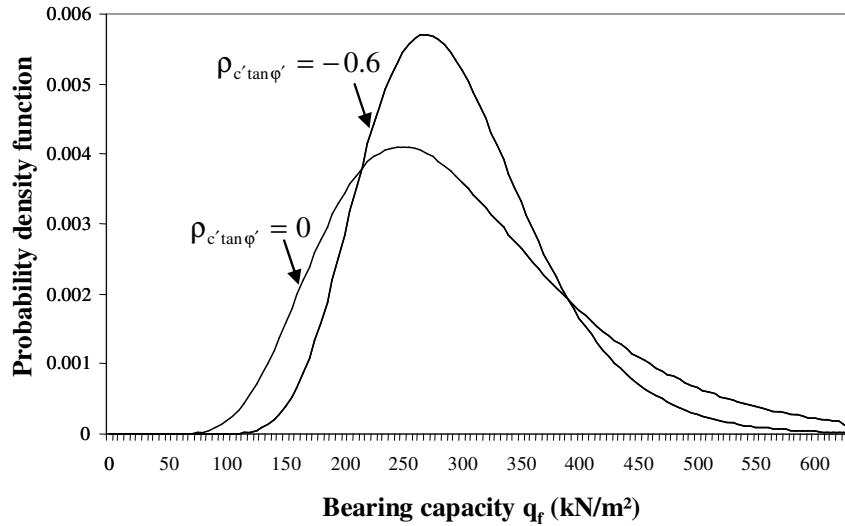


Figure 4.19: Comparison of probability density functions of q_f from SOSM method for benchmark 2 with $\rho_{c'tan\phi'} = 0$ and $\rho_{c'tan\phi'} = -0.6$

$\rho_{c'tan\phi'}$	μ_{q_f} (kN/m ²)	σ_{q_f} (kN/m ²)
-1.0	290.878	27.570
-0.9	292.175	44.777
-0.8	293.472	57.008
-0.7	294.770	67.043
-0.6	296.067	75.761
-0.5	297.364	83.574
-0.4	298.662	90.717
-0.3	299.959	97.336
-0.2	301.257	103.534
-0.1	302.554	109.381
0.0	303.851	114.931

Table 4.18: Influence of $\rho_{c'tan\phi'}$ on the statistical values of q_f from SOSM method for benchmark 2

4.5 Results comparison and necessity of an alternative method

The aim of this section is to compare the results of the probabilistic methods MCS, FOSM and SOSM applied to the benchmarks described in this chapter. At the end, the necessity of an alternative probabilistic approach, which could overcome the drawbacks of MCS, FOSM and SOSM methods, will be discussed.

4.5.1 Comparison of MCS, FOSM and SOSM results

The statistical values estimated using MCS, FOSM and SOSM methods for benchmark 1 and 2 are summarised in Tables 4.19, 4.20 and 4.21.

For both benchmarks, MCS results are similar to those evaluated by FOSM and SOSM methods. The mean value provided by SOSM method is closer to MCS estimate due to the introduction of second order terms in Eq. (3.4). However the standard deviation is exactly the same as that found by FOSM method.

It is very important to remember that the FOSM and SOSM methods do not provide any skewness coefficient value. The fictitious skewness coefficients depending on the assumption of a standard lognormal distribution for approximating FOSM and SOSM results are listed in Tables 4.19, 4.20 and 4.21. If another type of density function were to be assumed then the skewness coefficients would change. However it seems that these values are very similar to those of MCS, especially for the first benchmark. A larger difference in the skewness coefficients is evident when a correlation of $\rho_{c'\tan\phi'} = -0.6$ is taken into account.

Method	μ_{q_f}	σ_{q_f}	COV_{q_f}	v_{q_f}
MCS	306.562 kN/m ²	102.242 kN/m ²	0.333	1.008
FOSM	290.878 kN/m ²	93.876 kN/m ²	0.323	1.003*
SOSM	303.851 kN/m ²	93.876 kN/m ²	0.309	0.956*

* value found with BENJAMIN and CORNELL's formula (1970) for a standard lognormal distribution

Table 4.19: Comparison of statistical values of q_f found using MCS, FOSM and SOSM methods for benchmark 1

4.5 Results comparison and necessity of an alternative probabilistic method

Method				
MCS	306.805 kN/m ²	123.367 kN/m ²	0.402	1.387
FOSM	290.878 kN/m ²	114.931 kN/m ²	0.395	1.247*
SOSM	303.851 kN/m ²	114.931 kN/m ²	0.378	1.188*

* value found with BENJAMIN and CORNELL's formula (1970) for a standard lognormal distribution

Table 4.20: Comparison of statistical values of q_f found using of MCS, FOSM and SOSM methods for benchmark 2 with uncorrelated soil parameters ($\rho_{c \tan \phi} = 0$)

Method				
MCS	297.848 kN/m ²	73.372 kN/m ²	0.246	0.911
FOSM	290.878 kN/m ²	75.761 kN/m ²	0.26	0.798*
SOSM	296.067 kN/m ²	75.761 kN/m ²	0.256	0.785*

* value found with BENJAMIN and CORNELL's formula (1970) for a standard lognormal distribution

Table 4.21: Comparison of statistical values of q_f found using MCS, FOSM and SOSM methods for benchmark 2 with negatively correlated parameters ($\rho_{c \tan \phi} = -0.6$)

Figs. 4.20, 4.21 and 4.22 show the Monte Carlo results plotted pointwise together with the standard lognormal distribution approximations for FOSM and SOSM methods.

For benchmark 1 and 2 with uncorrelated variables, the FOSM probability density function is shifted more to the left than MCS points and SOSM curve. Hence there is a better agreement between the SOSM curve and the MCS results, as Figs. 4.20 and 4.21 demonstrate. In any case FOSM and SOSM curves have a higher probability peak when compared with the MCS one. This is because their standard deviations are lower.

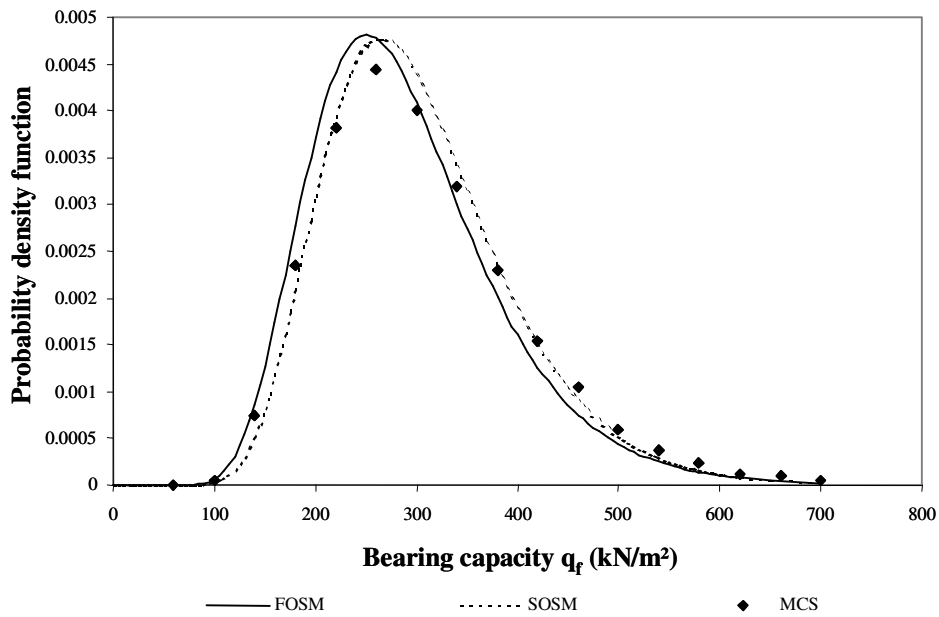


Figure 4.20: Comparison of MCS, FOSM and SOSM results in terms of probability distribution for benchmark 1

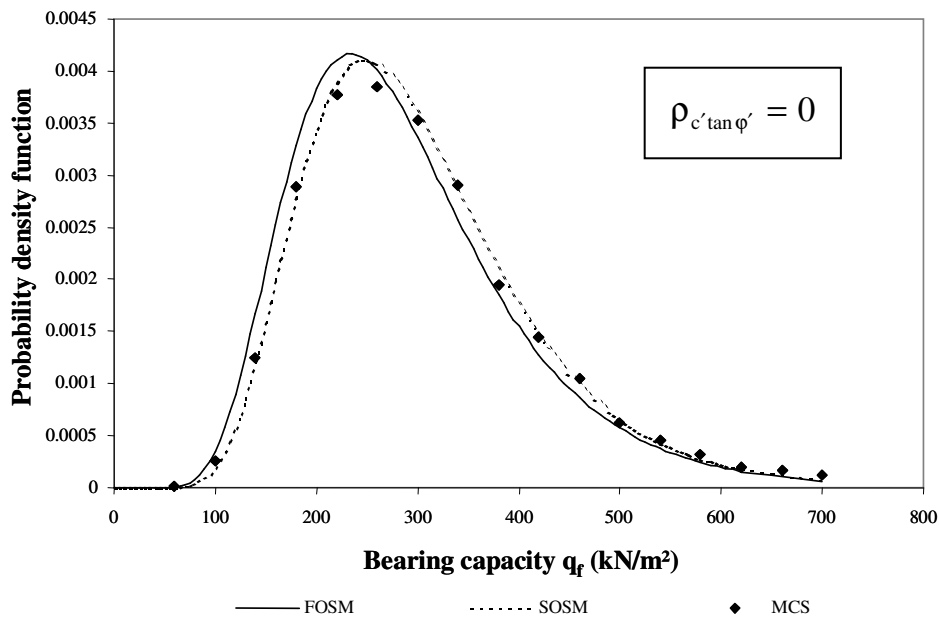


Figure 4.21: Comparison of MCS, FOSM and SOSM results in terms of probability distribution for benchmark 2 considering uncorrelated soil variables.

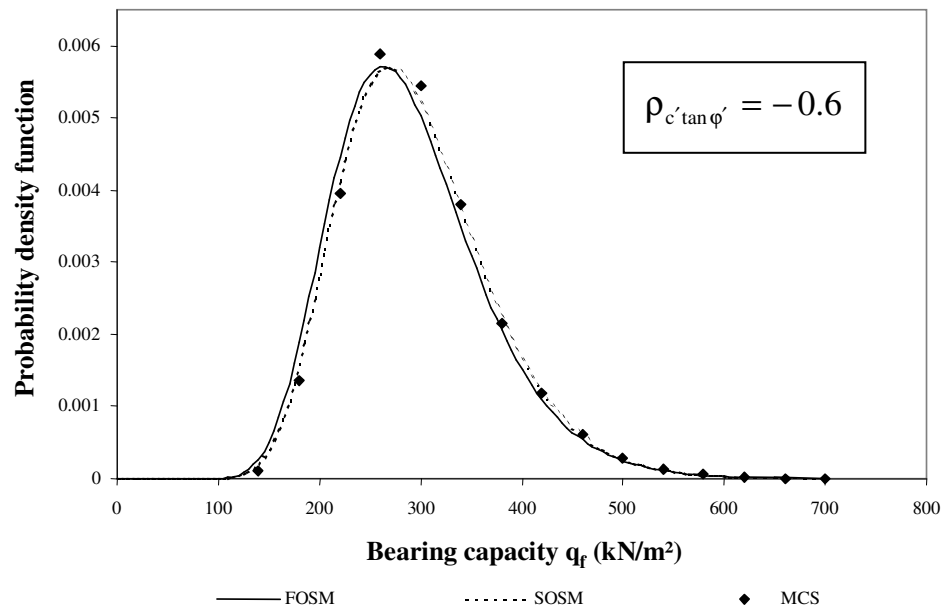


Figure 4.22: Comparison of MCS, FOSM and SOSM results in terms of probability distribution for benchmark 2 considering correlated soil variables

The opposite happens for benchmark 2 with negatively correlated parameters, where MCS probability peak is higher than FOSM and SOSM values, as Fig. 4.22 illustrates. This is due to the lower value of the MCS standard deviation.

In Fig. 4.22 the perfect matching of the FOSM and SOSM curves can be seen. In addition they are in good agreement with MCS results.

Having compared the results of the MCS, FOSM and SOSM methods, it can be concluded that similar results are found for the mean value and the standard deviation. On the other hand no skewness coefficient is provided by the FOSM and SOSM methods. Thus, it is not possible to guess the shape of the probability density function of the bearing capacity, as for the Monte Carlo method. A standard lognormal distribution has been assumed to approximate the final results. So doing, a satisfactory agreement between the curves of FOSM and SOSM methods and the MCS results has been observed.

4.5.2 Necessity of an alternative probabilistic method

It was seen in chapter 3 that the Monte Carlo approach is the most reliable technique between other well-known probabilistic methods, because not only mean value, standard deviation and skewness coefficient of a performance function can be estimated, but also the corresponding probability density function can be identified. However, as already seen in chapter 3, for geotechnical problems without an analytical solution, additional special programming for the MCS would be needed. Furthermore, to obtain a high accuracy, a large number of simulations are involved. Thus, in practice, this method requires a very high computational effort.

FOSM and SOSM methods were then chosen as alternative probabilistic approaches to replace MCS, both of which require only a limited amount of calculations. However these methods are accurate only for linear functions. The accuracy diminishes as the non-linearity of a function increases. In fact in this chapter it has been pointed out that the bearing capacity varies exponentially with $\tan\phi'$. Thus, using FOSM and SOSM methods for a probabilistic analysis of the bearing capacity problem, uncertainty is introduced in the calculations, giving less accurate results than MCS.

It has been observed that the SOSM method seems to refine the estimate of the bearing capacity mean value found by the FOSM method. However results show that the improvement is small and hardly worthwhile for the proposed benchmarks.

In addition these approaches require the computation and evaluation of partial derivatives. This could be exceedingly difficult or impossible for many problems, such as when relationships are only in the form of charts or graphics or for solutions involving finite element methods. Furthermore no skewness coefficient is provided by both these methods. For this reason no information about the shape of the probability density function of the output is given. It has to be assumed, thus introducing a source of inaccuracy.

Hence it is necessary to take into account another alternative, which can overcome the drawbacks of MCS, FOSM and SOSM methods, providing a skewness coefficient value together with the other statistical estimates, but with less computational effort.

In chapter 5 the Two Point Estimate Method (PEM) will be chosen as alternative approach to be applied to the bearing capacity benchmarks. The results will be then presented and compared to those of the MCS, FOSM and SOSM methods.

Although the PEM does not provide a full distribution of the output variable, as Monte Carlo does, it will show to be a simple but powerful technique for

4.5 Results comparison and necessity of an alternative probabilistic method

probabilistic analyses, as it requires less computational effort than MCS for a comparable degree of accuracy.

Moreover the PEM will provide not only mean value and standard deviation, but also the skewness coefficient of the bearing capacity, giving then more accurate results than FOSM and SOSM methods, with little or no increase in computational effort and without evaluation of partial derivatives.

In chapter 6 the PEM will be applied for the evaluation of the failure probability of the bearing capacity problem. It will be shown that also this method has some limitations, as already mentioned in chapter 3.

However, despite its limitations, the PEM will proof to be a more attractive method than MCS, from a computational point of view, and than FOSM and SOSM approaches, as it will overcome their drawbacks.

Chapter 5

The Two Point Estimate method applied to the bearing capacity problem

Introduction

It has been shown in chapter 3 that various probabilistic methods exist to quantify uncertainty. The most common are Monte Carlo simulations and the moments methods FOSM and SOSM. However these approaches present important shortcomings, as described in chapter 3 and demonstrated in chapter 4. These difficulties can be overcome, with some limitations, using the Two Point Estimate Method after ROSENBLUETH (1975, 1981), described in chapter 3.

In the present chapter, the PEM is applied to the bearing capacity problem. The PEM results are then compared with those of the MCS, FOSM and SOSM methods.

5.1 PEM results for benchmark 1

In order to assess the bearing capacity statistical values related to the first benchmark, illustrated in chapter 4, the Two Point Estimate method after ROSENBLUETH (1975) is applied. The procedure for implementing the PEM and the corresponding calculations are described step by step in next section.

5.1.1 Procedure of the PEM

1. The relationship (4.6) between the dependent variable q_f and the single random variable $\tan\phi'$ is considered.
2. The two sampling point locations for $\tan\phi'$, which is normally distributed ($v_{\tan\phi'} = 0$), have to be computed. First of all, the standard deviation units, giving locations of the sampling points to the right and to the left of the mean value, are evaluated using Eqs. (3.6), thus giving

$$\xi_{\tan \phi'_+} = \xi_{\tan \phi'_-} = 1 .$$

Then the corresponding sampling point locations can be found by using Eqs. (3.7), thus obtaining

$$\begin{aligned} \tan \phi'_- &= 0.406 \\ \tan \phi'_+ &= 0.527 . \end{aligned}$$

Figure 5.1 shows the sampling points located at $\tan \phi'_-$ and $\tan \phi'_+$.

3. Then the weights P_i are determined. In this case there is only one input variable, for this reason no correlation coefficient is considered in the weights formula. For $\tan \phi'$ the weights are simply given by formula (3.8) and, because of the symmetry of the normal distribution, they will have the same value, i.e.:

$$P_{\tan \phi'_+} = P_{\tan \phi'_-} = 0.5 .$$

4. The values of the bearing capacity are then evaluated at both sampling point locations of $\tan \phi'$. The results are shown in Table 5.1.

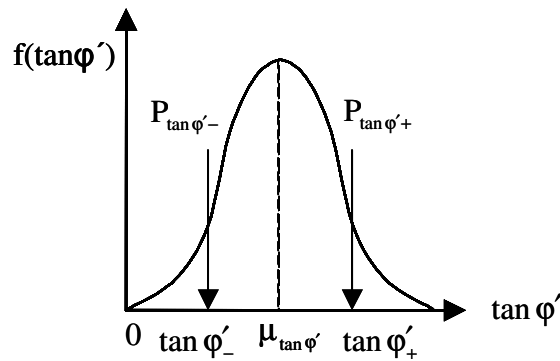


Figure 5.1: Sampling point locations and weights for $\tan \phi'$

P_{\pm}	$\tan \phi'_{\pm}$	$q_{f\pm}$
0.5	0.406	209.619 kN/m ²
0.5	0.527	403.953 kN/m ²

Table 5.1: Weights and sampling points of $\tan \phi'$ and bearing capacity values for PEM

5. Now the first three moments of the bearing capacity can be evaluated using Eqs. (3.15), (3.16) and (3.17), where $n = 1$.

The results of the bearing capacity predicted by PEM are presented in Table 5.2. From this table, it can be seen that the mean value is 6.2% higher than the deterministic value (i.e. 287.6 kN/m²). In addition the skewness coefficient is nil, thus suggesting a symmetric probability density function for the bearing capacity.

However, for a better definition of the shape of the bearing capacity distribution more sampling points would be needed.

Assuming both a standard lognormal and a normal distribution, as suggested by the skewness value in Table 5.2, the shape of the bearing capacity distribution can be plotted for both cases obtaining the curves in Fig. 5.2.

In the literature (e.g. ANG and TANG, 1975; FENTON, 2006) it is frequently reported that, for values of the variation coefficient lower than 30%, there is not much difference between the shape of a normal and a lognormal distribution. On the other hand, when the COV is higher than 30%, then a discrepancy exists between the shape of these two important density functions. For the first benchmark, the bearing capacity has a variation coefficient of approximately 32%, thus a certain discrepancy exists between the curves of Fig. 5.2.

μ_{q_f}	σ_{q_f}	COV_{q_f}	v_{q_f}
306.785 kN/m ²	97.167 kN/m ²	0.317	0

Table 5.2: Statistical values of q_f predicted by PEM

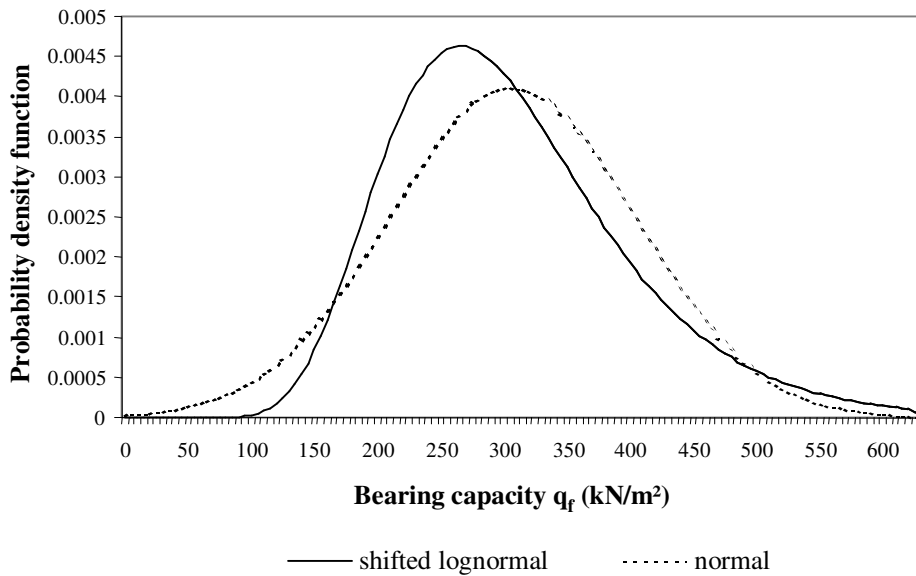


Figure 5.2: Approximation of PEM results using the standard lognormal and the normal distributions

5.2 PEM results for benchmark 2 with uncorrelated soil parameters

For the second benchmark the number of input variables increases, thus increasing the number of PEM calculations from 2 to 4 (because $n=2$). As the soil parameters are uncorrelated, the determination of the bearing capacity statistical values, the procedure as is described stepwise in next section, is still very simple, as for benchmark 1.

5.2.1 Procedure of the PEM

1. The relationship (4.6) between the dependent variable q_f and the random input variables $\tan\phi'$ and c' is considered.

2. Then the sampling point locations for $\tan\phi'$ and c' are computed. The standard deviation units will be evaluated for both soil parameters by applying formulas (3.6), thus leading to

$$\begin{aligned} \xi_{\tan\phi'+} &= \xi_{\tan\phi'-} = 1 \\ \xi_{c'+} &= 3.222 \\ \xi_{c'-} &= 0.310. \end{aligned}$$

The corresponding sampling point locations can be evaluated with Eqs. (3.7)

$$\tan \phi'_- = 0.527$$

$$\tan \phi'_+ = 0.406$$

$$c'_+ = 14.311 \text{ kN/m}^2$$

$$c'_- = 3.007 \text{ kN/m}^2.$$

3. The weights P_i , giving each of the four point estimates of soil parameters considered as single random variable, are then determined using Eq. (3.8), thus obtaining

$$P_{\tan \phi'_+} = P_{\tan \phi'_-} = 0.5$$

$$P_{c'_+} = 0.088$$

$$P_{c'_-} = 0.912.$$

Figure 5.3 shows how the sampling points of both soil parameters $\tan \phi'$ and c' are located. The corresponding weights are also shown in these diagrams. Then the associated weights need to be found, considering the input parameters as multiple uncorrelated variables. Formula (3.9) gives the following weights:

$$P_{++} = P_{\tan \phi'_+} \cdot P_{c'_+} = 0.044$$

$$P_{+-} = P_{\tan \phi'_+} \cdot P_{c'_-} = 0.456$$

$$P_{-+} = P_{\tan \phi'_-} \cdot P_{c'_+} = 0.044$$

$$P_{--} = P_{\tan \phi'_-} \cdot P_{c'_-} = 0.456$$

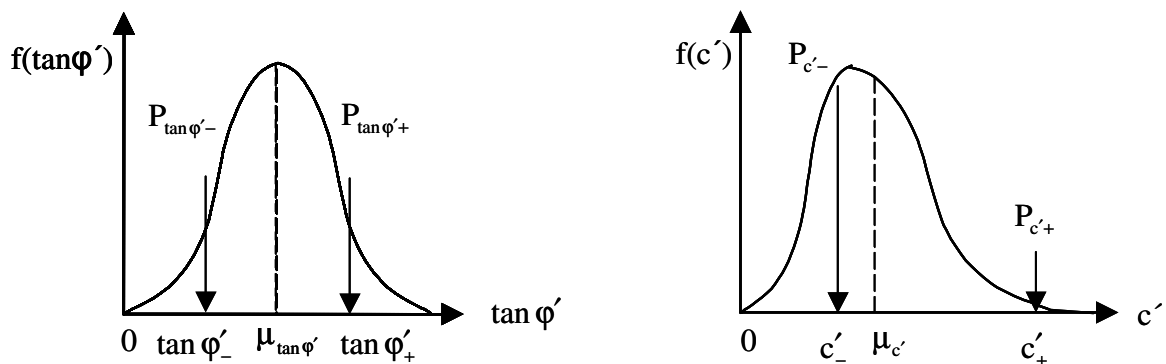


Figure 5.3: Sampling point locations and weights of the soil parameters $\tan \phi'$ and c'

4. The value of the bearing capacity at each sampling point can now be evaluated. The results are shown in Table 5.3.

$P_{\pm\pm}$	c'_{\pm}	$\tan \phi'_{\pm}$	$q_{f\pm\pm}$
0.044	14.311 kN/m ²	0.527	665.755 kN/m ²
0.456	3.007 kN/m ²	0.527	378.740 kN/m ²
0.044	14.311 kN/m ²	0.406	384.650 kN/m ²
0.456	3.007 kN/m ²	0.406	192.762 kN/m ²

Table 5.3: Associated weights, sampling points and bearing capacity values for $\tan\phi'$ and c'

5. The mean value, variance and skewness coefficient of the bearing capacity can be determined using Eqs. (3.15), (3.16) and (3.17), where $n = 2$. The results of the statistical estimates of the bearing capacity predicted by PEM are presented in Table 5.4.

Comparing these results with those of Table 5.2, it can be seen that the mean value is constant, while the standard deviation increases. This also increases the skewness and the variation coefficients. The higher standard deviation is due to the consideration of the effective cohesion as input random variable, which introduces more uncertainty in the final results. Moreover, it can be deduced from the positive skewness coefficient that the probability density function of the bearing capacity is no longer symmetric, as found in the first benchmark.

μ_{q_f}	σ_{q_f}	COV_{q_f}	v_{q_f}
306.786 kN/m ²	119.236 kN/m ²	0.389	0.912

Table 5.4: Statistical values of q_f predicted by PEM with uncorrelated soil variables

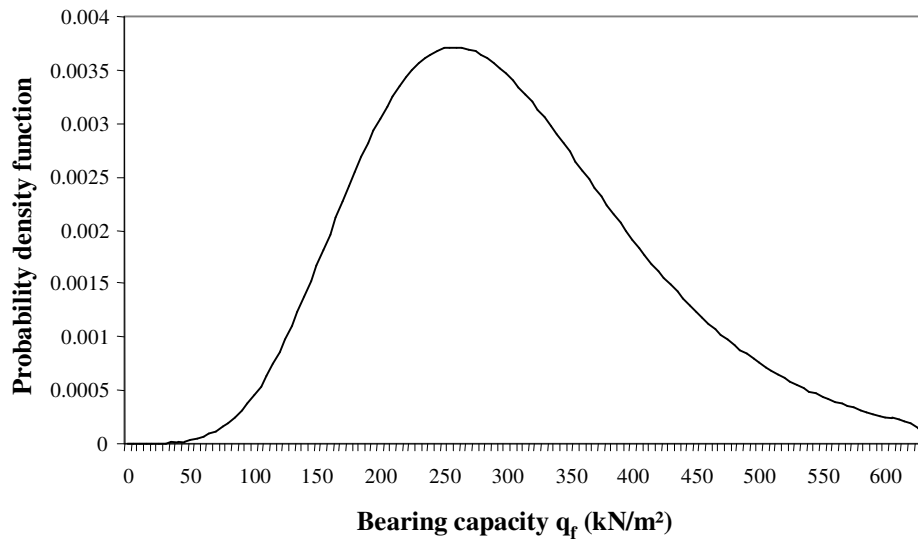


Figure 5.4: Approximation of PEM results using a shifted lognormal distribution with uncorrelated soil variables

Assuming a shifted lognormal distribution to approximate the results of Table 5.4, the bearing capacity curve can be plotted and shown in Fig. 5.4. This function is positively (right) skewed with respect to the mean value of the bearing capacity.

5.3 PEM results for benchmark 2 with correlated soil parameters

If the soil parameters $\tan\phi'$ and c' are correlated, then Rosenblueth's formula (3.9) can not be applied for this benchmark, because negative weights are found. For this reason Christian's formula (3.13) is used. As this formula is valid only for symmetrical random variables, instead of the lognormal variable c' , the normal variable $\ln c'$ will be considered with its corresponding statistical values listed in Fig. 4.2 (b). In this way it is possible to simplify calculations working with two symmetrically distributed and correlated variables and applying formula (3.13) without any mathematical difficulties.

However, it will be seen in this chapter that formula (3.13) also presents some problem when applied to correlated soil parameters. This fact will be clearer when PEM results are compared with those of MCS in section 5.4.

The bearing capacity statistical values are found by following the usual procedure for implementing the PEM, as shown stepwise in next section.

5.3.1 Procedure of the PEM

1. The relationship (4.6) between q_f and the soil variables $\tan\phi'$ and c' is again considered.

2. As $\tan\phi'$ and $\ln c'$ are both symmetrically distributed, then the standard deviation units of the soil parameters will be both equal to unity. In fact Eqs. (3.6) lead to

$$\xi_{\tan\phi'_+} = \xi_{\tan\phi'_-} = 1$$

$$\xi_{\ln c'_+} = \xi_{\ln c'_-} = 1.$$

The sampling point locations for $\tan\phi'$ and $\ln c'$ are then computed by applying formulas (3.7), thus obtaining

$$\tan\phi'_- = 0.406$$

$$\tan\phi'_+ = 0.527$$

$$\ln c'_+ = 1.842 \text{ kN/m}^2$$

$$\ln c'_- = 0.436 \text{ kN/m}^2.$$

$\rho_{\ln c' \tan\phi'}$	Associated weights			
	P_{++}	P_{+-}	P_{-+}	P_{--}
-1.0	0.000	0.500	0.500	0.000
-0.9	0.025	0.475	0.475	0.025
-0.8	0.050	0.450	0.450	0.050
-0.7	0.075	0.425	0.425	0.075
-0.6	0.100	0.400	0.400	0.100
-0.5	0.125	0.375	0.375	0.125
-0.4	0.150	0.350	0.350	0.150
-0.3	0.175	0.325	0.325	0.175
-0.2	0.200	0.300	0.300	0.200
-0.1	0.225	0.275	0.275	0.225
0.0	0.250	0.250	0.250	0.250

Table 5.5: Associated weights of $\tan\phi'$ and $\ln c'$ varying the correlation coefficient

3. The weights P_i , giving each of the four point estimates of the soil parameters considered as single random variable, are then determined using formula (3.8), thus leading to

$$P_{\tan \phi'_+} = P_{\tan \phi'_-} = 0.5$$

$$P_{\ln c'_+} = P_{\ln c'_-} = 0.5.$$

Formula (3.13) is then used to find the associated weights. The sampling weights calculated for various correlation coefficients between 0 to -1.0 are listed in Table 5.5.

4. To determine the bearing capacity values at each sampling point, the sampling point locations of $\ln c'$ need to be transformed into the sampling point locations of the lognormal cohesion. This is done simply using the exponential function, i.e.

$$c'_+ = e^{\ln c'_+} = 6.311 \text{ kN/m}^2$$

$$c'_- = e^{\ln c'_-} = 1.546 \text{ kN/m}^2.$$

Then the relationship (4.6) can be easily applied to evaluate the bearing capacity values listed in Table 5.6 for $\rho_{c' \tan \phi'} = -0.6$.

Eqs. (3.15), (3.16) and (3.17) can now be used to define the statistical values of the bearing capacity corresponding to a correlation coefficient of -0.6 . The results are shown in Table 5.7.

Comparing results of Tables 5.4 and 5.7, one sees a slight change in the mean value, while the standard deviation decreases down to around 35% when compared with the value obtained considering uncorrelated soil parameters. Consequently the skewness and the variation coefficients also decrease. Thus the bearing capacity variability and the uncertainty in the analysis are strongly reduced.

Assuming a shifted lognormal distribution and considering uncorrelated and negatively correlated soil parameters with $\rho_{c' \tan \phi'} = -0.6$, the probability density functions of the bearing capacity for both cases can be compared in one diagram, as shown in Fig. 5.5. When uncorrelated variables are taken into account then the density function shows a higher variability, being wider than the curve for negatively correlated parameters. Also the peak values of these distributions is clearly different, being around 0.0037 for the case with $\rho_{c' \tan \phi'} = 0$ and around 0.0052 for the case with $\rho_{c' \tan \phi'} = -0.6$.

$P_{\pm\pm}$	$\ln c'_{\pm}$	$\tan \phi'_{\pm}$	$q_{f\pm\pm}$
0.1	1.843 kN/m ²	0.527	462.628 kN/m ²
0.4	0.436 kN/m ²	0.527	341.645 kN/m ²
0.4	1.843 kN/m ²	0.406	248.846 kN/m ²
0.1	0.436 kN/m ²	0.406	167.961 kN/m ²

Table 5.6: Associated weights, sampling points and bearing capacity values for $\tan \phi'$ and $\ln c'$

μ_{q_f}	σ_{q_f}	COV_{q_f}	v_{q_f}
299.255 kN/m ²	78.282 kN/m ²	0.262	0.394

Table 5.7: Statistical values of q_f predicted by PEM with $\rho_{c'\tan\phi'} = -0.6$

Varying the correlation coefficient from 0 to -1.0 , the statistical values of the bearing capacity change as shown in Table 5.8. By decreasing the correlation coefficient and considering the normal variable $\ln c'$ as input for the analysis, the mean value changes slightly (less than 4% difference for uncorrelated soil parameters to parameters with $\rho_{c'\tan\phi'} = -1.0$), while the standard deviation decreases significantly down to about 60% reduction for the case with $\rho_{c'\tan\phi'} = -1.0$. The skewness coefficient increases up to a maximum value when $\rho_{c'\tan\phi'} = -0.7$, then it decreases to a value of zero for a correlation of $\rho_{c'\tan\phi'} = -1.0$. This strange behaviour of the skewness is influenced mainly by the standard deviation reduction.

At the bottom of Table 5.8 the bearing capacity statistical values from Table 5.4 found considering uncorrelated soil parameters and the lognormal cohesion c' , instead of the normal variable $\ln c'$, are also listed. Comparing the results for both cases, the mean value is practically unchanged, while there is a clear difference between standard deviations and even more between skewness coefficients. This divergence is due to the different associated weights

evaluated, respectively, by Eq. (3.9) for c' and Eq. (3.13) for $\ln c'$, which are listed in Tables 5.3 and 5.6.

Unfortunately Rosenblueth's formula can not be applied for benchmark 2 to estimate any statistical values of the bearing capacity considering different correlation coefficients, because, as already mentioned, negative associated weights are found. Also Christian's formulas can only be used when the normal variable $\ln c'$ is taken into account, because this formula refers only to symmetrically distributed variables.

Hence the results of Table 5.8 referred to negative correlation coefficients can not be compared with other statistical values, as done for the case with uncorrelated variables.

As the results of Table 5.8 are the outcome of the application of formulas (3.13) using a mathematical trick for considering the input variable cohesion as normally distributed, i.e. $\ln c'$ instead of c' , then the correlation between the input variables is different, thus influencing the values of the associated weights.

For this reason these results will be used as reference for further comparisons with other probabilistic methods results only for the case with negatively correlated variables. Whereas the statistical values of Table 5.4 will be considered as reference for further comparisons in case of uncorrelated soil parameters, i.e. when $\rho_{\tan \phi' c'} = 0$. For these comparisons the author refers to section 5.4.

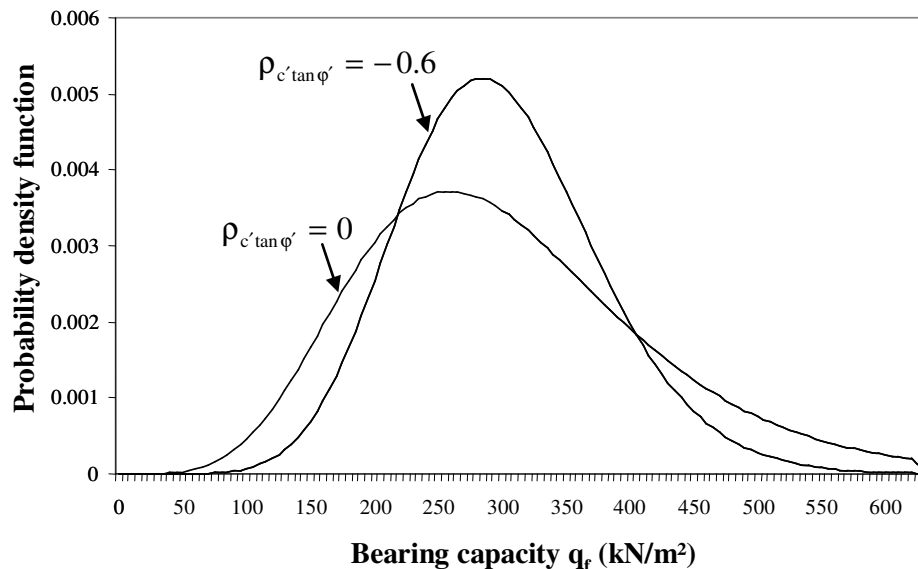


Figure 5.5: Comparison of the probability density functions of q_f with $\rho_{c' \tan \phi'} = 0$ and with $\rho_{c' \tan \phi'} = -0.6$

$\rho_{c'\tan\phi'}$	μ_{q_r} (kN/m ²)	σ_{q_r} (kN/m ²)	v_{q_r}
-1.0	295.246	46.399	0.000
-0.9	296.248	56.122	0.318
-0.8	297.250	64.378	0.399
-0.7	298.253	71.675	0.409
-0.6	299.255	78.282	0.394
-0.5	300.258	84.361	0.369
-0.4	301.260	90.020	0.340
-0.3	302.263	95.333	0.309
-0.2	303.265	100.354	0.280
-0.1	304.268	105.127	0.251
0.0 (considering $\ln c'$)	305.270	109.683	0.223
0.0 (considering c')	306.785	119.236	0.912

Table 5.8: Statistical values of the bearing capacity for different correlation coefficients

Fig. 5.6 shows the influence of the correlation coefficient variation on the shape of the shifted lognormal fit of the bearing capacity. As already pointed out for Fig. 5.5, the curves become narrower for lower correlation coefficients, thus decreasing the bearing capacity variability, which means less uncertainty in the analysis. As a consequence the distribution peaks increase.

It should be noted that, for $\rho_{\tan\phi'c'} = -1.0$, the skewness coefficient of the bearing capacity is nil, as reported in Table 5.8, meaning a symmetrical distribution. For this reason a Gaussian distribution is assumed for plotting the bearing capacity function in Fig. 5.6.

In this Figure the curve for $\rho_{\tan\phi'c'} = 0$ taking into account the lognormal cohesion c' as input variable is also plotted. Comparing this curve to that obtained considering the normal variable $\ln c'$ instead of c' , a clear divergence is seen. The curve referred to c' is in fact wider because of the higher standard deviation. Furthermore, it is shifted more to the left because of the extremely higher positive skewness coefficient.

Summarising it is possible to conclude that the choice of a negative correlation between soil parameters is reasonable, because the uncertainty in the probabilistic analysis is effectively reduced.

In addition it is shown in Table 5.8 and Fig. 5.6 that, depending on the weights formula applied for benchmark 2 with uncorrelated soil variables, the bearing capacity results are different, particularly in terms of skewness coefficient, thus producing some difficulty in the interpretation of the outcome.

As already mentioned in chapter 3, ROSENBLUETH (1981) noted that when multiple random variables are taken into account in the application of the PEM, the value of the skewness coefficient can only be reliably calculated using Eq. (3.17) if the variables are uncorrelated. Also CHRISTIAN and BAECHER (1999) pointed out that the PEM should not be applied for evaluating the skewness coefficient for non-linear functions, as in the case of the bearing capacity formula.

Moreover, they observed that the larger the variation coefficient of the input variables, the larger is the error in the estimates. In this study a variation coefficient of 80% is considered for the cohesion. This value is higher than the values usually found in the literature, thus introducing some inaccuracy in the probabilistic results of the bearing capacity.

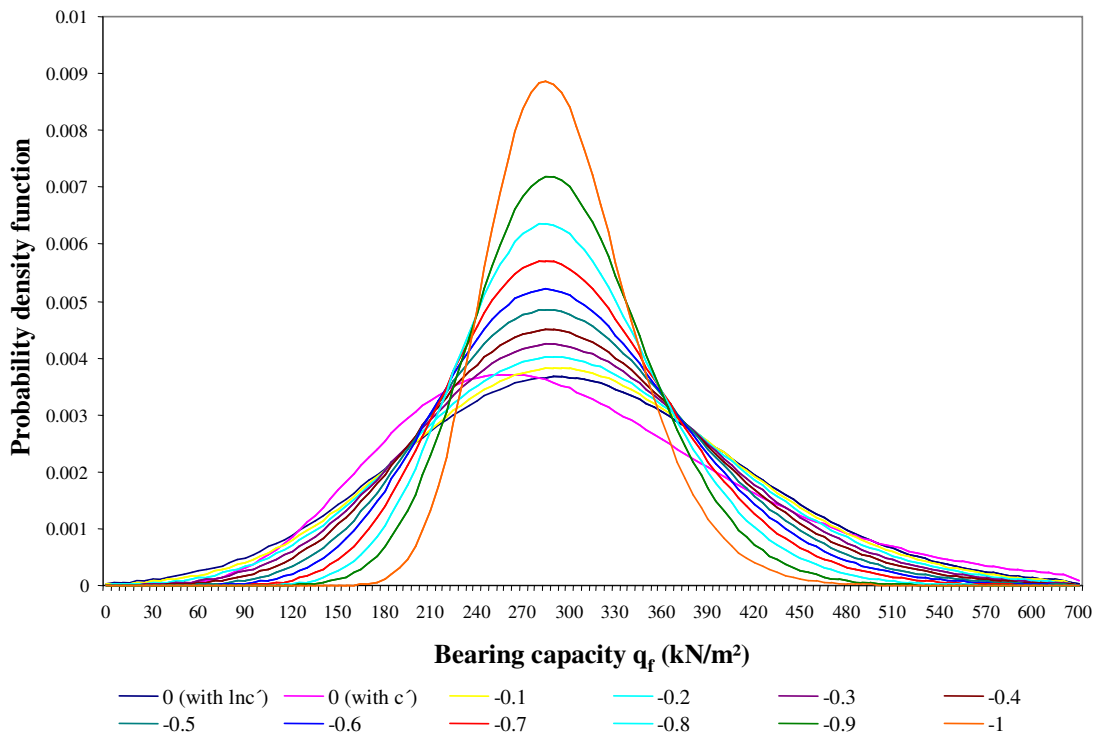


Figure 5.6: Influence of the correlation coefficient variation on the probability distribution of the bearing capacity

Finally, these authors stated that one should be careful when applying the PEM to cases in which the transformation of an input variable changes its distributional form, as it was done for the cohesion, for which important information on the correlation coefficient between shear strength parameters is lost. All these facts are confirmed in this chapter.

Thus, before applying a certain formula for evaluating the associated weights, one should be aware of the characteristics of the input variables, i.e. if these are symmetrically distributed or not and if a certain correlation exists between them.

5.4 Comparison of PEM, MCS, FOSM and SOSM results

The scope of this section is to compare PEM results for benchmark 1 and 2 already shown in chapter 4 to those of FOSM and SOSM methods, using the Monte Carlo approach as a reference for the comparison.

In chapters 3 and 4 it has been shown that MCS are too time consuming for practical purposes, which means consequently too expensive. Moreover, the FOSM and SOSM methods do not provide information about the skewness coefficient.

The PEM is chosen as alternative probabilistic method to be applied to the bearing capacity problem, instead of MCS, FOSM and SOSM methods, because it requires much less computational effort than MCS and it also provides information about the skewness coefficient. Furthermore this approach does not require the determination and evaluation of partial derivatives of the bearing capacity formula as FOSM and SOSM, thus being more straightforward to use.

Nevertheless, as already discussed in section 5.3, the PEM has also some drawbacks. These are highlighted in this section when the skewness coefficients of MCS and PEM methods are compared.

5.4.1 Comparison of results for benchmark 1

In Table 5.9 the statistical values of the bearing capacity for benchmark 1 found by applying the probabilistic methods PEM, FOSM, SOSM and MCS are listed. Mean values, standard deviations and, consequently, variation coefficients are quite similar, while a significant difference is observed between the skewness coefficients. In fact the FOSM and SOSM method do not provide any skewness coefficient, while the PEM provides a nil value. Thus the PEM is more accurate than FOSM and SOSM methods, giving the additional information about the shape of the bearing capacity distribution. However this value is extremely different from the skewness coefficient found by MCS, which is 1.008.

Assuming a standard lognormal distribution, the probability density function of PEM, FOSM and SOSM results can be drawn together with the results derived from 10000 MCS plotted pointwise, as shown in Fig. 5.7.

Actually, the PEM skewness coefficient suggests that a normal distribution should be assumed for approximating the bearing capacity statistical values. However, following the conclusions reported in section 5.1 about the variation coefficient and referring to Fig. 5.2, a standard lognormal distribution is preferred, because it seems to be more representative for the bearing capacity.

Despite the different skewness coefficient, the PEM curve matches very well the points indicating the MCS results, even if PEM distribution is a little bit skewed to the right and up. Hence PEM apparently seems to be insensitive to the skewness and gives virtually the same distribution as the computationally not so attractive MCS.

It is important to observe that PEM requires only two calculations, against the 10000 simulations for Monte Carlo method, to get the results of Table 5.9. Thus, by applying PEM, the computational effort considerably decreases.

Considering Benjamin and Cornell's formula (4.1) valid for a standard lognormal distribution, it is possible to assign fictitious skewness coefficients for the FOSM and SOSM results. These values are then compared with the skewness coefficient found by PEM and MCS, as shown in Table 5.9. These fictitious values are very similar to the skewness coefficient found by MCS, whereas they are extremely different from the value of PEM. Nevertheless, because a standard lognormal distribution is assumed as approximation for the PEM results, it is then possible to determine a fictitious skewness also for this method. The value is approximately 0.983 and it is similar to the fictitious skewness coefficients assigned to FOSM and SOSM methods and to the skewness coefficient of the MCS. For this reason the curves in Fig. 5.7 are in good agreement. However, the FOSM curve is skewed more to left due to the lower mean value. If another type of distribution were to be assumed for approximating the results of Table 5.9, then the fictitious skewness coefficients would also change.

For more detail about the assumption of different distribution functions as an approximation for the probabilistic results of the bearing capacity the author refers to section 5.5. For example, by assuming a Gaussian distribution, the skewness coefficients of all probabilistic approaches would be the same. The difference reported in Table 5.9 for the skewness would then disappear.

However, the author would like to point out that one of the goal of this work is to find the most suitable probability distribution which approximates MCS and PEM results best and not those of FOSM and SOSM methods.

Method	μ_{q_r}	σ_{q_r}	COV_{q_r}	v_{q_r}
PEM	306.785 kN/m ²	97.167 kN/m ²	0.317	0
FOSM	290.878 kN/m ²	93.876 kN/m ²	0.323	1.003*
SOSM	303.851 kN/m ²	93.876 kN/m ²	0.309	0.956*
MCS	306.562 kN/m ²	102.242 kN/m ²	0.333	1.008

*value found with BENJAMIN and CORNELL's formula (1970) for a standard lognormal distribution

Table 5.9: Statistical values of q_f found using PEM, FOSM, SOSM and MCS methods

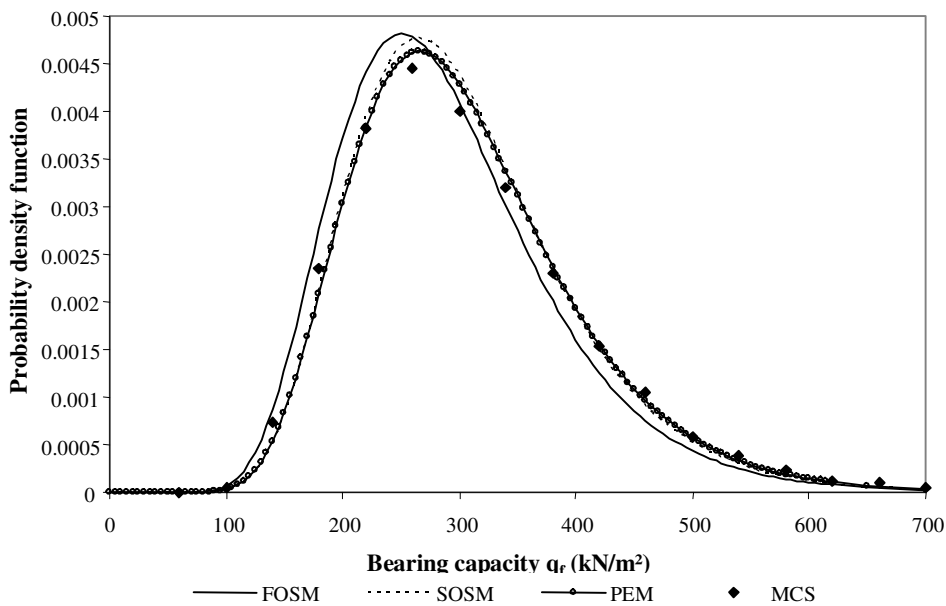


Figure 5.7: Comparison of PEM, FOSM, SOSM and MCS results in terms of probability density function

From this results comparison it would seem that no real advantage exists by applying PEM or FOSM and SOSM method, as PEM does not provide a

meaningful skewness coefficient for benchmark 1 as compared with the MCS results.

However it will be seen in next sections that PEM, not only strongly decreases the number of calculations, but can give more significant skewness values when multiple input variables are considered, as for benchmark 2, where both cohesion and $\tan\phi'$ are taken into account.

Nevertheless, some difficulty will be encountered in the evaluation of the skewness when correlated soil variables are considered.

5.4.2 Comparison of results for benchmark 2 with uncorrelated soil parameters

Table 5.10 summarizes the statistical values of the bearing capacity previously evaluated by PEM, FOSM, SOSM and MCS methods for benchmark 2 considering uncorrelated soil parameters. Comparing these results, it can be seen that mean values and standard deviations are quite similar, while there is a difference between the skewness coefficients. However, when compared with the results of benchmark 1 in Table 5.9, the difference between MCS and PEM skewness coefficient is now decreased down to about 35%, instead of the earlier 100%.

Considering a standard lognormal distribution and using again formula (4.1), fictitious skewness coefficients can be assigned to the FOSM and SOSM methods, which are listed in Table 5.10. In contrast to benchmark 1, these values are similar to the skewness coefficient of the PEM. This is certainly due to the introduction of the cohesion c' as additional input variable, whose skewness strongly influences that of the bearing capacity. Of course if another distribution were to be assumed for approximating the FOSM and SOSM results, then other skewness values would be found.

Assuming a shifted lognormal distribution for PEM and a standard lognormal distribution for FOSM and SOSM methods, then the results of Table 5.10 can be drawn in Fig. 5.8 together with MCS results plotted pointwise. When compared with benchmark 1, the PEM curve is now more skewed right down than those of FOSM and SOSM methods, due to the fact that a shifted lognormal, and not a standard lognormal distribution is assumed as an approximation.

If a standard lognormal distribution were to be assumed for plotting PEM results, then this difference would disappear. The fictitious skewness coefficient of the PEM of approximately 1.226 is very similar to the FOSM, SOSM and MCS values and all the fitting curves would be then in good agreement.

It is important to notice that, for this case, PEM requires only four calculations, against the 10000 Monte Carlo simulations, to get the results of Table 5.10.

Method	μ_{q_f}	σ_{q_f}	COV_{q_f}	v_{q_f}
PEM	306.786 kN/m ²	119.236 kN/m ²	0.389	0.912
FOSM	290.878 kN/m ²	114.931 kN/m ²	0.395	1.247*
SOSM	303.851 kN/m ²	114.931 kN/m ²	0.378	1.188*
MCS	306.805 kN/m ²	123.367 kN/m ²	0.402	1.387

*value found with BENJAMIN and CORNELL's formula (1970) for a standard lognormal distribution

Table 5.10: Statistical values of q_f found using PEM, FOSM, SOSM and MCS methods with uncorrelated soil parameters

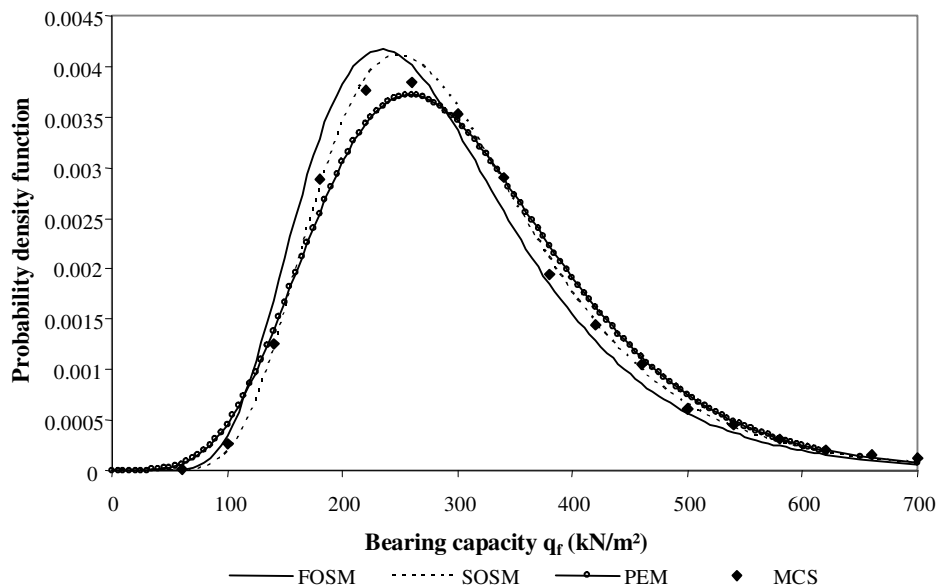


Figure 5.8: Comparison of PEM, FOSM, SOSM and MCS results in terms of probability density function with $\rho_c \tan \phi = 0$

5.4.3 Comparison of results for benchmark 2 with correlated soil parameters

The statistical values of the bearing capacity found by applying PEM, FOSM, SOSM and MCS methods to benchmark 2 taking into account a negative correlation of $\rho_{c' \tan \phi'} = -0.6$ are listed in Table 5.11. Mean values and standard deviations are quite similar, even considering a correlation between input variables. On the other hand, a significant discrepancy exists between skewness coefficients.

In fact FOSM and SOSM methods do not provide any value, while the skewness coefficient of the PEM is about 60% lower than MCS value. This difference is due to the inconvenience of applying PEM formulas (3.13) to the non-symmetric variable c' , as described in section 5.3. In order to apply Christian's formula to evaluate the associated weights, the normal variable $\ln c'$ needs to be considered, thus influencing the correlation coefficient between cohesion and friction angle, because of the different mean value and standard deviation of $\ln c'$ and c' .

Assuming a shifted lognormal distribution for PEM and a standard lognormal distribution for FOSM and SOSM methods, then results of Table 5.11 can be plotted in Fig. 5.9 together with MCS results. Despite the different skewness coefficients, the curves are in good agreement.

Method	μ_{q_f}	σ_{q_f}	COV_{q_f}	v_{q_f}
PEM	299.255 kN/m ²	78.282 kN/m ²	0.262	0.394
FOSM	290.878 kN/m ²	75.761 kN/m ²	0.26	0.798*
SOSM	296.067 kN/m ²	75.761 kN/m ²	0.256	0.785*
MCS	297.848 kN/m ²	73.372 kN/m ²	0.246	0.911

*value found with BENJAMIN and CORNELL's formula (1970) for a standard lognormal distribution

Table 5.11: Statistical values of q_f found using PEM, FOSM, SOSM and MCS methods with $\rho_{c' \tan \phi'} = -0.6$

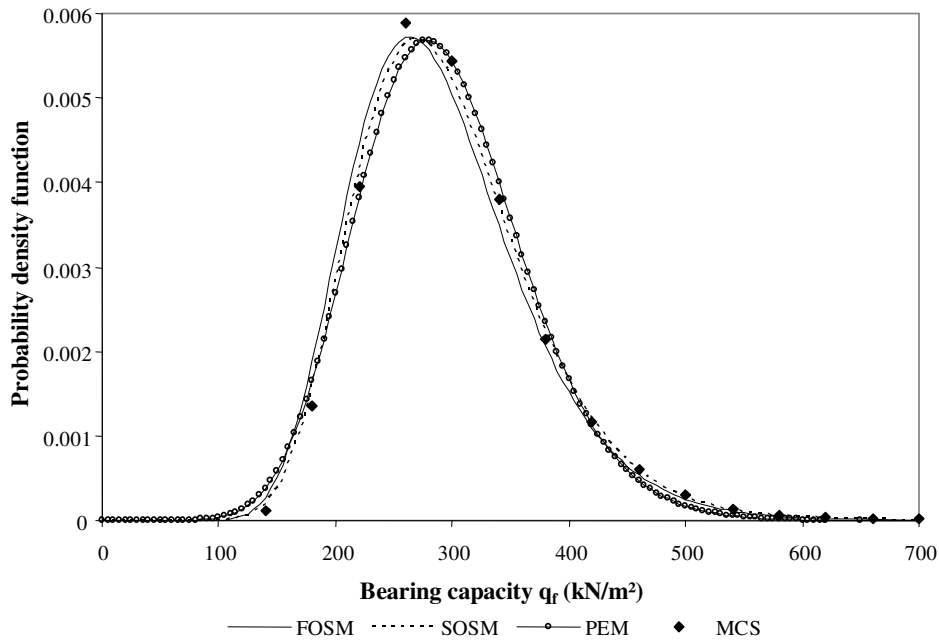


Figure 5.9: Comparison of PEM, FOSM, SOSM and MCS results in terms of probability density function with $\rho_{c \tan \phi} = -0.6$

Benjamin and Cornell’s formula (4.1) is applied to evaluate a fictitious value for the skewness coefficient of FOSM and SOSM methods, as reported in Table 5.11. Thus the skewness coefficients of all methods can be compared. One notes that PEM skewness is around 50% lower than FOSM and SOSM fictitious values, while the value of MCS is less than 15% higher. If another distribution were to be assumed for approximating FOSM and SOSM results, then it would be possible to find other skewness coefficients, maybe more similar to the PEM or MCS values.

Also in this case, if a standard lognormal distribution were to be assumed for approximating PEM results, then the fictitious skewness coefficient of PEM would be approximately 0.804, which is very similar to the fictitious values found for FOSM and SOSM methods and slightly lower than the MCS value.

5.5 Discussion of the assumption of the shifted lognormal distribution

The use of a certain probability density function in preference to others plays an important role in the probabilistic analysis of the bearing capacity problem, as shown in this chapter.

From the results of Monte Carlo simulations reported in chapter 4, it is possible to define the shape of the bearing capacity density function.

Considering, for example, the frequency diagram of 10000 MCS in Fig. 4.10 for benchmark 2 with uncorrelated soil parameters, it is reasonable to assume a positively (right) skewed probability distribution for the bearing capacity statistical values. Certain continuous probability distributions can be used to approximate these results, such as the lognormal, the beta or the Weibull distributions.

In geotechnical literature the normal and the standard lognormal distributions are frequently used, because of their mathematical simplicity. In addition, the necessary statistical information about these functions is widely available, including probability tables.

For this study the shifted lognormal distribution is chosen to represent the distribution of the bearing capacity. Not only it is strictly non-negative and can be treated mathematically straightforward, but it also matches very well all the three moments of the bearing capacity found by applying the Monte Carlo and the Point Estimate methods.

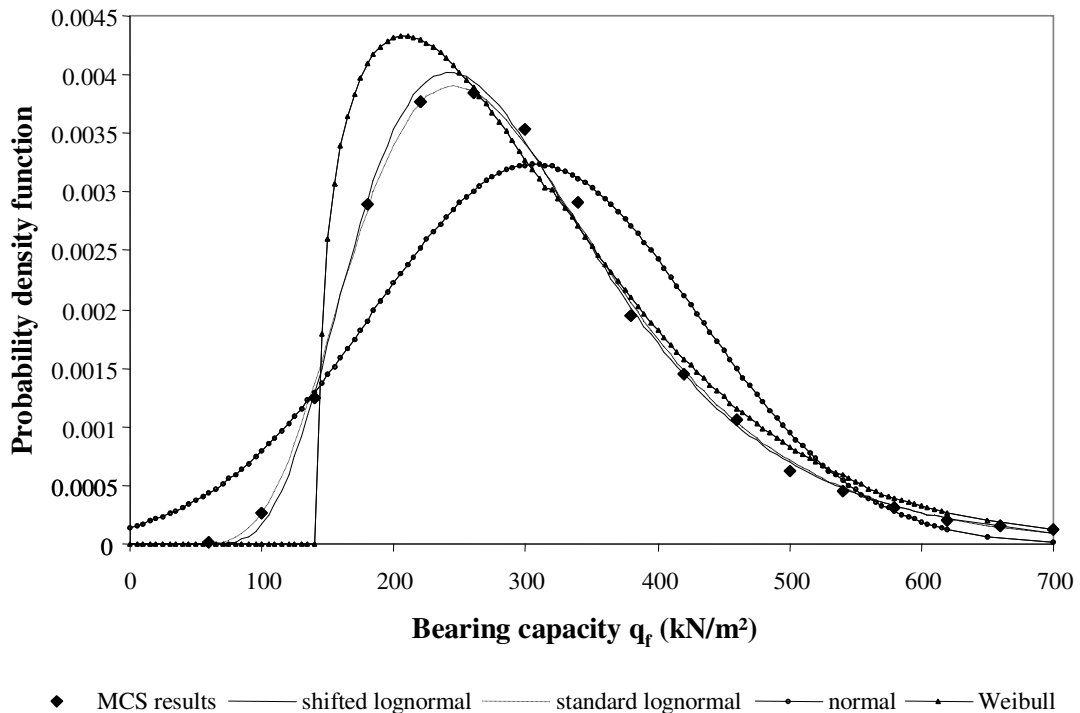


Figure 5.10: Different probability density functions assumed as approximation of 10000 MCS for benchmark 2 with $\rho_{c \sim \tan \phi} = 0$

The pointwise results of 10000 MCS for benchmark 2 considering $\rho_{c'\tan\phi'} = 0$ are shown in Fig. 5.10 together with four possible fits using well-known probability density functions.

A large discrepancy exists between the Gaussian normal distribution assumed as approximation and the MCS results described pointwise. This is due to the fact that the skewness coefficient evaluated using the Monte Carlo method is not nil. Furthermore, as Fig. 5.10 shows, the Gaussian distribution allows negative bearing capacity values, which are physically unrealistic. Then the Gaussian distribution could only be seen as a rough approximation.

The Weibull distribution shows a good agreement with MCS results for values of the bearing capacity higher than around $q_f = 270 \text{ kN/m}^2$. However this curve can not be a good fit because it does not describe the entire interval of the bearing capacity variability as Monte Carlo method does. This curve is truncated at about $q_f = 140 \text{ kN/m}^2$.

The standard and the shifted lognormal distributions seem to approximate MCS results at best. In fact the curves found considering these two distributions match very well the points referred to the MCS results.

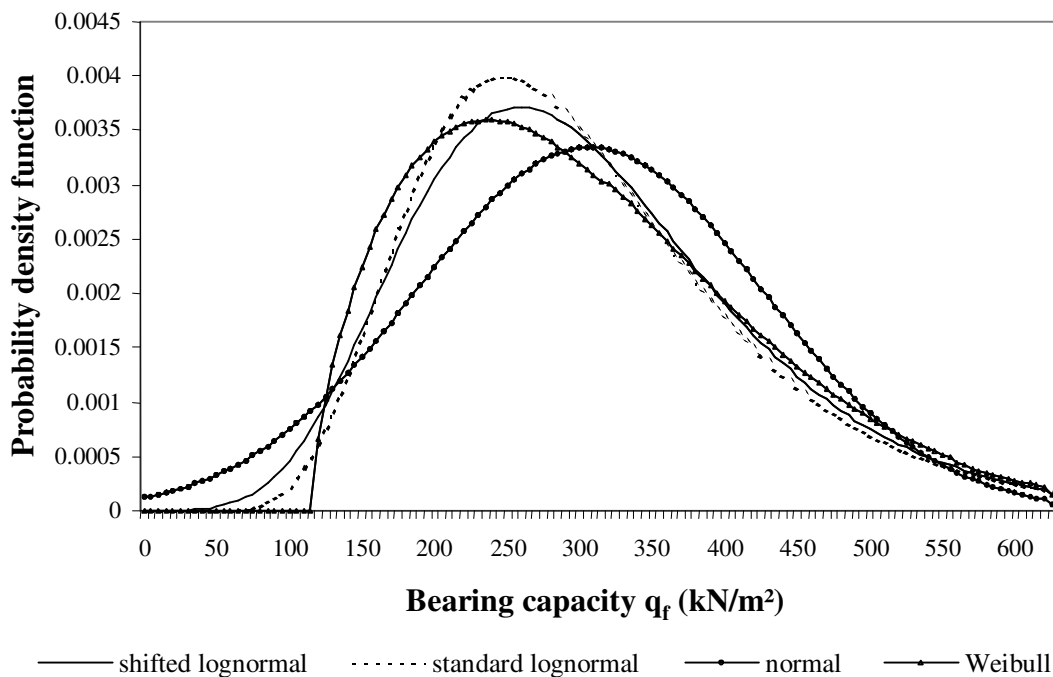


Figure 5.11: Different probability density functions assumed as approximation for PEM results of benchmark 2 with $\rho_{c'\tan\phi'} = 0$

Moreover, looking at the first term of the bearing capacity formula (A.4) in Appendix A, this is given as the product of the two input variables c' and $\tan\phi'$. Hence, for the central limit theorem, the distribution of the bearing capacity should tend to a lognormal distribution.

Apparently, it seems to be that the standard lognormal distribution is more appropriate than the shifted one, especially around the peak of the curve. Nevertheless only the shifted lognormal distribution can match the skewness coefficient of the bearing capacity. This is why this function is preferred to others as an approximation of the results of this probabilistic analysis.

Fig. 5.11 shows possible probability density functions assumed for approximating PEM results of benchmark 2 considering uncorrelated soil variables. In this diagram the good matching of the standard and the shifted lognormal functions can be seen, while there is a high divergence between these two curves and the Weibull and the Gaussian distributions.

It should be pointed out that the differences showed in Figs. 5.10 and 5.11 would become less important if the method of maximum likelihood would be applied. However its results could not be directly compared to the results of the other probabilistic methods considered for the bearing capacity problem, as the method of maximum likelihood is not moment oriented.

Figs. 5.12 shows the comparison of the shifted lognormal (a), standard lognormal (b), normal (c) and Weibull (d) distributions for MCS, PEM, FOSM and SOSM results referred to benchmark 2 taking into account uncorrelated soil parameters.

As the FOSM and SOSM methods do not provide any skewness, their results can not be approximated by a shifted lognormal distribution, as this function requires the knowledge of all the first three moments of the bearing capacity. Thus in Fig. 5.12 a) only the curves for MCS and PEM results are plotted. These have been already compared in section 5.4.2.

The fitting curves of Fig. 5.12 b) and c) seem to agree satisfactorily. However, the assumption of a standard lognormal and of a normal distributions is not the best choice. In fact the standard lognormal distribution does not match the real skewness coefficients evaluated using MCS and PEM. Instead, fictitious skewness values, estimated with formula (4.1), are assigned to these methods.

In addition, the Gaussian normal distribution allows negative bearing capacity values for every probabilistic approach, which are physically impossible. In Fig. 5.12 c) these negative values do not appear, because the curves are truncated at the origin.

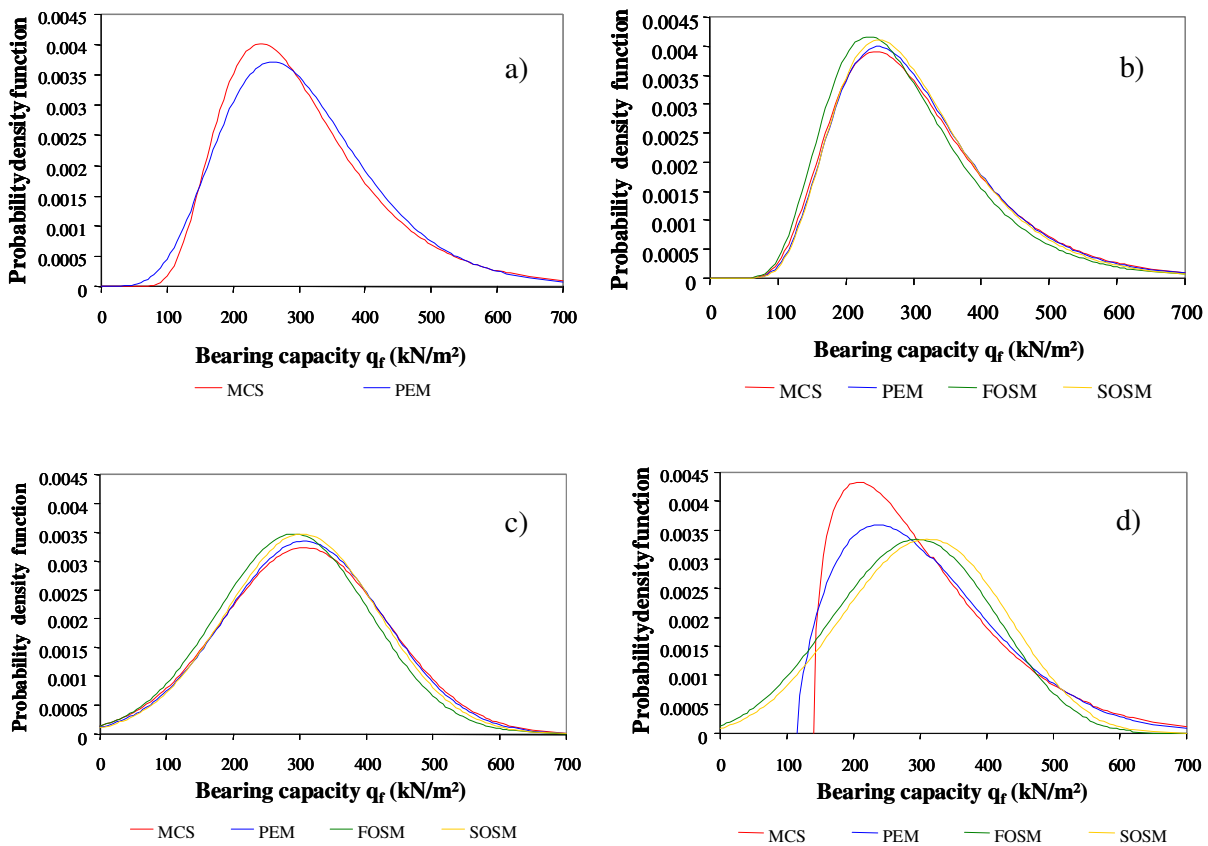


Figure 5.12: Comparison of different probability density functions for MCS, PEM, FOSM and SOSM results for benchmark 2 with $\rho_{c \tan \phi} = 0$: a) shifted lognormal, b) standard lognormal, c) normal and d) Weibull distributions

Finally one can see in Fig. 5.12 d) how the Weibull distribution presents the largest discrepancy. In fact for FOSM and SOSM method, whose skewness coefficient does not exist, the curves seem to be very similar to a normal distribution, giving negative values for the bearing capacity, here truncated at the origin.

On the other hand the well-known shape of the Weibull distribution with a lower bound is clearer for MCS and PEM methods, for which the skewness coefficient is not zero.

The Weibull curve for PEM results is wider, meaning more variability of the bearing capacity, and with lower peak than the MCS function. This is mostly due to the lower skewness coefficient of PEM results, as already seen in section

5.5.2 and shown in Fig. 5.12 a), when the assumption of the shifted lognormal distribution is considered.

As described in Fig. 5.12, the probability density functions behaviour for the bearing capacity results of benchmark 1 is shown in Fig. 5.13. However some differences can be highlighted:

- In Fig. 5.13 a) only the MCS fit can be plotted. In fact to find the three parameters of the shifted lognormal distribution using Eqs. (2.16), (2.17) and (2.18), the skewness coefficient should be different to zero. This is not the case for PEM results of benchmark 1, where the bearing capacity skewness is nil.
- In Fig. 5.13 b) and c), the density function referred to the MCS results, for a lognormal and a normal distribution, is wider and has a lower peak when compared with the other methods. In fact, by neglecting the real skewness coefficient and because the standard deviation of MCS is larger than the values of PEM, FOSM and SOSM methods, the variability of the bearing capacity will be higher.
- Finally, when compared to Fig. 5.12 d), in Fig. 5.13 d) the PEM approximation using the Weibull distribution seems to match well the FOSM and SOSM curves. This is due to the value of the skewness coefficient, which is nil for benchmark 1.

It should be pointed out that the differences showed in Figs. 5.10 and 5.11 would become less important if the method of maximum likelihood would be applied. However its results could not be directly compared to the results of the other probabilistic methods considered for the bearing capacity problem, as the method of maximum likelihood is not moment oriented.

Figs. 5.12 shows the comparison of the shifted lognormal (a), standard lognormal (b), normal (c) and Weibull (d) distributions for MCS, PEM, FOSM and SOSM results referred to benchmark 2 taking into account uncorrelated soil parameters.

As the FOSM and SOSM methods do not provide any skewness, their results can not be approximated by a shifted lognormal distribution, as this function requires the knowledge of all the first three moments of the bearing capacity. Thus in Fig. 5.12 a) only the curves for MCS and PEM results are plotted. These have been already compared in section 5.4.2.

The fitting curves of Fig. 5.12 b) and c) seem to agree satisfactorily. However, the assumption of a standard lognormal and of a normal distributions is not the best choice.

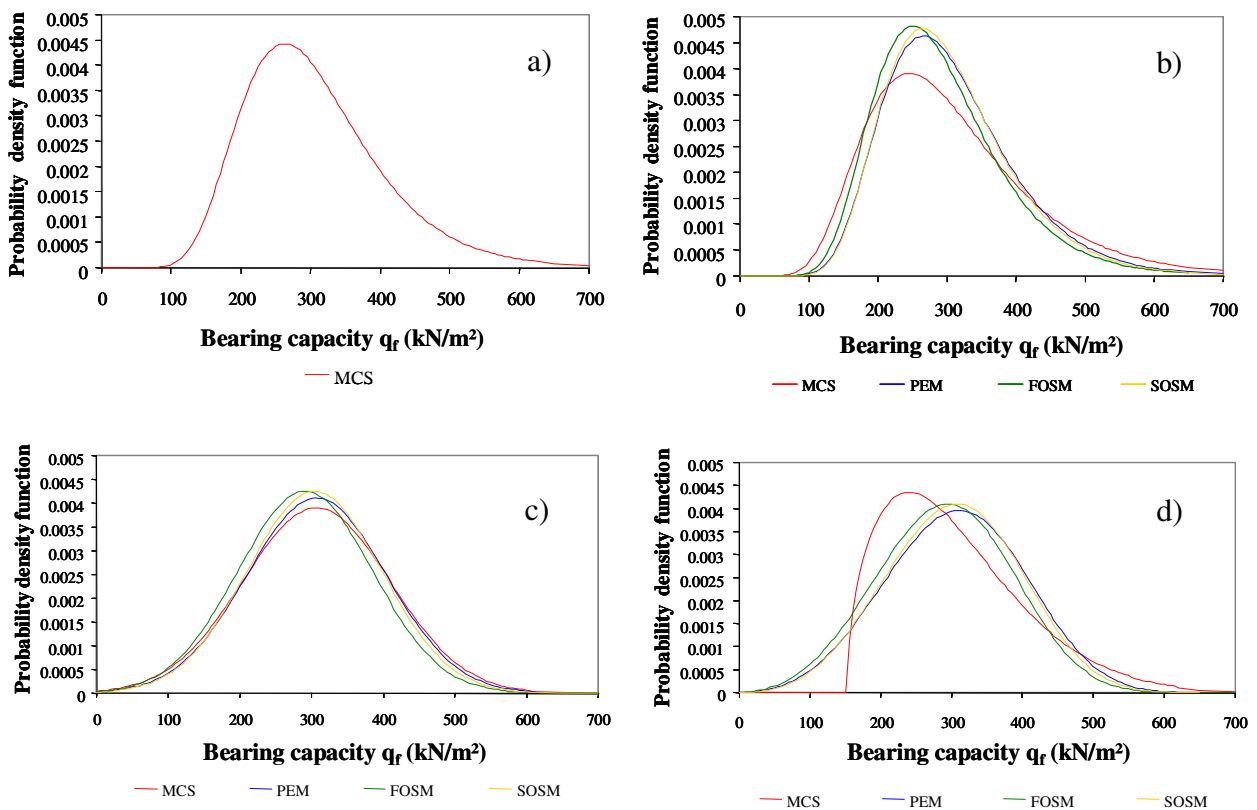


Figure 5.13: Comparison of different probability density functions for MCS, PEM, FOSM and SOSM results for benchmark 1: a) shifted lognormal, b) standard lognormal, c) normal and d) Weibull distribution

In fact the standard lognormal distribution does not match the real skewness coefficients evaluated using MCS and PEM. Instead, fictitious skewness values, estimated with formula (4.1), are assigned to these methods.

In addition, the Gaussian normal distribution allows negative bearing capacity values for every probabilistic approach, which are physically impossible. In Fig. 5.12 c) these negative values do not appear, because the curves are truncated at the origin.

To understand the influence of the skewness coefficient on the shape of the shifted lognormal distribution, different values of this coefficient are considered in Fig. 5.14. In this diagram PEM results for benchmark 2 with $\rho_{c \tan \phi} = 0$ are plotted keeping the mean value and the standard deviation constant. One can also see in this diagram the curve obtained by considering $v_{qf} = 0.912$, which

gives the real shifted lognormal approximation of PEM results listed in Table 5.10.

For skewness coefficients lower than 0.1 the curves practically do not change their shape, while for values higher than 0.1 the difference between the shape of these functions increases. In particular for skewness coefficients higher than 1.0 this difference is very large.

As the PEM and the MCS mean values and standard deviations are very similar for all the benchmarks analysed, but the MCS skewness is always higher, it is now clear why MCS approximation curves are narrower and present a higher peak than PEM functions, as seen in Figs. 5.12 a).

The only exception are the PEM results of benchmark 1, for which is not possible to draw a shifted lognormal distribution, because the skewness is nil. This fact was already noticed in Fig. 5.13 a).

Summarising all these findings, it can be concluded that the shifted lognormal distribution is an important and useful density curve for fitting the results of a probabilistic analysis. As there is very little information about the application of this function in geotechnical literature, the author suggests that the shifted lognormal distribution should be considered in further studies.

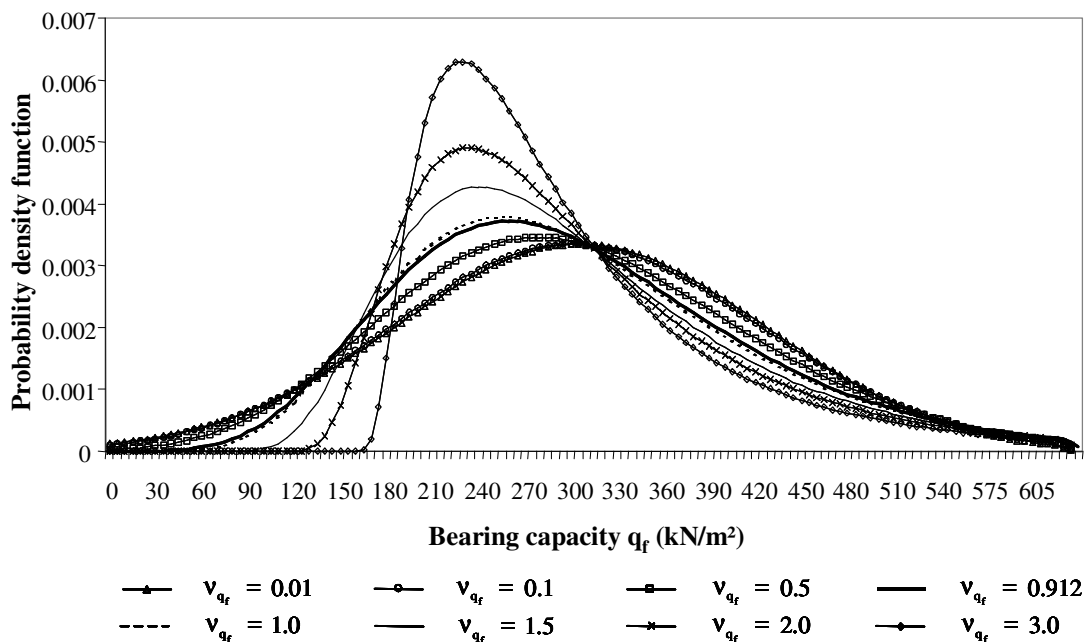


Figure 5.14: Influence of the skewness variation on the shape of the shifted lognormal distribution with constant mean value and standard deviation for PEM results of benchmark 2 with $\rho_c \cdot \tan \phi = 0$

5.6 Conclusions on the application of the PEM to the bearing capacity problem

In this chapter the Two Point Estimate Method was applied to the bearing capacity problem and the results were then compared with those of MCS, FOSM and SOSM methods.

It has been shown that, in spite of some limitations, PEM proves to be a simple, but powerful technique for probabilistic analysis, as it requires much less computational effort than Monte Carlo Simulations for a comparable degree of accuracy in terms of mean value and standard deviation. However, a high discrepancy is observed for the skewness coefficient. For this reason, mathematicians who are familiar with the principles and formulas of this method would emphasise that the PEM should be used only under the conditions mentioned at the end of section 5.3, for which the PEM is expected to give good results.

As an alternative to the PEM, the First Order Second Moment and the Second Order Second Moment methods were applied, which gave results similar to those of PEM. However they do not allow the evaluation of the skewness coefficient, and are therefore less accurate.

As already seen in chapter 4, when a negative correlation between strength parameters is considered, the variability of the bearing capacity is lower, as shown in Figs. 5.5 and 5.6, thus reducing the uncertainty in the final results.

Finally, another important finding of this chapter is that the probability density function of the bearing capacity can be well-approximated by a shifted lognormal distribution. In fact this function matches well not only the mean value and the standard deviation of the bearing capacity, as the standard lognormal function does, but also the skewness coefficient. In this way the final approximation is more precise and reliable.

Chapter 6

The Advanced Point Estimate Method (APEM) for the reliability analysis

Introduction

The goal of a reliability-based design is the evaluation of the probability that a system is safe or unsafe over its expected lifetime, identified numerically respectively by the reliability index or the failure probability.

In recent years different attempts (e.g.: CHERUBINI, 1998; GRIFFITHS, FENTON and MANOHARAN, 2002; HONJO and AMATYA, 2005) have been made to estimate the reliability of the bearing capacity of shallow foundations using probabilistic analyses.

The results of the present chapter are meant as a further contribution to the probabilistic approaches, by which attempts are made to provide a rational framework to include the relevant uncertainties of a certain geotechnical problem consistently and to evaluate the corresponding failure probability.

For the reliability study only benchmark 2 with uncorrelated and negatively correlated soil parameters is considered, because this is of major interest from an engineering point of view.

6.1 Basic problems concerning the evaluation of failure probabilities

It was seen in chapter 2 that, traditionally, the reliability of engineering systems is achieved through the definition of a safety factor, adopting some conservative assumption on the available strength of the system and on the lifetime maximum load. However, this approach can not properly take into account uncertainties related to the system resistance and load. Consequently, a reliability level can not be assessed quantitatively. Thus reliability can only be assured in terms of probability, by modelling the system resistance and load as random variables.

Unfortunately, for most people it is difficult to interpret the meaning of a failure probability, especially if it is a small value. Since many parameters are

not usually considered in order to simplify probabilistic analyses, the computed failure probability could only be seen as a lower bound to the absolute probability of failure. A more elaborate probabilistic risk analysis would be needed to evaluate the absolute risk due to all unforeseen events. However, for most practical problems, the estimate of relative failure probabilities is sufficient to define the inability of a system to perform adequately.

In chapter 2 it has been shown that, considering the resistance and the load of a certain engineering system as random variables together with the corresponding probability density functions, the failure probability can be estimated from the convolution integral (2.22). This calculation requires the knowledge of the joint distribution shape of the input variables.

However, in many cases, the available information may only be sufficient to evaluate the mean value and the standard deviation of load and resistance, but not the skewness coefficient, which describes the shape of a certain density function better. Additionally, even knowing the form of the required distributions, the exact evaluation of the failure probability using the integral (2.22) may be difficult. A practical alternative could be to consider equivalent normal distributions as approximation of the real density function.

In the next section the results of the reliability analysis of the bearing capacity problem by applying different probabilistic methods are presented, discussed and compared. Afterwards, the enhancement of the Point Estimate Method, here named Advanced PEM, or shortly APEM, is described. This approach represents the PEM improvement to solve the problem of evaluating low failure probabilities when a significant divergence exists between Monte Carlo results and the probability density function assumed as an approximation of the traditional PEM statistical values. Or, more specifically, when a high difference between the skewness coefficients of these methods exists.

Not all the probabilistic methods applied provide information regarding lifetimes or time-based probabilities of failure. In order to achieve a time-based reliability analysis other input variables should have a time basis such as some time random event. In this analysis the input soil variables c' and $\tan\phi'$ are considered time independent and the failure probability is referenced to the lifetime of the strip footing.

6.2 Reliability analysis of the bearing capacity problem

In this section the results of the reliability analysis of benchmark 2, considering both uncorrelated ($\rho_{c'\tan\phi'} = 0$) and negatively correlated ($\rho_{c'\tan\phi'} = -0.6$) soil variables, are illustrated and compared. The limitations of every approach in

estimating the failure probability of the bearing capacity are discussed. Finally, the necessity of an enhancement of the traditional PEM is stressed. This new method proves to be a more competitive alternative to MCS, especially when a large number of random variables has to be considered and when small failure probabilities need to be calculated.

6.2.1 Failure probability from Monte Carlo simulations

It has been seen in chapter 3 that, by applying the Monte Carlo method, the soil variables c' and $\tan\phi'$ are simulated according to their known probability density function and the system reliability is evaluated deterministically for each simulation.

Knowing all the bearing capacity values obtained by thousands of Monte Carlo simulations, the failure probability can then be evaluated as

$$P_f = \frac{n_f}{N} \quad (6.1)$$

where n_f is the number of trials for which failure occurs and N is the total number of realisations. The number n_f depends on a certain value of the bearing capacity, for which a target failure probability should be evaluated. In this work the estimated mean value is considered as reference of the ultimate (i.e. at failure) bearing capacity value for finding the number n_f .

The mean value should then be divided by the safety factor FS to evaluate the allowable bearing capacity value for the system safety. More precisely it should be

$$n_f = \text{number of trials for which } q_f < \frac{\mu_{q_f}}{FS} \quad (6.2)$$

For this work a factor of safety $FS=2$ is assumed, as usual for strip footings.

The failure frequency n_f , however, gives an approximation of the target failure probability. If more accurate values are required then the number of simulations has to be increased.

In Tables 6.1, 6.2 and 6.3 the failure probability for 1000, 10000 and 100000 MCS for benchmark 2 are reported. Two cases with correlation coefficient $\rho_{c'\tan\phi'} = 0$ and $\rho_{c'\tan\phi'} = -0.6$ are considered.

1000 Monte Carlo Simulations			
Correlation	μ_{q_f}	n_f	P_f
$\rho_{c'\tan\phi'} = 0$	310.807 kN/m ²	51	0.051
$\rho_{c'\tan\phi'} = -0.6$	294.288 kN/m ²	2	0.002

Table 6.1: Failure probability from 1000 MCS for benchmark 2 with uncorrelated and correlated soil parameters

10000 Monte Carlo Simulations			
Correlation	μ_{q_f}	n_f	P_f
$\rho_{c'\tan\phi'} = 0$	306.805 kN/m ²	496	0.0496
$\rho_{c'\tan\phi'} = -0.6$	297.848 kN/m ²	14	0.0014

Table 6.2: Failure probability from 10000 MCS for benchmark 2 with uncorrelated and correlated soil parameters

100000 Monte Carlo Simulations			
Correlation	μ_{q_f}	n_f	P_f
$\rho_{c'\tan\phi'} = 0$	306.451 kN/m ²	3485	0.03485
$\rho_{c'\tan\phi'} = -0.6$	297.327 kN/m ²	139	0.00139

Table 6.3: Failure probability from 100000 MCS for benchmark 2 with uncorrelated and correlated soil parameters

The corresponding bearing capacity mean value and the number of trials n_f , which give failure, are also indicated. It is evident that the failure probability decreases with increasing the number of simulations, obtaining the highest accuracy at 100000 simulations.

To define the error referred to an estimated failure probability or, more essentially, the number of Monte Carlo simulations necessary to obtain a certain accuracy, the formula (6.3) after VRIJLING (1997) could be applied

$$E = K \cdot \sqrt{\frac{1 - P_f}{N \cdot P_f}} \quad (6.3)$$

where P_f is the estimated failure probability, N is the required number of simulations, K is the accuracy and E is the percent error associated with N .

Considering the failure probabilities of Table 6.2 for 10000 simulations with $\rho_{c' \tan \phi'} = 0$ and $\rho_{c' \tan \phi'} = -0.6$, the corresponding percent error found applying formula (6.3) with an accuracy of 95% will be, respectively, 4.2% and 25%. On the other hand, formula (6.3) can also be used to evaluate the number of simulations required for a higher accuracy. As an example, a percent error of 10% is desired to get the same failure probability of Table 6.2 for the case with a negative correlation. Thus the number of simulations should be at least $N \approx 64000$.

Table 6.4 shows how the failure probability of the bearing capacity is influenced by the correlation coefficient. These results show that much lower probabilities of failure are found when the correlation coefficient between c' and $\tan \phi'$ decreases from 0 to -1.0 . In particular, for higher negative values of the correlation coefficient the system is apparently safe with $P_f = 0$.

$\rho_{c' \tan \phi'}$	$P_f(1000 \text{ MCS})$	$P_f(10000 \text{ MCS})$	$P_f(100000 \text{ MCS})$
0	0.051	0.0496	0.0348
-0.1	0.030	0.0371	0.0214
-0.2	0.021	0.0292	0.0169
-0.3	0.014	0.0194	0.0122
-0.4	0.005	0.0125	0.0078
-0.5	0.003	0.0056	0.0044
-0.6	0.002	0.0014	0.0014
-0.7	0	0.0001	0.0002
-0.8	0	0	0
-0.9	0	0	0
-1	0	0	0

Table 6.4: Influence of the correlation coefficient on the failure probability for benchmark 2

These facts are also shown in Fig. 6.1, where the failure probability is plotted against the correlation coefficient of the soil strength parameters for different Monte Carlo realisations.

If a certain density function is assumed as an approximation to plot MCS results, as shown in Fig. 6.2, then different failure probabilities can be found.

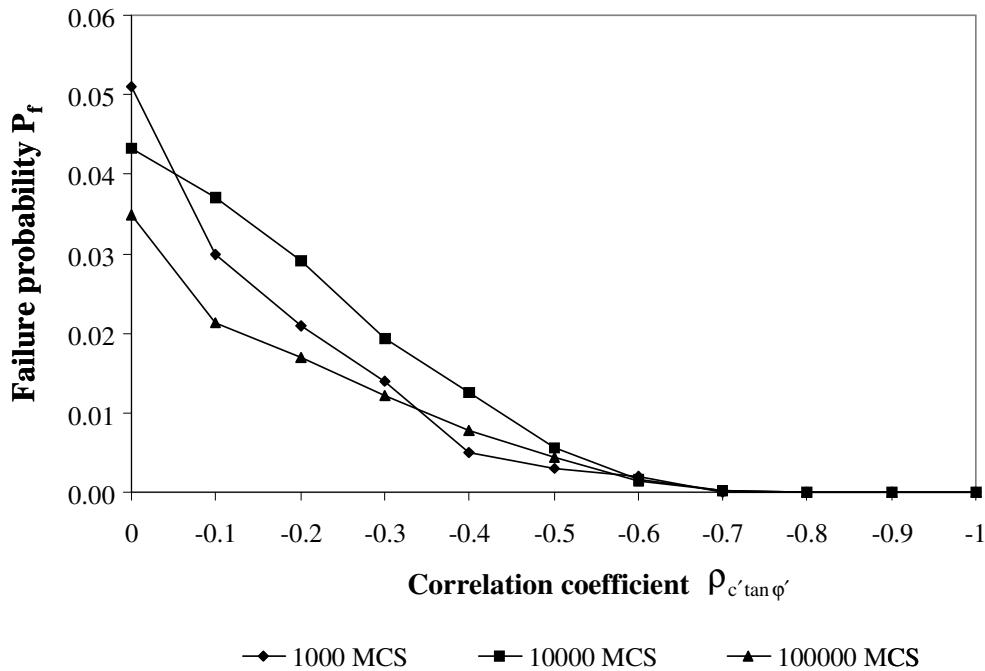


Figure 6.1: Failure probability versus correlation coefficient for benchmark 2

Failure probability of 10000 Monte Carlo Simulations		
assumed distribution	ρ _{c'tan φ'} = 0	ρ _{c'tan φ'} = -0.6
standard lognormal	0.0552	0.0031
shifted lognormal	0.0483	0.0013

Table 6.5: Failure probability of q_f assuming a standard lognormal and a shifted lognormal distribution as approximation of 10000 MCS with ρ_{c'tan φ'} = 0 and ρ_{c'tan φ'} = -0.6

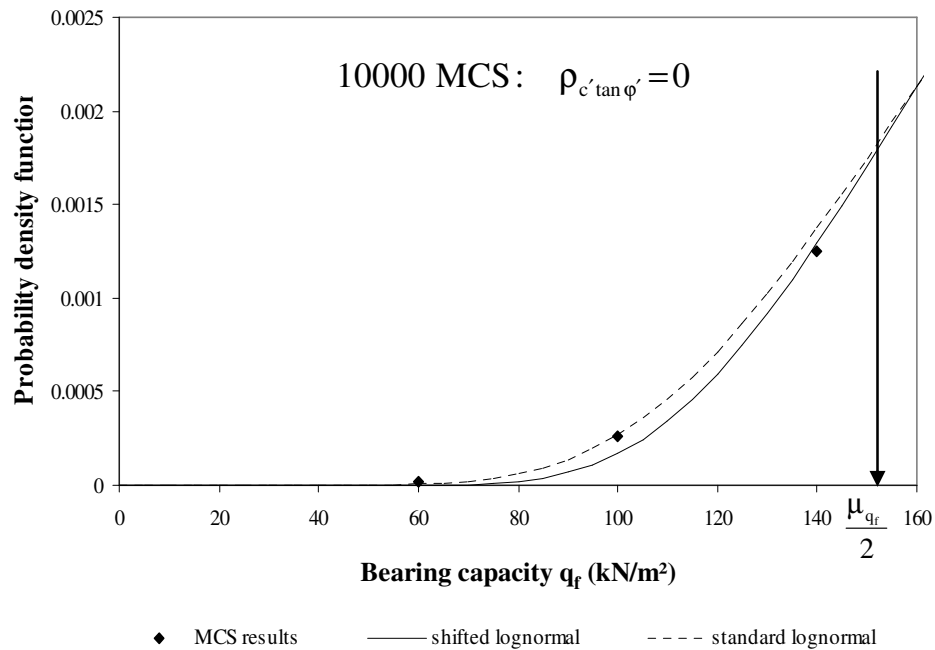


Figure 6.2: Unsafe regions of the bearing capacity assuming a standard lognormal and a shifted lognormal distribution for 10000 MCS with $\rho_{c' \tan \phi'} = 0$

Table 6.5 shows the failure probability values found by assuming a standard lognormal and a shifted lognormal distribution for 10000 MCS. The shifted lognormal distribution is the best choice, because it also matches the skewness coefficient of the bearing capacity.

In Table 6.5 it can be seen that the lowest values are those derived by the integration over the unsafe region described by the shifted lognormal distribution. This difference is clearly highlighted in Fig. 6.2, where the unsafe region given by the standard lognormal distribution is larger than that of the shifted lognormal density function.

The advantage of the Monte Carlo methodology is that it can be applied not only to linear, but also to non-linear performance functions, as in the case of the bearing capacity problem.

However, when the target failure probability is very small and a correlation between the input variables is taken into account, the number of simulations required to obtain an accurate result can be so large that it renders the application impractical.

6.2.2 Failure probability from FOSM and SOSM methods

As already mentioned in chapter 4, the FOSM and SOSM methods provide approximations only for the mean value and the standard deviation. Thus, one must assume a certain distribution function for plotting the bearing capacity results beforehand in order to estimate any failure probability. This can then be evaluated by integrating over the unsafe region of the assumed bearing capacity density function. In this way estimates of failure probabilities, especially with low values of P_f , are highly sensitive to the assumed distribution.

In Fig. 6.3 it can be seen the unsafe region of the bearing capacity given by assuming a standard lognormal distribution for FOSM results of benchmarks 2 considering uncorrelated soil variables. This region is found by taking into account values of the bearing capacity lower than the mean value divided by the safety factor $FS=2$.

In Tables 6.6 the failure probability values of the bearing capacity assuming a standard lognormal distribution to approximate FOSM and SOSM results, considering both uncorrelated and negatively correlated soil parameters are listed. If a negative correlation is considered much lower failure probabilities are found.

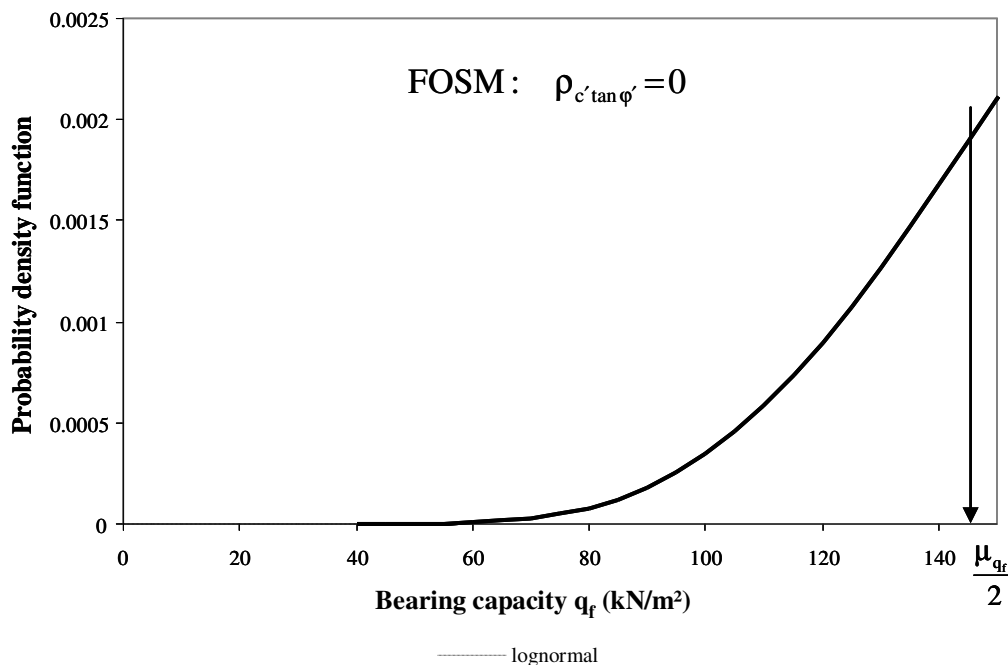


Figure 6.3: Unsafe region of the bearing capacity assuming a standard lognormal distribution for FOSM results with $\rho_{c' \tan \phi'} = 0$

When there is no information on the shape of the probability distribution, as in the case of FOSM and SOSM methods, for which no skewness is provided, another way of evaluating the reliability of the bearing capacity is to consider a normal distribution and then calculate the reliability index, which only depends on the first two moments of the performance function. Thus Eq. (2.24) can be easily applied, considering the limit state function Z as

$$Z = q_f - \frac{\mu_{q_f}}{2} \tag{6.4}$$

where q_f represents the resistance of the system, or ultimate bearing capacity, as a random variable with a certain probability density function. While $\mu_{q_f}/2$ is the deterministic load, given by the mean value of the bearing capacity divided by the safety factor $FS=2$. For a more detailed description about the ultimate bearing capacity and the corresponding safety factor the author refers to Appendix A.

Instead of considering the load deterministically, it can also be considered as a variable following a Dirac Delta function, given by

$$f(x) = \begin{cases} 1 & \text{if } x = \frac{\mu_{q_f}}{2} \\ 0 & \text{if } x \neq \frac{\mu_{q_f}}{2} \end{cases}$$

It has been shown that, when the soil parameters are negatively correlated, then the failure probability is lower than when uncorrelated variables are considered. Thus the reliability index is obviously higher, as this parameter is inversely related to the failure probability.

However, if an appropriate form of the bearing capacity density function is prescribed, the corresponding failure probability can be estimated by transforming this function into an equivalent normal distribution using special transformation formulas, such as the well-known Rosenblatt's transformation (ROSENBLATT, 1952).

Table 6.7 shows the reliability indices of the bearing capacity by assuming a standard lognormal distribution for FOSM and SOSM results for uncorrelated soil parameters and for a negative correlation of -0.6 . These values are obtained using Eq. (2.25), valid for a standard lognormal distribution and considering the limit state function Z as given by Eq. (6.4). The failure probability can then be

estimated by using Eq. (2.23). The results found are exactly those of Tables 6.6 and 6.7, thus confirming the failure probabilities estimated by integrating over the unsafe region of the bearing capacity plotted in Fig. 6.3.

lognormal distribution approximation		
Correlation	$P_f(\text{FOSM})$	$P_f(\text{SOSM})$
$\rho_{c' \tan \phi'} = 0$	0.0516	0.0434
$\rho_{c' \tan \phi'} = -0.6$	0.005	0.0043

Table 6.6: Failure probability of q_f assuming a standard lognormal distribution for FOSM and SOSM results considering $\rho_{c' \tan \phi'} = 0$ and $\rho_{c' \tan \phi'} = -0.6$

lognormal distribution approximation		
Correlation	$\beta(\text{FOSM})$	$\beta(\text{SOSM})$
$\rho_{c' \tan \phi'} = 0$	1.63	1.71
$\rho_{c' \tan \phi'} = -0.6$	2.58	2.63

Table 6.7: Reliability index of q_f assuming a standard lognormal distribution for FOSM and SOSM results considering $\rho_{c' \tan \phi'} = 0$ and $\rho_{c' \tan \phi'} = -0.6$

6.2.3 Failure probability from FORM

The First Order Reliability Method is also applied to evaluate the reliability of the bearing capacity problem.

As already seen in chapter 3, an iterative solution is required for the FORM to find the design point useful to identify the most probable combination of the input variables at failure. This procedure can lead to time consuming convergence problems when highly non-linear limit state functions are considered. However for the bearing capacity problem the iterative process converges rapidly, because only two input random variables are involved.

Gaussian normal distribution approximation		
Correlation	$P_f(\text{FORM})$	$\beta(\text{FORM})$
$\rho_{c' \tan \phi'} = 0$	0.0515	1.63
$\rho_{c' \tan \phi'} = -0.6$	0.0109	2.3

Table 6.8: Failure probability and reliability index of q_f from VaP application, assuming a normal distribution for FORM results with $\rho_{c' \tan \phi'} = 0$ and $\rho_{c' \tan \phi'} = -0.6$

For FORM application the soil cohesion, which is lognormally distributed, needs to be transformed into a standard normal variable with zero mean and standard deviation equal to unity, as, for example, described in VRIJLING (1997). In this publication, the analytical “modus operandi” of the FORM is reported. Results derived by the analytical procedure are then compared with those of the numerical optimisation routine of the VaP 2.2 software, already mentioned in chapter 3.

An advantage of the numerical method is that it offers the possibility to input different correlation values directly in the form of a matrix, thus overcoming the difficulties of the analytical procedure.

In addition, the level of accuracy of the VaP is very high. This is set at 10^{-6} . This value can also be changed according to the accuracy required.

Because of the higher accuracy of the numerical procedure, only FORM results derived by the VaP application are listed in Table 6.8. As the FORM requires the transformation of a non-normal distribution into a Gaussian distribution, the results are referred only to this function.

Compared to the case with $\rho_{c' \tan \phi'} = 0$, an almost 80% lower failure probability and a 30% higher reliability index are found when a negative correlation of -0.6 between cohesion and friction angle is considered.

6.2.4 Failure probability from PEM

It should be pointed out again that, contrary to the FOSM and SOSM methods, the PEM also provides the skewness coefficient of the bearing capacity.

This way it is possible to have an idea of the symmetry, or asymmetry, of the bearing capacity density function.

The results reported in Tables 5.4 and 5.7 show a positive skewness coefficient found using the PEM. Therefore a Gaussian distribution will not be assumed for approximating PEM results. In Fig. 6.4 the PEM results are plotted assuming both the standard lognormal and the shifted lognormal distributions.

The failure probability and the reliability index of the bearing capacity, evaluated considering the two approximation functions, can be therefore listed in Tables 6.9 and 6.10 and compared. The failure probability is estimated by integrating over the unsafe region of the assumed bearing capacity density functions. The reliability index is obtained by applying Eq. (2.25) for a lognormal distribution, where the limit state function Z is given by Eq. (6.4).

In Fig. 6.4 it is clear that the unsafe region given by the standard lognormal distribution is smaller than that given by the shifted lognormal distribution. This difference is confirmed by the failure probability and the reliability index values of Tables 6.9 to 6.10, when both uncorrelated and negatively correlated input variables are considered.

In fact, the highest failure probabilities are those referred to the shifted lognormal distribution, for which the lowest reliability index values obviously correspond. On the contrary, the lowest failure probabilities and the highest reliability index values are those related to the standard lognormal distribution.

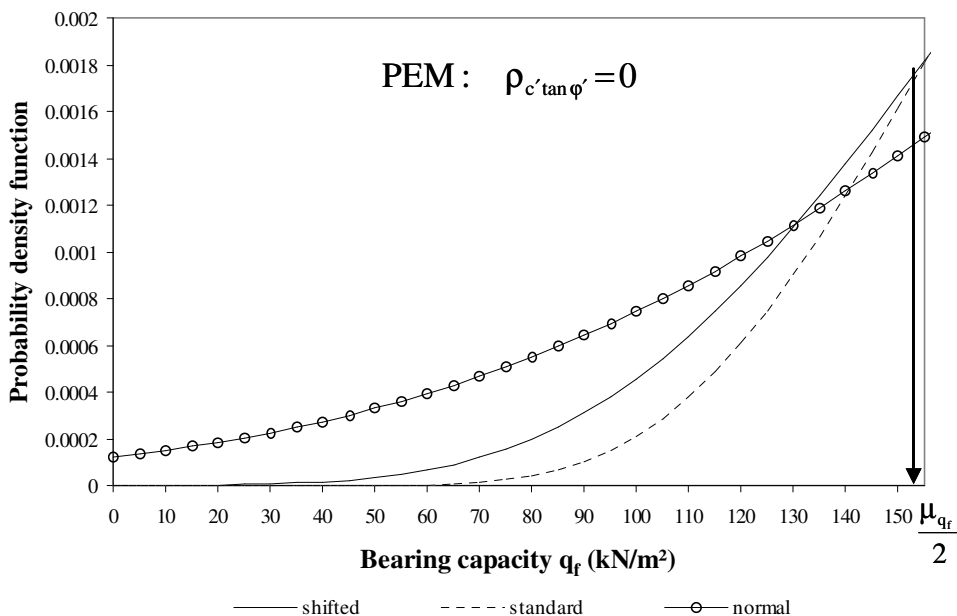


Figure 6.4: Unsafe regions of the bearing capacity assuming a standard lognormal and a shifted lognormal distribution for PEM results with $\rho_{c'tan\phi'} = 0$

standard lognormal distribution approximation		
Correlation	$P_f(\text{PEM})$	$\beta(\text{PEM})$
$\rho_{c' \tan \varphi'} = 0$	0.0484	1.66
$\rho_{c' \tan \varphi'} = -0.6$	0.0052	2.56

Table 6.9: Failure probability and reliability index of q_f assuming a standard lognormal distribution for PEM results considering $\rho_{c' \tan \varphi'} = 0$ and $\rho_{c' \tan \varphi'} = -0.6$

shifted lognormal distribution approximation		
Correlation	$P_f(\text{PEM})$	$\beta(\text{PEM})$
$\rho_{c' \tan \varphi'} = 0$	0.0651	1.56
$\rho_{c' \tan \varphi'} = -0.6$	0.0185	2.27

Table 6.10: Failure probability and reliability index of q_f assuming a shifted lognormal distribution for PEM results considering $\rho_{c' \tan \varphi'} = 0$ and $\rho_{c' \tan \varphi'} = -0.6$

6.2.5 Comparison of failure probabilities and necessity of a new approach

The aim of this section is to compare the failure probabilities of the bearing capacity previously estimated using Monte Carlo, PEM, FORM, FOSM and SOSM methods.

It is important to stress again that the MCS results do not need to be approximated by a certain probability density function, because this method already provides both the shape of the distribution curve and the failure probability for the bearing capacity problem. However different probability functions are considered here to show that one of these curves can more effectively approximate the results of the probabilistic methods applied.

The bearing capacity values representing the right extremes of the unsafe regions of the assumed probability density function, for which the target failure probability should be evaluated are listed in Table 6.11. As already mentioned, these values are estimated by dividing the bearing capacity mean values, found by applying different probabilistic methods, by a safety factor of 2. They are all very similar. The PEM values, however, are closer to those of MCS. Of course FOSM and FORM values are exactly the same, because they are found by applying the same formula, being the FORM an enhancement of FOSM.

Nevertheless, different right extreme values could be chosen to evaluate the failure probability, depending on the reliability level that one wants to achieve for the bearing capacity problem. In this section, only the values listed in Table 6.11 are taken into account.

The values 200 kN/m^2 and 250 kN/m^2 will be further considered for evaluating the failure probability of the bearing capacity by applying the advanced PEM. For more details, the author refers to section 6.3.

The unsafe regions found considering the right extremes of Table 6.11 and assuming a Gaussian normal, a standard lognormal and a shifted lognormal distribution as approximations of the bearing capacity results are plotted in Figs. 6.5, 6.6 and 6.7. These diagrams are drawn for both uncorrelated and negatively correlated soil parameters.

In particular, in Figs. 6.5 and 6.6 the unsafe regions referred to the results derived from all the probabilistic methods analysed, except for the FORM, are shown. The iterative procedure of the FORM method does not provide proper mean values and standard deviations of the bearing capacity (i.e. they vary depending on the choice of the design point), which can be compared with the statistical values of other methods. Nevertheless it gives the failure probability and the reliability index. In Fig. 6.7 only the MCS and PEM results are considered in the plot of the unsafe regions of the bearing capacity by assuming a shifted lognormal function. This is because the FOSM, SOSM and FORM methods do not provide any skewness values.

From these diagrams it is possible to see how the unsafe region decreases when a negative correlation is taken into account, especially for the MCS results approximated by a shifted lognormal distribution in Fig. 6.7.

This fact is more clear when Tables 6.12, 6.13 and 6.14 are examined. Here the failure probability evaluated by considering all probabilistic approaches and all assumed probability distributions are shown.

The analysis of the values of Tables 6.12, 6.13 and 6.14 illustrates, first of all, the importance of the correlation coefficient between c' and $\tan\phi'$ with respect to the failure probability (or conversely to the reliability index).

In fact when a negative correlation is considered in the calculation very different values of P_f , compared to the case with $\rho_{c'\tan\phi'} = 0$, are obtained, which are lower when $\rho_{c'\tan\phi'} = -0.6$. In other words, if the correlation is not considered, then the failure probabilities are higher than those actually observed when a negative correlation is imposed.

The real failure probabilities found by applying 10000 Monte Carlo simulations are those of Table 6.2. The fictitious failure probabilities in the hypothesis of assuming a certain probability distribution for the bearing capacity results of MCS are listed in Tables 6.12, 6.13 and 6.14.

An idea of the accuracy given by assuming different probability density functions when compared to the real values of the failure probability found by MCS is given in Table 6.15.

bearing capacity mean value μ_{q_f} (kN/m ²) / safety factor FS=2					
Correlation	10000 MCS	PEM	FOSM	SOSM	FORM
$\rho_{c'\tan\phi'} = 0$	153.403	153.393	145.439	151.925	145.439
$\rho_{c'\tan\phi'} = -0.6$	148.924	149.627	145.439	148.033	145.439

Table 6.11: Right extreme values of the bearing capacity unsafe regions for which the failure probability is evaluated

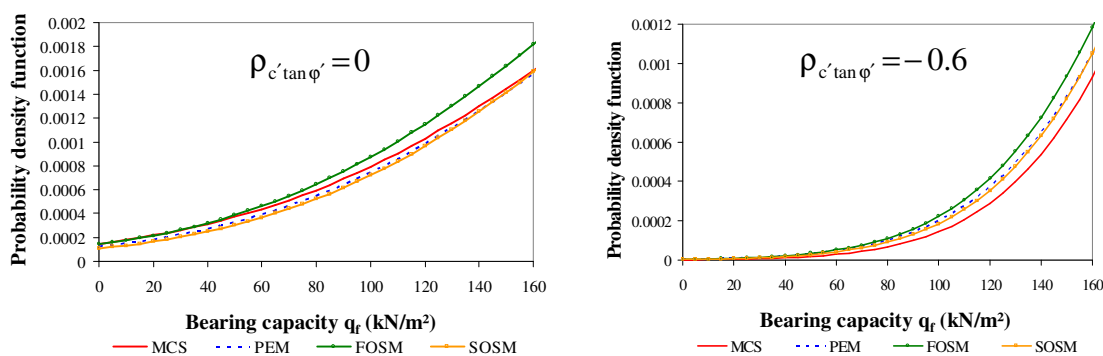


Figure 6.5: Unsafe regions of q_f assuming a normal distribution for different probabilistic methods considering $\rho_{c'\tan\phi'} = 0$ and $\rho_{c'\tan\phi'} = -0.6$

From this Table, it is clear that the fictitious failure probabilities found by assuming a shifted lognormal distribution are more accurate than when a normal and a standard lognormal distributions are considered. This is an additional good reason for choosing the shifted lognormal distribution as an approximation of the bearing capacity results. In fact, the fictitious failure probability of MCS increases greatly when a Gaussian distribution is taken into account, thus showing how a probabilistic result can deviate from reality depending on the assumption considered.

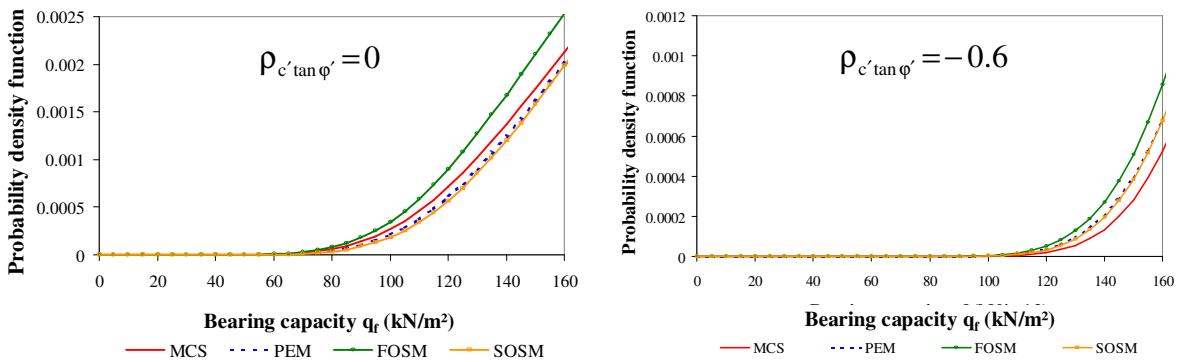


Figure 6.6: Unsafe regions of q_f assuming a standard lognormal distribution for different probabilistic methods considering $\rho_{c'\tan\phi'} = 0$ and $\rho_{c'\tan\phi'} = -0.6$

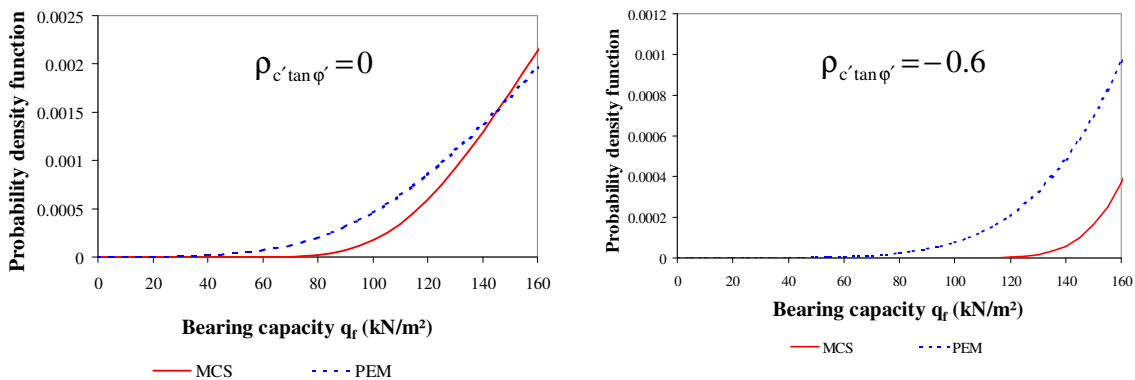


Figure 6.7: Unsafe regions of q_f assuming a shifted lognormal distribution for different probabilistic methods considering $\rho_{c'\tan\phi'} = 0$ and $\rho_{c'\tan\phi'} = -0.6$

A comparison of the FORM results of Table 6.12 with the MCS failure probabilities reported in Table 6.2 shows that the FORM method, based on the assumption of normal input variables, gives higher values than MCS. Two main causes of this discrepancy are: firstly, the bearing capacity is highly non-linear with $\tan\phi'$, which is one of the input variables that play an important role in this analysis. In fact, it is well-known that a linear approximation in the FORM design point causes some serious error in the estimation of the reliability index, thus influencing also the value of the failure probability. Secondly, the input variable cohesion follows a distribution, which is far from the normal distribution, thus introducing additional uncertainties in the final results when this is transformed to a normal variable.

Failure probability by assuming a Gaussian normal distribution					
Correlation	10000 MCS	PEM	FOSM	SOSM	FORM
$\rho_{c'\tan\phi'} = 0$	0.1005*	0.0936	0.1029	0.0931	0.0515
$\rho_{c'\tan\phi'} = -0.6$	0.0212*	0.0308	0.0275	0.0254	0.0109

* fictitious value. The real MCS failure probabilities are reported in Table 6.2.

Table 6.12: Failure probability of q_f assuming a normal distribution for different probabilistic methods considering $\rho_{c'\tan\phi'} = 0$ and $\rho_{c'\tan\phi'} = -0.6$

Failure probability by assuming a standard lognormal distribution					
Correlation	10000 MCS	PEM	FOSM	SOSM	FORM
$\rho_{c'\tan\phi'} = 0$	0.0552*	0.0484	0.0516	0.0434	-
$\rho_{c'\tan\phi'} = -0.6$	0.0031*	0.0052	0.005	0.0043	-

* fictitious value. The real MCS failure probabilities are reported in Table 6.2.

Table 6.13: Failure probability of q_f assuming a standard lognormal distribution for different probabilistic methods considering $\rho_{c'\tan\phi'} = 0$ and $\rho_{c'\tan\phi'} = -0.6$

Failure probability by assuming a shifted lognormal distribution					
Correlation	10000 MCS	PEM	FOSM	SOSM	FORM
$\rho_{c'\tan\phi'}=0$	0.0483*	0.0651	-	-	-
$\rho_{c'\tan\phi'}=-0.6$	0.0013*	0.0185	-	-	-

* fictitious value. The real MCS failure probabilities are reported in Table 6.2.

Table 6.14: Failure probability of q_f assuming a shifted lognormal distribution for different probabilistic methods considering $\rho_{c'\tan\phi'}=0$ and $\rho_{c'\tan\phi'}=-0.6$

Accuracy [%] of MCS results assuming different PDFs		
assumed PDF	$\rho_{c'\tan\phi'}=0$	$\rho_{c'\tan\phi'}=-0.6$
normal	50%	10%
standard lognormal	90%	45%
shifted lognormal	97%	93%

Table 6.15: Accuracy of the failure probability values found by assuming a normal, a standard lognormal and a shifted lognormal distribution to approximate MCS results

One should therefore be very careful in applying the approximation procedure of FORM in the reliability analysis of a structure that has a highly non-linear performance function, such as a shallow foundation design. This fact is also valid for FOSM and SOSM methods, as already stressed in chapter 3.

When a standard lognormal distribution is considered, it seems to be that the failure probabilities evaluated using the PEM are apparently closer to MCS values of Table 6.2, especially for the case with uncorrelated soil parameters.

However, it has been previously shown that the shifted lognormal distribution approximates MCS results best. Then only the failure probabilities referred to

this function should be taken into account. These values are listed in Table 6.14, where PEM failure probabilities are given together with the fictitious ones of MCS. The PEM, as a direct non-iterative method, overcomes the convergence problem of FORM, thus being a more promising alternative. Unfortunately, in this case the PEM results are even higher than those of FORM method, when compared with the real failure probability values of MCS, shown in Table 6.2. In order to cope with the shortcoming of the PEM in evaluating low failure probabilities, a new method is proposed, referred to as the advanced PEM. The methodology of the proposed approach is described in detail in the next section.

6.3 Application of the Advanced PEM to the bearing capacity problem

In the previous section the necessity of developing a new probabilistic method is stated. The aim of this section is to describe this new methodology, called Advanced Point Estimate Method, or shortly APEM, which is not yet available in the literature, and to show its application to the bearing capacity problem.

6.3.1 Short description of the Advanced PEM methodology

The basic idea of the Advanced PEM is to focus on the critical values of the input data, i.e. cohesion and friction angle, which could cause bearing capacity failure. The reduced intervals of the soil parameters can be found using an iteration procedure or by experts opinion.

Then the PEM is applied to these reduced intervals and the bearing capacity statistical values are plotted in a graph by assuming the well-known shifted lognormal distribution. It is then possible to evaluate low failure probabilities of the bearing capacity more precisely. These values are then compared with the Monte Carlo failure probabilities of Table 6.2 to verify the accuracy of the APEM.

6.3.2 The reduced intervals of the input soil parameters

In chapter 4 it has been seen that the effective soil cohesion and friction angle are described respectively by a standard lognormal and a normal distribution with their corresponding statistical values, as shown in Figs. 4.1(a), (b) and 4.2.

For the new probabilistic method, i.e. the APEM, a reduced interval of both parameters should be considered. These intervals contain values of the cohesion and friction angle, which can most probably cause bearing capacity failure.

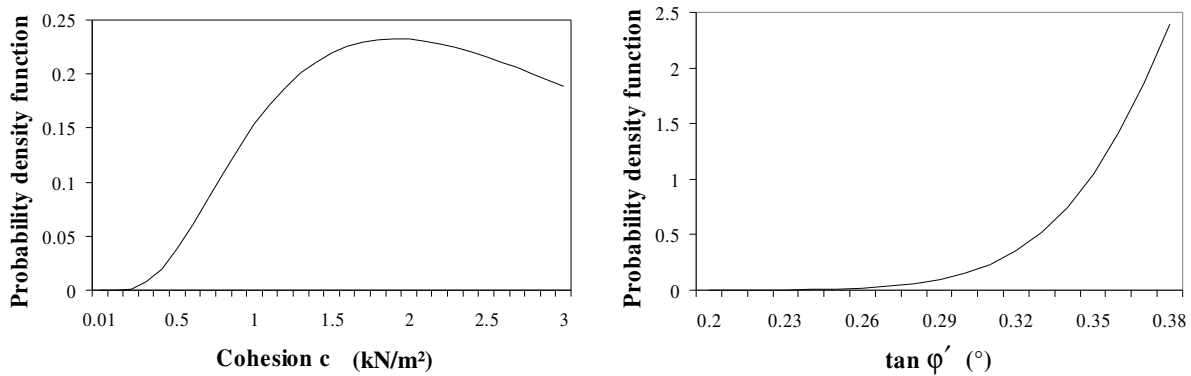


Figure 6.8: Reduced intervals of the soil input variables

There are two different ways of establishing these ranges, either by choosing them on the basis of experts knowledge or using an iteration procedure:

- “experts” are geotechnical engineers who know the behaviour of the soil layer in question, thus being able to better judge which values of the shear parameters can be more dangerous for the stability of the strip footing considered;
- the iteration procedure can be represented by an algorithm which considers different combinations of soil cohesion and friction angle values and finding those which give failure of the bearing capacity problem.

For this study an algorithm, described in appendix C, has been implemented in MATLAB[®] Version 7.0 to determine the reduced intervals of the soil parameters c' and $\tan\phi'$.

It has been observed that the cohesion has a negligible influence on the bearing capacity compared to the friction angle. For this reason a constant range of 0 - 3 kN/m² is considered for this soil parameter. While for the friction angle the algorithm finds a value of 21°, i.e. $\tan\phi' \approx 0.384$, if the right extreme value of the unsafe region of the bearing capacity is considered to be equal to its mean value divided by a safety factor 2. The reduced intervals are then plotted in Fig. 6.8. The corresponding statistical values are respectively

- for c' : $\mu_{c'_{red}} = 1.87 \text{ kN/m}^2$; $\sigma_{c'_{red}} = 0.65 \text{ kN/m}^2$; $\nu_{c'_{red}} = -0.08$

- for $\tan\phi'$: $\mu_{\tan\phi'_{red}} = 0.35$; $\sigma_{\tan\phi'_{red}} = 0.02$; $\nu_{\tan\phi'_{red}} = -1.37$

where “red” means “reduced intervals”. Comparing these values to those of Figs. 4.1(a), (b) and 4.2, the new ones are obviously different. The mean values and standard deviations are lower and the skewness coefficient negative because of the shape of the reduced probability density functions of the soil input data.

6.3.3 Application of the PEM to the reduced intervals of the soil parameters

As in chapter 5, the PEM is now applied step by step to the reduced intervals of c' and $\tan\phi'$ of Fig. 6.8, considering first of all no correlation between them, then a correlation of -0.6.

6.3.3.1 Case with $\rho_{c' \text{red} \tan\phi' \text{red}} = 0$

1. The relationship (4.6) between the dependent variable q_f and the input soil variables $\tan\phi'$ and c' is considered.
2. Then the sampling point locations for $\tan\phi'$ and c' are computed. First of all the standard deviation units are evaluated for both soil parameters by applying Eqs. (3.6), thus leading to

$$\xi_{\tan\phi' \text{red}+} = 0.527$$

$$\xi_{\tan\phi' \text{red}-} = 1.897$$

$$\xi_{c' \text{red}+} = 0.962$$

$$\xi_{c' \text{red}-} = 01.039.$$

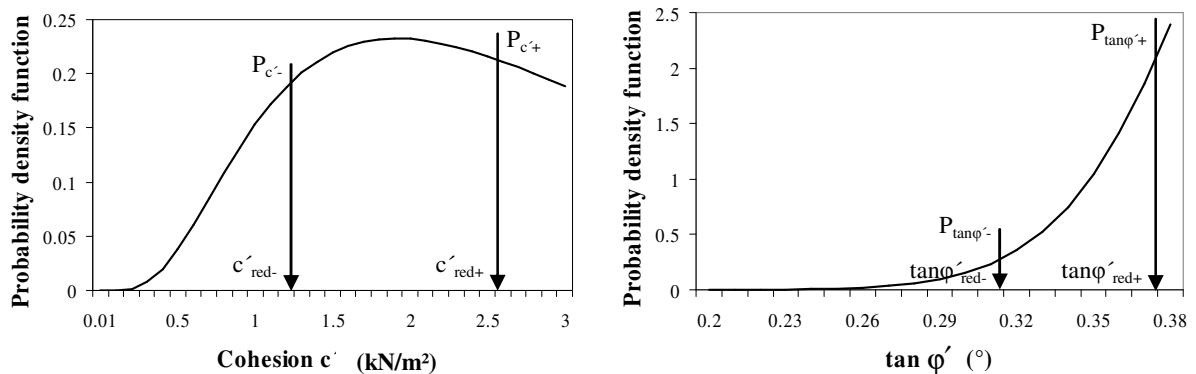


Figure 6.9: Sampling point locations and weights of the reduced soil parameters

Hence the corresponding sampling point locations can be evaluated using Eqs. (3.7), which give

$$\tan \phi'_{\text{red}_-} = 0.309$$

$$\tan \phi'_{\text{red}_+} = 0.368$$

$$c'_{\text{red}_+} = 2.503 \text{ kN/m}^2$$

$$c'_{\text{red}_-} = 1.192 \text{ kN/m}^2.$$

3. The weights P_i , giving each of the four point estimates of soil parameters considered as single random variables, are then determined using Eq. (3.8) valid for a single random variable,

$$P_{\tan \phi'_{\text{red}_+}} = 0.782$$

$$P_{\tan \phi'_{\text{red}_-}} = 0.217$$

$$P_{c'_{\text{red}_+}} = 0.519$$

$$P_{c'_{\text{red}_-}} = 0.481.$$

Figure 6.9 shows the locations of the sampling points of both soil parameters $\tan \phi'$ and c' . The corresponding weights are also shown in this diagram. Then the associated weights need to be found, considering the input parameters as multiple uncorrelated variables. For this aim Eq. (3.13) is here applied, which gives the following values

$$P_{++} = P_{\tan \phi'_{\text{red}_+}} \cdot P_{c'_{\text{red}_+}} = 0.406$$

$$P_{+-} = P_{\tan \phi'_{\text{red}_+}} \cdot P_{c'_{\text{red}_-}} = 0.376$$

$$P_{-+} = P_{\tan \phi'_{\text{red}_-}} \cdot P_{c'_{\text{red}_+}} = 0.113$$

$$P_{--} = P_{\tan \phi'_{\text{red}_-}} \cdot P_{c'_{\text{red}_-}} = 0.105.$$

4. The value of the bearing capacity at each sampling point can then be evaluated. The results are shown in Table 6.16.

$P_{\pm\pm}$	c'_{\pm}	$\tan \phi'_{\pm}$	$q_{f\pm\pm}$
0.406	2.503 kN/m ²	0.368	148.705 kN/m ²
0.376	1.192 kN/m ²	0.368	129.004 kN/m ²
0.113	2.503 kN/m ²	0.309	106.494 kN/m ²
0.105	1.192 kN/m ²	0.309	90.153 kN/m ²

Table 6.16: Associated weights, sampling points and bearing capacity values for the reduced intervals of $\tan\phi'$ and c'

5. Now the mean value, variance and skewness coefficient of the bearing capacity can be determined using Eqs. (3.15), (3.16) and (3.17), where $n = 2$. The results of the statistical estimates of q_f predicted by PEM considering small values of the input soil parameters are presented in Table 6.17.

μ_{q_f}	σ_{q_f}	COV_{q_f}	ν_{q_f}
130.641 kN/m ²	19.278 kN/m ²	0.148	-0.823

Table 6.17: Statistical values of q_f predicted by PEM considering reduced intervals of the uncorrelated soil parameters

The bearing capacity results reported in Tables 6.16 and 6.17 are clearly lower than those of Tables 5.3 and 5.4, due to the consideration of smaller values of the cohesion and friction angle. In addition, the skewness coefficient is negative, thus the probability density function of the bearing capacity should be negatively skewed. This distribution should be at the same time able to approximate the statistical results of Table 6.17 best and to give a failure probability similar to the MCS value of Table 6.2 for uncorrelated soil parameters.

The reason of choosing this particular density function the author refers to section 6.3.4, where a shifted lognormal distribution will be assumed to approximate the reduced bearing capacity results.

6.3.3.2 Case with $\rho_{c'_{red}\tan\phi'_{red}} = -0.6$

When negatively correlated soil parameters are considered then the steps 1 to 3 lead to the same results as the case with uncorrelated soil parameters. The only difference is that the associated weights change because of the contribution of the correlation coefficient -0.6 . The formula of Christian (3.13) can be easily applied here, thus giving

$$\begin{aligned}
 P_{++} &= P_{\tan\phi'_{red+}} \cdot P_{c'_{red+}} \cdot (1 - 0.6) = 0.163 \\
 P_{+-} &= P_{\tan\phi'_{red+}} \cdot P_{c'_{red-}} \cdot (1 + 0.6) = 0.602 \\
 P_{-+} &= P_{\tan\phi'_{red-}} \cdot P_{c'_{red+}} \cdot (1 + 0.6) = 0.181 \\
 P_{--} &= P_{\tan\phi'_{red-}} \cdot P_{c'_{red-}} \cdot (1 - 0.6) = 0.042.
 \end{aligned}$$

4. The values of the bearing capacity at each sampling point are reported in Table 6.18.

$P_{\pm\pm}$	c'_{\pm}	$\tan\phi'_{\pm}$	$q_{f\pm\pm}$
0.163	2.503 kN/m ²	0.368	148.956 kN/m ²
0.602	1.192 kN/m ²	0.368	129.244 kN/m ²
0.181	2.503 kN/m ²	0.309	106.695 kN/m ²
0.042	1.192 kN/m ²	0.309	90.342 kN/m ²

Table 6.18: Associated weights, sampling points and bearing capacity values for the reduced intervals of $\tan\phi'$ and c' with $\rho_{c'_{red}\tan\phi'_{red}} = -0.6$

5. Now the statistical values of the bearing capacity can be determined using Eqs. (3.15), (3.16) and (3.17), where $n = 2$. Then the results predicted by PEM considering small values of the input soil parameters are shown in Table 6.19.

The bearing capacity mean value and standard deviation reported in Tables 6.19 are slightly lower than those of Table 6.17, due to the consideration of a

negative correlation between the soil parameters. On the other hand the skewness coefficient is higher, thus the bearing capacity density function should be less left skewed than for the case with $\rho_{c' \text{red} \tan\phi' \text{red}} = 0$.

μ_{q_f}	σ_{q_f}	COV_{q_f}	v_{q_f}
125.045 kN/m ²	14.656 kN/m ²	0.122	-0.190

Table 6.19: Statistical values of q_f predicted by PEM considering reduced intervals of the soil parameters with $\rho_{c' \text{red} \tan\phi' \text{red}} = -0.6$

This fact will be seen in section 6.3.4, where a shifted lognormal distribution will be assumed as approximation of the bearing capacity statistical values. A comparison of the results reported in Tables 6.17 and 6.19 will be also shown graphically.

6.3.4 Shifted lognormal approximation of the bearing capacity results

In previous sections reduced intervals of c' and $\tan\phi'$, which can cause bearing capacity failure, have been considered and new statistical values of the bearing capacity have been evaluated, thus obtaining the results of Tables 6.17 and 6.19, for uncorrelated as well as for negatively correlated soil parameters.

Now it is necessary to choose a probability density function which can approximate these new results best and, at the same time can lead to failure probability values similar to those found by applying the Monte Carlo approach.

In chapters 4 and 5 it has been shown that, compared with other well-known probability distributions, the shifted lognormal distribution matches very well the results of PEM and MCS for the bearing capacity problem. Hence this function will be assumed here to approximate the reduced mean value, standard deviation and skewness coefficient of the bearing capacity and to evaluate the corresponding failure probability.

The aim of this section is to describe the procedure adopted to find the three parameters of the shifted lognormal distribution, which lead to a better approximation of the results listed in Tables 6.17 and 6.19 and to failure probabilities similar to those of 10000 Monte Carlo simulations, considering different values of the right extreme of the unsafe region.

It will be seen that, independent of Monte Carlo results, this procedure can also be useful to find different combinations of the shifted lognormal parameters which give different target failure probabilities, depending on the reliability level to be achieved.

6.3.4.1 Procedure to find the shifted lognormal parameters

In Figs. 5.10 and 5.11 bearing capacity results have been compared considering the entire curve of the shifted lognormal distribution for PEM and MCS estimates plotted pointwise. Now a reduced interval of the bearing capacity will be taking into account to compare the results of Tables 6.17 and 6.19 and to evaluate the corresponding failure probability.

For this reason one needs to evaluate the three parameters x_0 , $\mu_{\ln(X)}$ and $\sigma_{\ln(X)}$ of the shifted lognormal distribution that approximate the reduced results of the bearing capacity best. As only small values of the bearing capacity are of interest to estimate the target failure probability, attention will only be paid to the shape of the curve describing the unsafe region for this reduced interval.

To find the parameters already mentioned the following procedure, described stepwise, is adopted:

1. The shifted lognormal distribution $f_X(x)$ described by Eq. (2.15), depending on the three parameters x_0 , $\mu_{\ln(X)}$ and $\sigma_{\ln(X)}$, is considered. For practical reason this function is shown again below.

$$f_X(x) = \frac{1}{\sqrt{2\pi}(x-x_0)\sigma_{\ln(X)}} \exp\left\{-\frac{1}{2}\left[\frac{\ln(x-x_0)-\mu_{\ln(X)}}{\sigma_{\ln(X)}}\right]^2\right\}, \quad x_0 < x < +\infty$$

2. The mathematical definition of mean value, variance and skewness coefficient given, respectively, by Eqs. (2.4), (2.5) and (2.9), are taken into account to link up the reduced statistical values of the bearing capacity, reported in Tables 6.17 and 6.19, to the shifted lognormal distribution, as described by the following equations:

$$\mu_{q_f \text{ red}} = \frac{\int_{x_0^+}^{x_m} x \cdot f_X(x) dx}{\int_{x_0^+}^{x_m} f_X(x) dx} \quad (6.5)$$

$$\sigma_{q_f \text{ red}}^2 = \frac{\int_{x_0^+}^{x_m} (x - \mu_{q_f \text{ red}})^2 \cdot f_X(x) dx}{\int_{x_0^+}^{x_m} f_X(x) dx} \quad (6.6)$$

$$V_{q_f \text{ red}} = \frac{\int_{x_0^+}^{x_m} (x - \mu_{q_f \text{ red}})^3 \cdot f_X(x) dx}{\sigma_{q_f \text{ red}}^3 \int_{x_0^+}^{x_m} f_X(x) dx} \quad (6.7)$$

In Eqs. (6.5), (6.6) and (6.7), x represents the variable “bearing capacity” depending on the soil parameters c' and $\tan\phi'$; $f_X(x)$ is the probability density function of the shifted lognormal distribution. The left extreme x_0^+ of the integration interval is given by the location parameter x_0 summed up to a certain value. This value should be higher than zero because of the logarithm inside equation (2.15). For a practical solution a value of 10^{-1} is adopted, thus $x_0^+ = x_0 + 10^{-1}$ and Eqs. (6.5), (6.6) and (6.7) are then limit improprius integrals. The theoretical solution is given by considering the full integrals.

In addition, the value x_m is the right extreme of the unsafe region of the bearing capacity. To compare failure probabilities of APEM and MCS, the value x_m is first of all assumed for both methods equal to 150 kN/m^2 , which approximates the values listed in Table 6.11 for MCS and PEM. Then the bearing capacity values 200 kN/m^2 and 250 kN/m^2 are also taken into account to show that this procedure can be adopted to evaluate any target failure probability.

3. It should be pointed out that, as opposed to Eqs. (2.4), (2.5) and (2.9), in Eqs. (6.5) to (6.7) mean value, variance and skewness coefficient are given for an area smaller than the unity. This area, also referred to as unsafe region, is given by the integral of the denominator of these equations and quantitatively corresponds to the failure probability, defined by the following formula

$$P_f(q_f) = \int_{x_0^+}^{x_m} f_X(x) dx \quad (6.8)$$

4. So far four equations, i.e. Eqs. (6.5) to (6.8), with four unknowns, i.e. x_0 , $\mu_{\ln(X)}$, $\sigma_{\ln(X)}$ and P_f are given, which constitute a linear system to be solved to find the shifted lognormal distribution for approximating APEM results.

To solve this system an algorithm has been implemented in MATLAB[®] Version7, whose aim is to optimise the objective function F described by equation (6.9).

$$F = \left(\frac{\int_{x_0^+}^{x_m} x \cdot f(x) dx}{\int_{x_0^+}^{x_m} f(x) dx} - \mu_{q_f \text{ red}} \right)^2 + \left(\frac{\int_{x_0^+}^{x_m} (x - \mu_{q_f \text{ red}})^2 \cdot f(x) dx}{\int_{x_0^+}^{x_m} f(x) dx} - \sigma_{q_f \text{ red}}^2 \right)^2 + \left(\frac{\int_{x_0^+}^{x_m} (x - \mu_{q_f \text{ red}})^3 f(x) dx}{\sigma_{q_f \text{ red}}^3 \cdot \int_{x_0^+}^{x_m} f(x) dx} - \nu_{q_f \text{ red}} \right)^2 + \left(P_f(q_f) - \int_{x_0^+}^{x_m} f(x) dx \right)^2 \quad (6.9)$$

This optimisation problem consists basically in finding those values of the unknown parameters x_0 , $\mu_{\ln(X)}$, $\sigma_{\ln(X)}$ and of the failure probability P_f which minimise the function F . For this reason initial values of the unknowns, delimited by lower and upper bounds, are input in the algorithm, which runs until the minimum of F is reached. Unfortunately this algorithm can lead to different local minima of the function F when different combinations of the initial values of the 4 unknowns are considered. To overcome this problem, one of the four unknowns should be fixed. The failure probability value obtained by the Monte Carlo method is then considered as known parameter for the optimisation. In this way the model finds the three shifted lognormal parameters which give the minimum of the objective function for the desired reliability level given in the form of a target failure probability.

In Appendix C a more detailed description of the routine used to find the shifted lognormal parameters and to evaluate the failure probability is given together with the results of this study for both uncorrelated and negatively correlated soil variables.

6.4 Results comparison of MCS, traditional PEM and APEM

In this section the failure probabilities evaluated using 10000 Monte Carlo simulations, the traditional PEM and the advanced PEM are presented and compared for different intervals and correlation values of the soil parameters.

6.4.1 Case with $\rho_{c' \text{ red} \tan \phi' \text{ red}} = 0$

The results of 10000 Monte Carlo simulations for uncorrelated soil variables together with those of the traditional PEM approximated by the shifted

lognormal distribution are shown in Fig. 6.10. These results are listed, respectively, in Table 4.5 for MCS and 5.4 for PEM. Furthermore the APEM results, reported in Table 6.17, are also drawn assuming a shifted lognormal distribution.

q_f - interval of APEM application	friction angle
APEM(150): 0 - 150 kN/m ²	0 - 22.5°
APEM(200): 0 - 200 kN/m ²	0 - 24.5°
APEM(250): 0 - 250 kN/m ²	0 - 24.75°

Table 6.20: Bearing capacity range of APEM application for different friction angle intervals

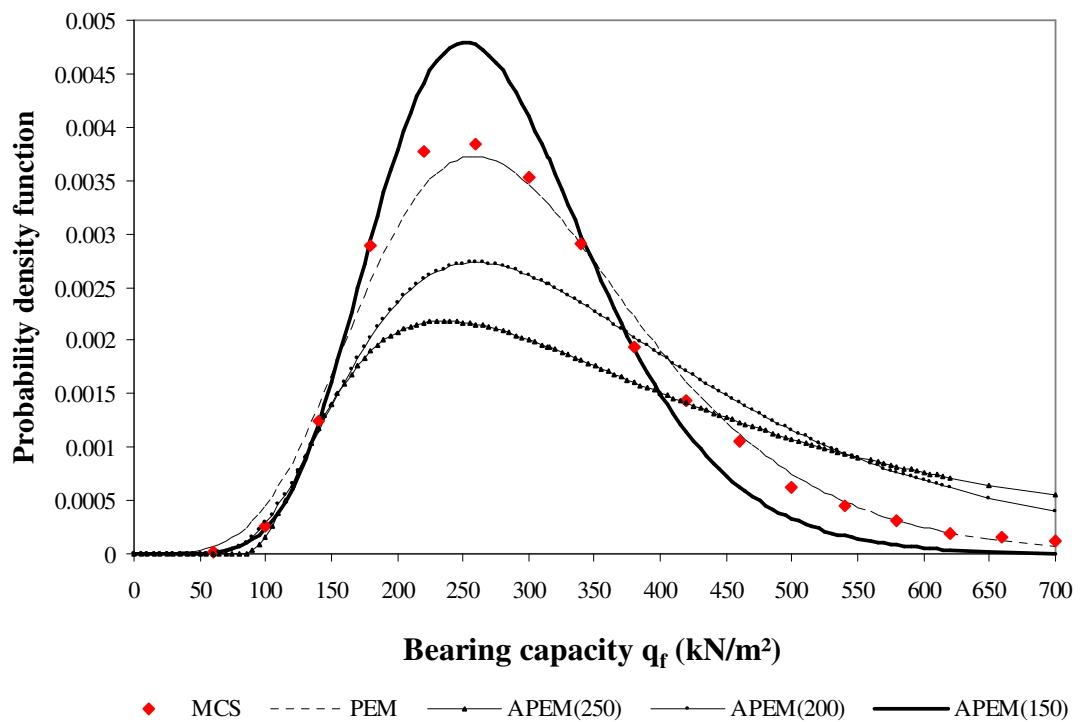


Figure 6.10: Results comparison of MCS and PEM with those of APEM considering different intervals of the friction angle and $\rho_{c'} \tan \phi'_{red} = 0$

To understand the influence of the friction angle on the behaviour of the bearing capacity, different intervals of this soil parameter are considered for APEM application, as described in Table 6.20. The interval of the cohesion is constant, always in the range of 0 - 3 kN/m².

As a first impression it is clear that, considering the entire interval of bearing capacity values, the curve referred to the traditional PEM matches well the MCS results, while those approximating the APEM statistical values are very different to these results.

However, to evaluate low failure probabilities, attention is paid only to the unsafe regions of the bearing capacity, as plotted in Fig. 6.11, and not to the entire probability density functions. In fact, looking at Fig. 6.11, it is clear that the APEM curves are effectively closer to Monte Carlo results than the traditional PEM when one focuses only on the unsafe regions.

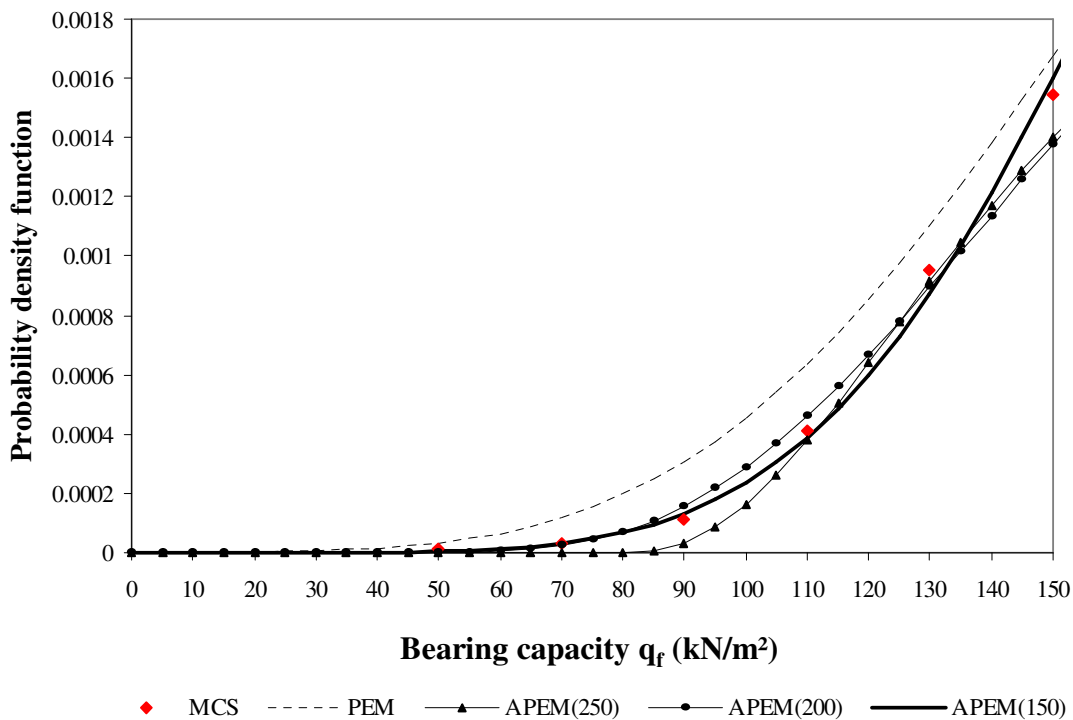


Figure 6.11: Results comparison of MCS and PEM with those of APEM considering different intervals of ϕ' , $\rho_{c'_{red}\tan\phi'_{red}} = 0$ and focusing on the unsafe regions

$P_f (\rho_{c'_{red}\tan\phi'_{red}} = 0)$					
right extreme of q_f	MCS	PEM	APEM(250)	APEM(200)	APEM(150)
250 kN/m ²	0.3656	0.3532	0.2565	-	-
200 kN/m ²	0.1767	0.1798	0.134	0.1392	-
150 kN/m ²	0.0432	0.0598	0.0463	0.0437	0.0433

Table 6.21: Failure probabilities of MCS, PEM and APEM for different bearing capacity right extreme of the unsafe region and considering $\rho_{c'_{red}\tan\phi'_{red}} = 0$

In particular, the prediction of the failure behaviour of the bearing capacity is remarkably improved by the optimisation on the shifted lognormal parameters, especially for the case defined as APEM(150), i.e. when smaller values of the friction angle are considered. This demonstrates how the assumed range of the friction angle can influence the final results of a bearing capacity reliability analysis.

Instead, when the shifted lognormal parameter $\mu_{\ln(X)}$ is considered fixed, then the model finds the failure probability values listed in Table 6.21 for different intervals of the friction angle. These values are here compared to the failure probabilities evaluated by means of the Monte Carlo and the traditional Point Estimate methods.

When a failure probability is evaluated for an unsafe region, whose right extreme is the value $q_f = 250 \text{ kN/m}^2$, the traditional PEM seems to give a value closer to that of MCS. On the other hand, when smaller unsafe region are considered, then the APEM failure probabilities are more similar to those of MCS. They are practically the same for reduced interval of the friction angle and when considering the right extreme $q_f = 150 \text{ kN/m}^2$.

6.4.2 Case with $\rho_{c'_{red}\tan\phi'_{red}} = -0.6$

For the case with negatively correlated soil parameters the results of 10000 MCS are plotted pointwise in Fig. 6.12 together with those of the traditional PEM and the APEM (applied for different friction angle intervals), approximated both by the shifted lognormal distribution. These results are given, respectively, in Table 4.8 for MCS, Table 5.7 for PEM and Table 6.21 for APEM.

From Fig. 6.12 one can also see the divergence between the APEM approximation curves and Monte Carlo results, when the entire probability density function of the bearing capacity is taken into account. Thus the PEM is, apparently, more accurate than the APEM.

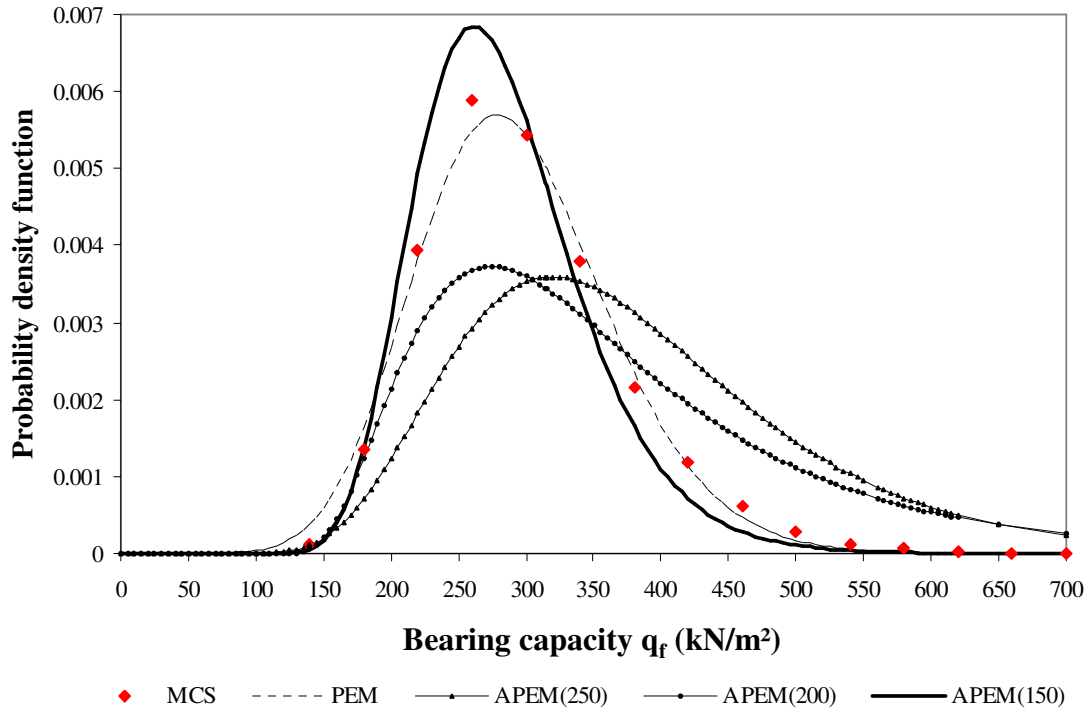


Figure 6.12: Results comparison of MCS and traditional PEM with those of APEM considering different intervals of the friction angle and $\rho_{c' \text{red} \tan \phi' \text{red}} = -0.6$

On the other hand, when one concentrates only on the unsafe region of the bearing capacity, zoomed in Fig. 6.13, then APEM curves are closer to MCS results than the traditional PEM. In particular, when smaller values of the friction angle are considered, i.e. for APEM(150), the curve is in perfect agreement with MCS results.

When the shifted lognormal parameter $\mu_{\ln(X)}$ is considered as known instead of the failure probability and when a negative correlation exists between soil parameters, the improvement of the results using the APEM is even clearer, both graphically, as Fig. 6.13 shows, and quantitatively in terms of failure probabilities, as reported in Table 6.22.

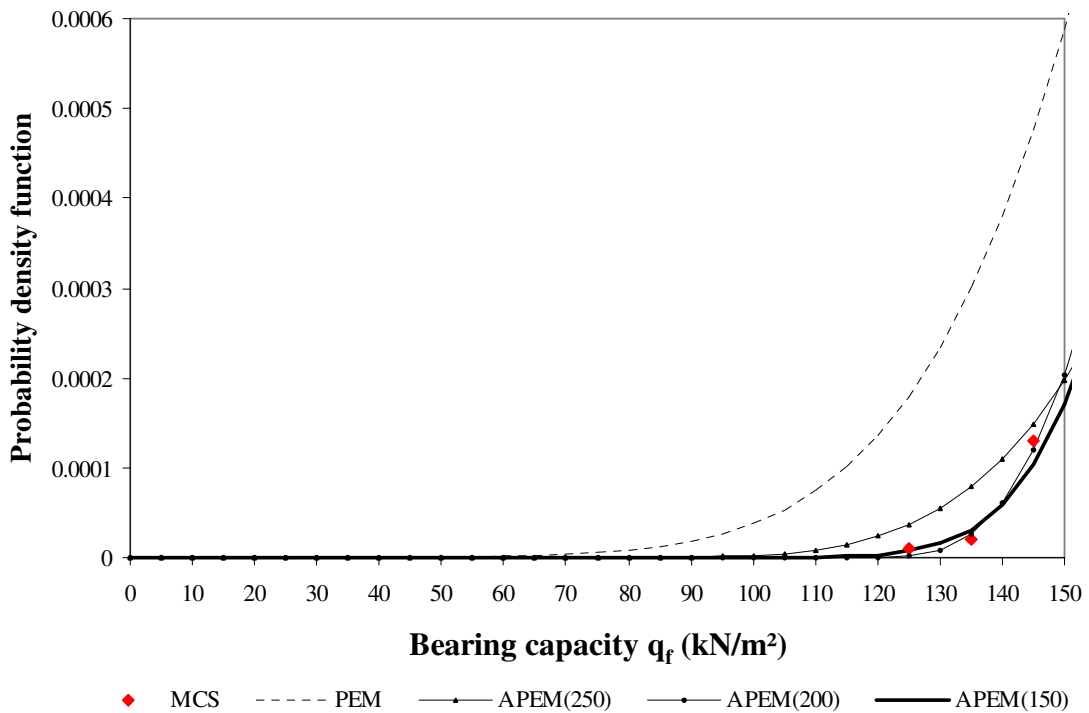


Figure 6.13: Results comparison of MCS and PEM with those of APEM considering different intervals of ϕ' , with $\rho_{c' \text{redtan}\phi' \text{red}} = -0.6$ and focusing on the unsafe regions

On the other hand, when one concentrates only on the unsafe region of the bearing capacity, zoomed in Fig. 6.13, then APEM curves are closer to MCS results than the traditional PEM. In particular, when smaller values of the friction angle are considered, i.e. for APEM(150), the curve is in perfect agreement with MCS results.

When the shifted lognormal parameter $\mu_{\ln(X)}$ is considered as known instead of the failure probability and when a negative correlation exists between soil parameters, the improvement of the results using the APEM is even clearer, both graphically, as Fig. 6.13 shows, and quantitatively in terms of failure probabilities, as reported in Table 6.22.

The observations of the failure probability values calculated for uncorrelated soil variables are valid also when $\rho_{c' \text{redtan}\phi' \text{red}} = -0.6$, except that now the failure probability given by APEM(150) considering the right extreme $q_f = 150 \text{ kN/m}^2$ is exactly the same as the value estimated using 10000 MCS.

$P_f (\rho_{c'_{red}\tan\phi'_{red}} = -0.6)$					
right extreme of q_f	MCS	PEM	APEM(250)	APEM(200)	APEM(150)
250 kN/m ²	0.2686	0.2885	0.1330	-	-
200 kN/m ²	0.0601	0.0866	0.0345	0.0551	-
150 kN/m ²	0.0015	0.0117	0.0029	0.0016	0.0015

Table 6.22: Failure probabilities of MCS, PEM and APEM for different bearing capacity right extreme of the unsafe region and considering $\rho_{c'_{red}\tan\phi'_{red}} = -0$

Summarising all the findings about the APEM, it can then be concluded that this new promising probabilistic approach gives excellent predictions of the failure behaviour of the bearing capacity, especially when negatively correlated soil parameters and reduced friction angle intervals are considered.

6.5 Applicability of the estimated failure probability of the bearing capacity

After having estimated the failure probability of the bearing capacity problem in the previous chapter, the next step is to assess whether it is an acceptable value or not.

Typically, this is achieved through comparing the computed failure probabilities with a probabilistic design criterion or using diagrams usually used in decision-making, such as the one of BAECHER (1982) shown in Fig. 6.14. This kind of diagrams has proven to be a useful tool for describing the meaning of failure probabilities and risks in the context of other risks familiar to the society.

In Fig. 6.14 the annual failure probability of well-known engineering structures is plotted against the cost in dollars or the number of lives lost in a year. Both axes are in logarithmic scale.

This experimental diagram reveals the rates of failure and costs that the society finds acceptable, or, can live with nowadays.

In particular for foundations, the annual failure probability considered as acceptable by the society is included in the range $10^{-2} - 10^{-3}$, thus having, for example, a higher frequency of failure than dams, but lower annual lost of lives and money.

6.5 Applicability of the estimated failure probability of the bearing capacity

For the strip footing of the bearing capacity problem it has been seen in Tables 6.21 and 6.22 that a magnitude order of $10^{-1} - 10^{-3}$ is found when the unsafe region has a right extreme of the bearing capacity equals to 250 kN/m^2 . Whereas this order of magnitude decreases down to $10^{-2} - 10^{-3}$ when the right extreme is 150 kN/m^2 . Hence the failure probabilities evaluated for the bearing capacity problem seem to be realistic when compared with the annual failure rates indicated in the diagram of Fig.6.14.

In any case, whenever one is dealing with estimated failure probabilities, it must be clear that these values have to be considered as lower bounds of the real failure probabilities. This is due to the fact that some effects of important factors, which might cause failure, are perhaps ignored in the reliability analysis. Thus engineers should be careful not to be too confident in the computed failure probabilities.

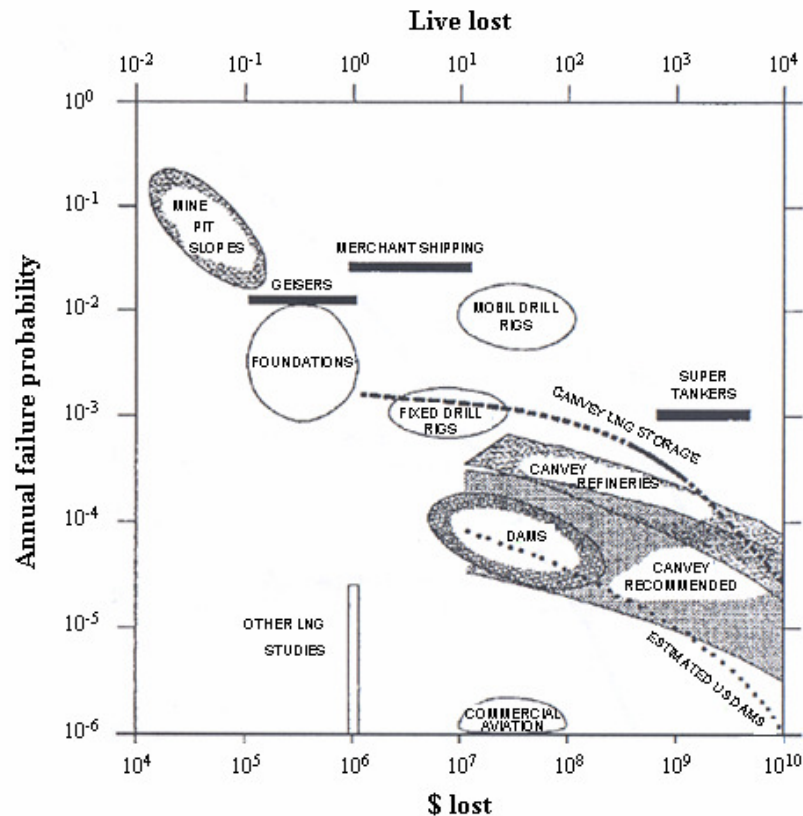


Figure 6.14: Annual failure probability versus annual risk cost in dollars and number of lives lost for various engineering structures (BAECHER, 1982)

Chapter 7

Conclusions and further research

Introduction

The aim of this research was to give a further contribution to the application of well-known probabilistic methods to the study of the bearing capacity problem, showing that a probabilistic analysis does not require more effort than that needed in a conventional deterministic study, but it provides a very useful means of modelling uncertainties involved in the calculations.

It is fundamental for engineers to ensure safety and reliability of geotechnical structures. Another important aim of this work was to find a method able to evaluate small failure probabilities of the bearing capacity. As a consequence, the Advanced Point Estimate Method, described in chapter 6, was developed. This was a big challenge. For this reason the author hopes that this promising tool can be applied to a more comprehensive reliability analysis, helping engineers in interpreting the probabilistic results and, thus, representing a new perspective in the field of geotechnical engineering.

In the next sections the most important conclusions of the present thesis will be given, followed by some recommendations for further research.

7.1 General conclusions

In chapter 2 the primary sources and types of uncertainties, which strongly affect geotechnical engineering, were described. In spite of the advances in modern computational resources and information technology for dealing with uncertainties, the knowledge of engineers on uncertain parameters involved in a design remains imperfect. As CHRISTIAN (2004) pointed out, uncertainty can be ignored by applying the deterministic approach, with the risk of being too conservative, thus leading to too expensive projects. On the other hand engineers can decide to quantify uncertainties, thus contributing to a more rational reliability analysis. It was seen that probabilistic and statistical analyses are a powerful means for dealing with uncertainties, providing them with a more logical mathematical framework. In spite of the reluctance of experts in applying probabilistic concepts and methods, in recent years these techniques are finding increasing application in the geotechnical field.

In chapters 3 the methodology of the most widely known probabilistic methods were exhaustively illustrated and their advantages and limitations were discussed.

7.2 Conclusions with respect to the probabilistic methods applied to the bearing capacity problem

In chapter 4 well-known probabilistic methods were applied to the study of two benchmarks on the bearing capacity of a strip footing on a homogeneous soil layer, considering different correlation coefficients between the soil parameters.

It has been shown that the Monte Carlo approach requires only fundamental knowledge of statistics and probability theory to solve the bearing capacity problem. It is generally considered as the most accurate and reliable probabilistic method, because not only mean value, standard deviation and skewness coefficient of a certain performance function can be obtained, but also the corresponding probability distribution can be built up. However, as for practical problems this method is too time consuming, other approaches were considered.

The moments methods FOSM and SOSM were chosen as alternative approaches to replace the Monte Carlo simulations, because they involved a limited amount of calculations. In spite of the similar results in terms of mean value and standard deviation with MCS, these methods did not provide any skewness coefficient of the bearing capacity, as Monte Carlo did. Thus, no information was given about the shape of the probability density function of the bearing capacity. It had to be assumed to approximate the final results. In addition, these approaches are generally accurate only for linear functions, thus the accuracy diminishes as the non-linearity of a function increases. Since the bearing capacity is a highly non-linear function of the effective friction angle, then some inaccuracies were introduced in the final results of FOSM and SOSM methods. Consequently, it was necessary to choose another probabilistic alternative, which could be able to overcome the drawbacks of MCS, FOSM and SOSM methods, providing the skewness coefficient together with the other statistical estimates, but with less computational effort than Monte Carlo method.

7.3 Conclusions with respect to the Two Point Estimate Method

In chapter 5 the Two Point Estimate Method after ROSENBLUETH (1975) was applied to the bearing capacity problem and the results were compared with those of MCS, FOSM and SOSM methods.

Similar results were obtained for all the probabilistic methods applied in terms of mean value and standard deviation of the bearing capacity. On the other hand, different conclusions can be drawn for the skewness coefficient. Actually, the First Order Second Moment and the Second Order Second Moment methods did not allow the evaluation of the skewness coefficient, thus being substantially less accurate than the Point Estimate Method. Moreover, a significant difference was observed between the skewness coefficients provided by the PEM and the Monte Carlo method.

However, it is important to stress that the PEM significantly decreased the computational effort of the probabilistic study of the bearing capacity problem. In fact, on one hand, the PEM did not involve the evaluation of partial derivatives of the bearing capacity formula, thus being more straightforward applied than FOSM and SOSM methods. On the other hand, when both soil cohesion and friction angle were considered as input variables (i.e. in benchmark 2), at least ten thousands of Monte Carlo simulations were necessary to get accurate statistical values of the bearing capacity, while only four calculations were required by the PEM to get results as accurate and reliable as those of the Monte Carlo method in terms of mean value and standard deviation.

In the last decades, the PEM is finding increasing application in practical problems and efforts are carried out to implement this method in finite elements codes. However experts, who are familiar with the mathematical background of this method, suggest the use of the PEM only under special conditions, for which it is expected to give good results. These conditions were mentioned in chapter 5 and are summarised here:

a) in order to reduce the error in the PEM results, the variation coefficient of the input random variables should not be large. For the probabilistic analysis of the bearing capacity problem a variation coefficient of 80% was taken into account for the soil cohesion, which is larger than the values usually found in the literature;

b) when multiple input random variables are considered, the skewness coefficient can only be reliably calculated by applying formula (3.17) of the PEM after ROSENBLUETH if the variables are uncorrelated and if the performance function is linear, which is not the case for the bearing capacity formula;

c) to cope with the problem of condition b), different formulas are available in the literature to evaluate the sampling point weights of the PEM for correlated input parameters, such as those proposed by CHRISTIAN et al. (1999) and shown in chapter 3. Unfortunately these formulas are valid only for symmetrical input variables. Thus, one should be careful in applying them to cases in which the transformation of an input variable changes its distributional form. In this research, in fact, in order to apply CHRISTIAN's formula, the lognormal soil cohesion c' had to be transformed into the normal variable $\ln c'$. So doing, the correlation coefficient between the input soil variables cohesion and friction angle changed, because of the different mean value and standard deviation of c' and $\ln c'$, thus influencing the evaluation of the sampling point weights.

These three conditions influenced the probabilistic results of the bearing capacity problem, thus being the primary reason of the difference between the skewness estimates of the PEM and the MCS. Despite its limitations, the PEM was shown to be a simple, but powerful technique for probabilistic analysis, as it required less computational effort than MCS for a comparable degree of accuracy.

7.4 Conclusions with respect to the shifted lognormal distribution

In chapter 5 the importance of assuming a certain probability density function as opposed to others to approximate and plot the results of the probabilistic analysis of the bearing capacity problem were discussed.

Considering the Monte Carlo results, it was possible to define the shape of the bearing capacity density function. In fact, from these results it was clear that a reasonable assumption for the bearing capacity estimates should be a positively (right) skewed probability distribution.

Different continuous probability distributions are available in the literature to approximate these results. In Geotechnics the Gaussian normal and the standard lognormal distributions are frequently used, because of their mathematical simplicity. Furthermore, the necessary statistical information about these functions is widely available, including probability tables.

In this research, the shifted lognormal distribution was chosen to plot the probability distribution of the bearing capacity, not only because it is strictly non-negative and can be treated mathematically straightforward, but especially because it matches well all the three moments of the bearing capacity, i.e. mean value, standard deviation and skewness. Hence, the final approximation is more

accurate and reliable than other probability density functions. This represents one of the most basic findings of this work.

Other good reasons for preferring the shifted lognormal distribution to other well-known continuous probability density curves are listed below:

- the first term of the bearing capacity formula (A.4) after Terzaghi is given as the product of the soil parameters c' and $\tan\phi'$. For the central limit theorem, the distribution of the bearing capacity should then tend to a lognormal distribution;
- generally the Gaussian distribution allows negative values of a certain performance function, which is physically unrealistic for soil parameters. For this reason this distribution could only be considered as a rough approximation;
- the Weibull distribution presented a high discrepancy with the other functions considered in this work. In addition, as this distribution is usually truncated at a lower bound, it did not describe the entire interval of the bearing capacity results, as the others did;
- for the reliability analysis of the bearing capacity problem, the shifted lognormal distribution showed to be the best fit-curve of all considered for approximating MCS results, leading to failure probabilities in good agreement with those evaluated using the Monte Carlo method.

It can be concluded that the shifted lognormal distribution was shown to be an important and useful density curve for approximating the results of a probabilistic analysis. As there is little information about the application of this function in geotechnical literature, it is suggested that the shifted lognormal distribution has to be considered for further probabilistic studies.

7.5 Conclusions with respect to the correlation between the soil parameters c' and $\tan\phi'$

Another important finding in this research refers to the correlation between the soil parameters cohesion and friction angle. In the literature some authors have often based their probabilistic studies considering uncorrelated parameters to simplify calculations, thus being more conservative. Other authors found negative correlation between cohesion and friction angle on the basis of experimental data. However, in geotechnical literature it is hard to find

probabilistic studies based on the assumption of a negative correlation between soil parameters.

In this work, different correlations between cohesion and friction angle was taken into account for the probabilistic analysis of the bearing capacity.

Independent of the probabilistic method applied, a lower bearing capacity variability was shown in chapter 5 and much lower failure probabilities (conversely, much higher reliability indices) were found in chapter 6 when a negative correlation is considered, thus affecting the final results of the probabilistic and reliability analyses significantly.

It can be then concluded that the choice of a negative correlation between soil parameters is reasonable, because the uncertainty in the probabilistic analysis is effectively reduced and the reliability level strongly increased.

7.6 Conclusions with respect to the reliability analysis

In chapter 6 the results of the reliability analysis of the bearing capacity problem were shown in terms of failure probability and reliability index for both uncorrelated and negatively correlated soil parameters. All the probabilistic methods described in chapter 3 were applied and the corresponding results were then compared.

Since many parameters are not incorporated in the reliability analysis to simplify calculations, then the estimated failure probability, referred to the lifetime of the shallow foundation, should be considered as a lower bound to the absolute probability of failure. If a more elaborate probabilistic risk analysis would be executed, taking into account all the uncertain contingencies, then the absolute risk could be evaluated.

Initially the Monte Carlo method was considered to evaluate the failure probability of the bearing capacity. It was found that, increasing the simulations number, the failure probability decreased thus increasing the reliability level. The MCS were easily applied to the non-linear performance function “bearing capacity”. However, in practice, when the target failure probability is very small and a correlation between the input variables is taken into account, the number of simulations required to obtain an accurate result can be so large that it renders the application impractical.

For this reason, the PEM, FOSM, SOSM and FORM methods were also applied to evaluate the reliability of the bearing capacity. As these approaches did not provide any probability density function, one had to assume a certain distribution to plot the bearing capacity results and then estimate the corresponding failure probability by integrating over the unsafe region of the

assumed density function. In this way, estimates of the failure probability are highly sensitive to the assumed distribution.

Moreover, the approximation procedures FORM, FOSM and SOSM showed some additional drawbacks in the reliability analysis of the bearing capacity problem. First of all, the iterative procedure of the FORM method overestimated the failure probability when compared with MCS results. This is due to the fact that the bearing capacity is highly non-linear with $\tan\phi'$, which is one of the input variables that play an important role in this analysis. In fact, it is well-known that a linear approximation in the FORM design point causes some serious error in the estimation of the reliability index, thus influencing also the value of the failure probability. One should therefore be very careful in applying the approximation procedures of FORM, FOSM and SOSM in the reliability analysis of a structure that has a highly non-linear performance function, such as a shallow foundation design. In addition, the input variable cohesion follows a distribution, which is far from the normal distribution for which the FORM method can be applied, thus introducing additional uncertainties in the final results when this is transformed to a normal variable.

Furthermore, as all of these methods did not provide any skewness, then their results could not be approximated by the shifted lognormal distribution, which proved to be the best-fit curve for MCS results, also in term of failure probabilities.

The PEM, as a direct non-iterative method, overcomes the convergence problem of FORM, and provides a value for the skewness coefficient, thus being a more promising alternative. Hence, only the PEM failure probabilities were considered to be compared with those of the MCS. Unfortunately, these values were in this analysis even higher than those of FORM method, when compared with the real failure probability values of MCS.

It can be concluded that, apparently, the FORM method showed to give better failure probability results than PEM. However FORM estimates were found by considering a normal distribution, which is not the best-fit curve for approximating MCS results.

7.7 Conclusions with respect to the APEM

In order to overcome the drawback of the PEM for the assessment of low failure probabilities, a so called advanced PEM, or shortly APEM, was developed. This method is not yet available in the literature.

The basic idea of the APEM is to focus on the relatively small values of the cohesion and the friction angle, which could cause most probably bearing

capacity failure. The reduced intervals of the soil parameters were found using an iterative procedure. The PEM was then applied to these intervals and the results were approximated by the shifted lognormal distribution to evaluate a target failure probability.

It was seen that, reducing the interval of the friction angle, the failure probability decreased. On the other hand, the width of the cohesion interval was shown not to have a great influence on the bearing capacity results.

This new promising probabilistic approach was shown to give the best predictions of the failure behaviour of the bearing capacity when compared with the traditional PEM, FOSM, SOSM and SOSM methods and excellent estimates when compared with MCS, especially if negatively correlated soil parameters were considered.

The application of the proposed method on the bearing capacity problem was feasible, since the mathematical and probabilistic background required to understand its methodology is not very complicated. Furthermore, the idea of considering reduced intervals of the cohesion and the friction angle is in practice more logical for the evaluation of small failure probabilities of the bearing capacity. Therefore the APEM should be easily accepted by practical engineers.

7.8 Recommendations for further research

The application of well-known probabilistic methods to the bearing capacity problem showed the necessity of providing a mathematical framework for dealing with uncertainties in a more rational manner. Combining the traditional deterministic approach and the probabilistic analysis in further research can be beneficial to geotechnical engineering practice, supporting engineering judgement and improving the decision-making process.

Also, the proposed APEM could in future be an important tool for evaluating small failure probabilities of geotechnical structures. Therefore, the next step should be an user-friendly implementation of this approach into finite element codes and its extension to some real case studies, such as the slope stability problem. This would improve its applicability in practical design and allow a more definitive judgement on its advantages and limitations.

It must be clear that this research showed the results of a simplified probabilistic analysis of the bearing capacity problem, ignoring some important factors of uncertainties, such as the heterogeneity of soil properties. So doing the failure probability can be overestimated, leading to erroneous results. Thus the next

challenge is to include the APEM into more complex geotechnical models (e.g. highly non-linear; 3D) considering all significant sources of uncertainty, such as the inherent spatial variability of soil parameters.

Appendix

A. The Terzaghi's bearing capacity formula

The function of a foundation is to transfer the load of a structure to the soil on which it is resting without overstressing it. Overstressing the soil can result in either excessive settlement or shear failure of the soil, both of which could damage the structure. Thus the bearing capacity of soils must be evaluated to avoid these problems.

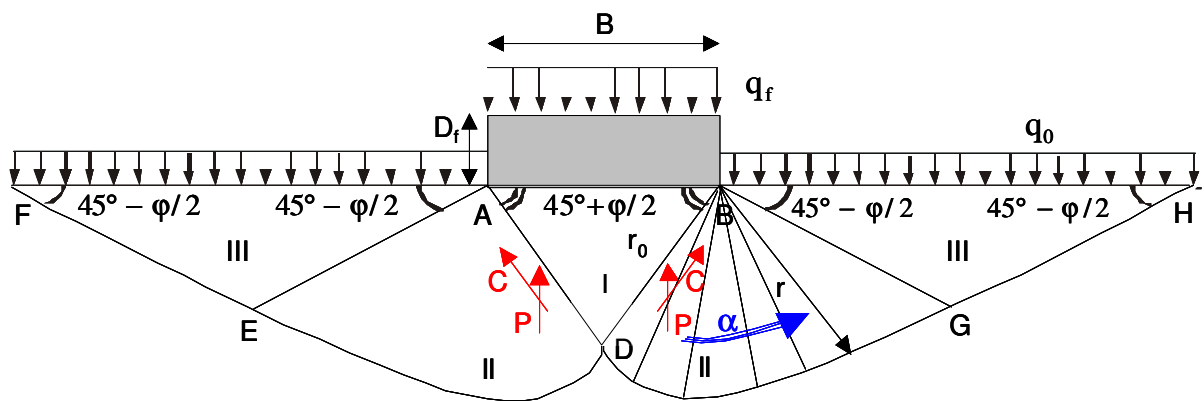


Figure A.1: Terzaghi's failure mechanism for the bearing capacity analysis

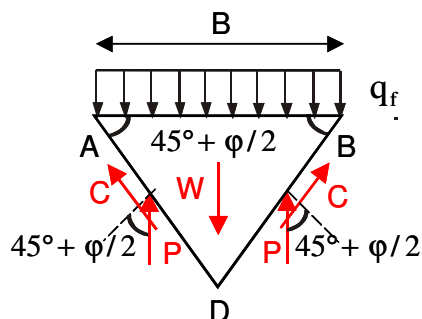


Figure A.2: Forces acting on the soil wedge I

The failure mechanism assumed by TERZAGHI (1943) for determining the ultimate bearing capacity of a shallow foundation is shown in Fig. A.1. The soil-zone I is an elastic zone, zones III are the radial shear zones and zones II are arcs of a logarithmic spiral, whose equation is given as

$$r = r_0 \cdot e^{(\alpha - \alpha_0) \cdot \tan \phi'} \quad (\text{A.1})$$

The lines EF and GH are straight lines. If the load per unit area q_f is applied to the shallow foundation and general shear failure occurs, the passive force P is acting on each of the faces of the soil wedge ABD.

Considering the soil wedge I and a unit length of the foundation, as in Fig. A.2, one has for equilibrium conditions

$$q_f \cdot B \cdot 1 = -W + 2 \cdot C \cdot \sin \phi' + 2 \cdot P \quad (\text{A.2})$$

where

$$W = \gamma \cdot \frac{B^2}{4} \cdot \tan \phi' = \text{weight of the soil wedge}$$

$$C = \frac{c \cdot B / 2}{\cos \phi'} = \text{cohesive force}$$

$$P = \frac{1}{2} \cdot \gamma \cdot \left(\frac{B}{2} \cdot \tan \phi' \right)^2 \cdot K_\gamma + c \cdot \left(\frac{B}{2} \tan \phi' \right) \cdot K_c + q_0 \cdot \left(\frac{B}{2} \cdot \tan \phi' \right) K_q = \text{passive force} \quad (\text{A.3})$$

K_q , K_c and K_γ are earth pressure coefficients depending on the soil friction angle which are very tedious to evaluate. Introducing the values of Eqs. (A.3) in Eq. (A.2) the ultimate bearing capacity equation will be then given by

$$q_f = c \cdot N_c + q_0 \cdot N_q + \frac{1}{2} \cdot \gamma \cdot B \cdot N_\gamma \quad (\text{A.4})$$

where c is the soil cohesion, q_0 is the surcharge (or overburden stress), γ is the unit soil weight, B is the footing width and N_q , N_c and N_γ are the bearing capacity factors defined by the following equations:

$$N_q = K_q \cdot \tan \varphi' = e^{\pi \cdot \tan \varphi'} \cdot \tan^2 \cdot \left(\frac{\pi}{4} + \frac{\varphi'}{2} \right) \quad \text{after PRANDTL (1921)}$$

$$N_c = (K_c + 1) \cdot \tan \varphi' = (N_q - 1) \cdot \cot \varphi' \quad \text{after PRANDTL (1921)}$$

$$N_\gamma = \frac{\tan \varphi'}{2} \cdot (K_\gamma \cdot \tan \varphi' - 1) = 1.8 \cdot (N_q - 1) \cdot \tan \varphi' \quad \text{after BRINCH-HANSEN (1961)} \quad (\text{A.5})$$

Equation (A.4) shows in a simple way that the ultimate bearing capacity is a function of three contributions, i.e. the soil weight inside the failure surface, the soil cohesion acting along the failure surface and the surcharge applied at the surface.

The bearing capacity factors depend on the friction angle of the soil. The equations (A.5) for evaluating N_q and N_c were first obtained by PRANDTL (1921), which are exact closed-form solutions obtainable using the limit analyses. In the German literature these two factors are denoted respectively as N_d and N_c .

On the other hand no closed-form solution exists for N_γ and the equation (A.5) for this factor is only one of the approximations available in the literature. The difference between these solutions is up to a factor of two, depending on the wedge angle below the foundation.

The first solution for N_γ was obtained by CAQUOT and KERISEL (1953) and can be expressed in the form

$$N_\gamma = 2 \cdot (N_q - 1) \cdot \tan \varphi' \quad (\text{A.6})$$

Equation (A.6) is for example applied in the EUROCODE 7 (1994). This formula has been further extended by BRINCH-HANSEN (1970), as given in Eq. (A.5). This solution is considered in this work for the evaluation of the bearing capacity.

In the German literature the bearing capacity factor N_γ obtained by MEYERHOF (1963), denoted as N_b , is applied, which can be evaluated with the following equation

$$N_b = N_\gamma = (N_q - 1) \cdot \tan(1.4 \cdot \varphi') \quad (\text{A.7})$$

The scope of this study is not to demonstrate how to derive the bearing capacity factors. For more information, the reader could refer to TERZAGHI (1943), LANCELLOTTA (1993), LANCELLOTTA and CALAVERA, (1999).

Generally a factor of safety of about 2 or more is applied to the ultimate bearing capacity to reach the allowable value of q_f .

B. Derivatives of the bearing capacity for the FOSM and SOSM methods

The first derivatives of the bearing capacity computed analytically with respect to the soil parameters c' and $\tan \phi'$ are given by Eqs. (B.1) and (B.2):

$$\frac{\partial q_f}{\partial c'} = \frac{1}{\tan \phi'} \cdot \left\{ e^{\pi \cdot \tan \phi'} \cdot \left[\tan \phi' + (1 + \tan^2 \phi')^{1/2} \right]^2 - 1 \right\} \quad (\text{B.1})$$

$$\frac{\partial q_f}{\partial \tan \phi'} = \quad (\text{B.2})$$

$$\begin{aligned} &= -22.5 + c' \cdot \left\{ \frac{1}{\tan^2 \phi'} - \frac{1}{\tan^2 \phi'} \cdot e^{\pi \cdot \tan \phi'} \cdot \left[\tan \phi' + (1 + \tan^2 \phi')^{1/2} \right]^2 + \frac{\pi}{\tan \phi'} \cdot e^{\pi \cdot \tan \phi'} \cdot \right. \\ &\cdot \left[\tan \phi' + (1 + \tan^2 \phi')^{1/2} \right]^2 + 4 \cdot e^{\pi \cdot \tan \phi'} \cdot \left[\tan \phi' + (1 + \tan^2 \phi')^{1/2} \right] \cdot \left[1 + \frac{1}{2} \cdot (1 + \tan^2 \phi')^{-1/2} \right] \left. \right\} + \\ &+ q_0 \cdot \left\{ \pi \cdot e^{\pi \cdot \tan \phi'} \cdot \left[\tan \phi' + (1 + \tan^2 \phi')^{1/2} \right]^2 + 4 \cdot e^{\pi \cdot \tan \phi'} \cdot \tan \phi' \cdot \left[\tan \phi' + (1 + \tan^2 \phi')^{1/2} \right] \cdot \right. \\ &\cdot \left[1 + \frac{1}{2} \cdot (1 + \tan^2 \phi')^{-1/2} \right] \left. \right\} + 1.5 \cdot \gamma \cdot \left\{ e^{\pi \cdot \tan \phi'} \cdot \left[\tan \phi' + (1 + \tan^2 \phi')^{1/2} \right]^2 + \pi \cdot \tan \phi' \cdot e^{\pi \cdot \tan \phi'} \cdot \right. \\ &\cdot \left[\tan \phi' + (1 + \tan^2 \phi')^{1/2} \right]^2 + 4 \cdot \tan^2 \phi' \cdot e^{\pi \cdot \tan \phi'} \cdot \left[\tan \phi' + (1 + \tan^2 \phi')^{1/2} \right] \cdot \left[1 + \frac{1}{2} \cdot (1 + \tan^2 \phi')^{-1/2} \right] \left. \right\} \end{aligned}$$

The second derivatives of the bearing capacity computed analytically with respect to the soil parameters c' and $\tan\phi'$ are given by Eqs. (B.3) and (B.4):

$$\frac{\partial^2 q_f}{\partial^2 c'} = 0 \quad (\text{B.3})$$

$$\frac{\partial^2 q_f}{\partial^2 \tan \phi'} = \quad (\text{B.4})$$

$$\begin{aligned} &= -\frac{2 \cdot c'}{\tan^3 \phi'} + c' \cdot e^{\pi \tan \phi'} \cdot [\tan \phi' + (1 + \tan^2 \phi')^{1/2}] \cdot \left\{ \frac{2}{\tan^3 \phi'} \cdot [\tan \phi' + (1 + \tan^2 \phi')^{1/2}] - \frac{\pi}{\tan^2 \phi'} \cdot [\tan \phi' + (1 + \tan^2 \phi')^{1/2}] - \right. \\ &\quad - \frac{4}{\tan \phi'} \cdot \left[1 + \frac{1}{2} \cdot (1 + \tan^2 \phi')^{-1/2} \right] + \pi \cdot \left[-\frac{1}{\tan^2 \phi'} \cdot [\tan \phi' + (1 + \tan^2 \phi')^{1/2}] + \frac{\pi}{\tan \phi'} \cdot [\tan \phi' + (1 + \tan^2 \phi')^{1/2}] + \right. \\ &\quad \left. \left. + 4 \cdot \left[1 + \frac{1}{2} \cdot (1 + \tan^2 \phi')^{-1/2} \right] + 4 \cdot \left[\pi \cdot \left[1 + \frac{1}{2} \cdot (1 + \tan^2 \phi')^{-1/2} \right] + 2 \cdot \tan \phi' \cdot \left[1 + \frac{1}{2} \cdot (1 + \tan^2 \phi')^{-1/2} \right] + \tan \phi' \cdot \left[-\frac{1}{2} \cdot (1 + \tan^2 \phi')^{-3/2} \right] \right] \right\} + \\ &\quad + q \cdot \left\{ \pi \cdot e^{\pi \tan \phi'} \cdot \left[\pi \cdot [\tan \phi' + (1 + \tan^2 \phi')^{1/2}]^2 + 4 \cdot \tan \phi' \cdot [\tan \phi' + (1 + \tan^2 \phi')^{1/2}] \cdot \left[1 + \frac{1}{2} \cdot (1 + \tan^2 \phi')^{-1/2} \right] \right] + \right. \\ &\quad \left. + 4 \cdot \left[\pi \cdot e^{\pi \tan \phi'} \cdot \tan \phi' \cdot [\tan \phi' + (1 + \tan^2 \phi')^{1/2}] \cdot \left[1 + \frac{1}{2} \cdot (1 + \tan^2 \phi')^{-1/2} \right] + e^{\pi \tan \phi'} \cdot \left[2 \cdot \tan \phi' + (1 + \tan^2 \phi')^{1/2} \right] + \right. \right. \\ &\quad \left. \left. + \tan \phi' \cdot (1 + \tan^2 \phi')^{-1/2} \right] \cdot \left[1 + \frac{1}{2} \cdot (1 + \tan^2 \phi')^{-1/2} \right] + \tan \phi' \cdot e^{\pi \tan \phi'} \cdot \left[-\frac{1}{2} \cdot (1 + \tan^2 \phi')^{-3/2} \right] \cdot [\tan \phi' + (1 + \tan^2 \phi')^{1/2}] \right\} \\ &\quad + 225 \cdot e^{\pi \tan \phi'} \cdot \left\{ \pi \cdot [\tan \phi' + (1 + \tan^2 \phi')^{1/2}]^2 + 4 \cdot \tan \phi' \cdot [\tan \phi' + (1 + \tan^2 \phi')^{1/2}] \cdot \left[1 + \frac{1}{2} \cdot (1 + \tan^2 \phi')^{-1/2} \right] + \right. \end{aligned}$$

$$\begin{aligned}
 & +\pi \cdot \left[\tan\phi' + (1 + \tan^2\phi')^{1/2} \right]^2 + \pi \cdot \tan\phi' \cdot \left[\tan\phi' + (1 + \tan^2\phi')^{1/2} \right]^2 + 4 \cdot \tan^2\phi' \cdot \left[\tan\phi' + (1 + \tan^2\phi')^{1/2} \right] \\
 & \cdot \left[1 + \frac{1}{2} \cdot (1 + \tan^2\phi')^{-1/2} \right] + 4 \cdot \tan\phi' \cdot \left[\pi \cdot \tan\phi' \cdot \left[\tan\phi' + (1 + \tan^2\phi')^{1/2} \right] \cdot \left[1 + \frac{1}{2} \cdot (1 + \tan^2\phi')^{1/2} \right] + \left[1 + \frac{1}{2} \cdot (1 + \tan^2\phi')^{-1/2} \right] \right. \\
 & \left. \cdot \left[3 \cdot \tan\phi' + 2 \cdot (1 + \tan^2\phi')^{1/2} + \tan\phi' \cdot (1 + \tan^2\phi')^{-1/2} \right] + \tan\phi' \cdot \left[\tan\phi' + (1 + \tan^2\phi')^{1/2} \right] \cdot \left[-\frac{1}{2} \cdot (1 + \tan^2\phi')^{-3/2} \right] \right] \Bigg\}
 \end{aligned}$$

The second derivative of the bearing capacity with respect to both soil parameters c' and $\tan\phi'$ is given by Eq. (B.5):

$$\begin{aligned}
 & \frac{\partial^2 q_f}{\partial \tan\phi' \cdot \partial c'} = \tag{B.5} \\
 & = \left\{ \frac{1}{\tan^2\phi'} - \frac{1}{\tan^2\phi'} \cdot e^{\pi \cdot \tan\phi'} \cdot \left[\tan\phi' + (1 + \tan^2\phi')^{1/2} \right]^2 + \frac{\pi}{\tan\phi'} \cdot e^{\pi \cdot \tan\phi'} \cdot \right. \\
 & \left. \cdot \left[\tan\phi' + (1 + \tan^2\phi')^{1/2} \right]^2 + 4 \cdot e^{\pi \cdot \tan\phi'} \cdot \left[\tan\phi' + (1 + \tan^2\phi')^{1/2} \right] \cdot \left[1 + \frac{1}{2} \cdot (1 + \tan^2\phi')^{-1/2} \right] \right\}
 \end{aligned}$$

C. Algorithm to evaluate the reduced intervals of the input soil parameters

In this appendix the routine implemented in MATLAB[®] Version 7.0 to find the reduced intervals of the effective soil cohesion and friction angle are given. The reduced intervals are then considered when using the advanced Point Estimate method to the bearing capacity problem, as described in chapter 6.

% finds the reduced intervals of the soil parameters

I=1;

par1=[];

par2=[];

- The effective cohesion and friction angle range from 0 to their mean values, respectively 4 kN/m² and 25°.

for c=0.0000001:0.004:4

for phi=0.0000001:0.025:25

- The Terzaghi's bearing capacity formula

$$q_f = (c / (\tan(\phi * \pi / 180))) * (\exp(\pi * \tan(\phi * \pi / 180)) * (\tan(\phi * \pi / 180) + (1 + (\tan(\phi * \pi / 180))^2)^{0.5})^2 - 1) + 10 * (\exp(\pi * \tan(\phi * \pi / 180)) * (\tan(\phi * \pi / 180) + (1 + (\tan(\phi * \pi / 180))^2)^{0.5})^2) + 22.5 * \tan(\phi * \pi / 180) * (\exp(\pi * \tan(\phi * \pi / 180)) * (\tan(\phi * \pi / 180) + (1 + (\tan(\phi * \pi / 180))^2)^{0.5})^2 - 1);$$

- The $q_{f\text{failure}}$ can be any value considered as the right extreme of the unsafe region of the q_f . Values of 150 kN/m², 200 kN/m² and 250 kN/m² and the mean value of the bearing capacity divided by a safety factor of 2 are considered. The intervals of the friction angle found for these values of the bearing capacity at failure are reported in table 6.22.

if qf <= qffailure

par1(I)=c;

par2(I)=phi;

I=I+1;

end

end

end

- The right extreme values of the cohesion and friction angle intervals can then be found.

maxc=max(par1)

maxphi=max(par2)

D. Algorithm to evaluate the shifted lognormal parameters and the failure probability of the bearing capacity problem

The aim of this appendix is to describe the algorithm implemented in MATLAB[®] Version 7.0 to evaluate the three parameters of the shifted lognormal distribution and the failure probability of the bearing capacity problem by considering the results of the advanced PEM shown in tables 6.19 and 6.21 of chapter 6.

The objective function F to be optimised is given by Eq. (6.8).

D.1 Main routine for the estimation of the three shifted lognormal parameters

In the main routine the parameters of the shifted lognormal distribution, described by Eq. (2.15), are indicated respectively as $m=\mu_{\ln(X)}$, $s=\sigma_{\ln(X)}$ and $u=x_0$, while the failure probability is simply given by $P_f=PF$.

% main program for the estimation of the shifted lognormal distribution parameters and the failure probability of the bearing capacity problem

- Initial values of the 4 unknown parameters are input together with their corresponding lower (lb) and upper (ub) bounds to start the optimization problem

% initial values are m, s, u, Pf

par0 = [m0 s0 u0 Pf0];

- The `optimset` command creates an optimization option structure. More precisely, after for example 10000 runs, it displays the output of each iteration, checks whether the objective function F values are valid giving a warning when the function returns an invalid value (complex or not a number) and it displays the maximum number of function evaluations allowed.

% options


```
option = optimset('Display','iter','MaxFunEvals',10000);  
% lower and upper bounds of the input parameters m, s, u, Pf  
lb = [ml sl ul Pfl];  
ub = [mu su uu Pfu];
```

- The gradient based solver `fmincon` finds the constrained minimum of the function `F` starting at initial bounded values `par0`. It returns a structure output with information about the optimization, i.e.: `par` indicates the results of the four unknowns, `fval` is the minimum of the function reached, `exitflag` describes the exit condition of `fmincon`.

```
% minimiser of the function F  
[par,fval,exitflag,output] =fmincon(@integralmod,par0,[],[],[],[],lb,ub,[],opti);
```

- The results of the optimization problem can be displayed

```
% results of the shifted lognormal parameters m, s, u and of the failure  
probability Pf  
m = par(1)  
s = par(2)  
u = par(3)  
Pf = par(4)
```

```
% extreme values of the integration intervals of the objective function F  
x0=par(3)+0.1  
xm=0.5*(par(3)+exp(par(1)+0.5*((par(2))^2)))
```

```
% statistical values of the entire shifted lognormal distribution of the bearing  
capacity to be found  
mean_value=par(3)+exp(par(1)+0.5*((par(2))^2))  
standard_deviation=(-1+(exp(par(2)^2))^0.5)*(exp(par(1)+0.5*((par(2))^2)))
```

$$\text{skewness} = 3 * (\text{standard_deviation} / (\text{mean_value} - \text{par}(3))) \\ + (\text{standard_deviation} / (\text{mean_value} - \text{par}(3)))^3$$

D.2 Subroutine for the evaluation of the integrals of the objective function

% Subroutine for evaluating the integrals inside the objective function F

function F = integralmod(par)

- Different extreme values of the integration interval can be considered to evaluate the integrals of the objective function F. The case a) considers a certain value x of the bearing capacity, while cases b), c) and d) refer to specific bearing capacity values. All these values describe a certain unsafe region of the probability density function of the bearing capacity to be found.

% a) extreme values of the integration interval of function F for a certain value x of the bearing capacity

limx = [par(3)+0.1; 0.5(par(3)+exp(par(1)+0.5*((par(2))^2)))];*

% extreme values of the integration interval of function F for a bearing capacity of, respectively, b) 250 kN/m², c) 200 kN/m² and d) 150 kN/m²

limx250 = [par(3)+0.1; 250];

limx200 = [par(3)+0.1; 200];

limx150 = [par(3)+0.1; 150];

- The quad command means “quadrature”, which is a numerical method used to find the area under the graph of a function, that is, to compute a definite integral.

% evaluation of the integrals of the objective function F for different values of the right extreme of the unsafe region of the bearing capacity

% a) general formula

```
qu = [quad(@Q1mod,limx(1),limx(2),[],[],par)
      quad(@Q2mod,limx(1),limx(2),[],[],par)
      quad(@Q3mod,limx(1),limx(2),[],[],par)
      quad(@Q4mod,limx(1),limx(2),[],[],par)];
```

% b) right extreme value of the unsafe region given by $q_f = 250 \text{ kN/m}^2$

```
qu250 = [quad(@Q1mod,limx250(1),limx250(2),[],[],par)
         quad(@Q2mod,limx250(1),limx250(2),[],[],par)
         quad(@Q3mod,limx250(1),limx250(2),[],[],par)
         quad(@Q4mod,limx250(1),limx250(2),[],[],par)];
```

% c) right extreme value of the unsafe region given by $q_f = 200 \text{ kN/m}^2$

```
qu200 = [quad(@Q1mod,limx200(1),limx200(2),[],[],par)
         quad(@Q2mod,limx200(1),limx200(2),[],[],par)
         quad(@Q3mod,limx200(1),limx200(2),[],[],par)
         quad(@Q4mod,limx200(1),limx200(2),[],[],par)];
```

% d) right extreme value of the unsafe region given by $q_f = 150 \text{ kN/m}^2$

```
qu150 = [quad(@Q1mod,limx150(1),limx150(2),[],[],par)
         quad(@Q2mod,limx150(1),limx150(2),[],[],par)
         quad(@Q3mod,limx150(1),limx150(2),[],[],par)
         quad(@Q4mod,limx150(1),limx150(2),[],[],par)];
```

- Definition of the objective function according to Eq. (6.8). The mean value, standard deviation and skewness coefficient of the bearing capacity listed in Tables 6.19 and 6.21 can be input respectively for uncorrelated

- and negatively correlated soil parameters. Initially the failure probability is considered as unknown and equal to par(4). However in this way different parameters combinations, which minimize the function F, are found. As a consequence one of the four unknown parameters could be considered as known. Here the failure probability is taken into account as a known target failure probability target_Pf, depending on the reliability level to be reached.

% Objective function F to be optimized

$$F = ((qu(2)/qu(1))-mean_value_qf_red).^2+((qu(3)/qu(1))-((standard_deviation_qf_red).^2)).^2+((qu(4)/qu(1))+skewness_qf_red).^2+(qu(1)-target_Pf)^2;$$

- The integration results of the optimization problem can be evaluated. These results are useful to evaluate the low failure probability of the bearing capacity considering reduced intervals of the effective cohesion and friction angle. Additionally they can be used to estimate the mean value, standard deviation and skewness coefficient for the entire shifted lognormal function of the bearing capacity to be found

% Integration results of the objective function useful for evaluating the failure probability of the bearing capacity considering a reduced interval for the soil parameters

% general formula

$$integrals=[qu(1) qu(2) qu(3) qu(4)]$$

% Integration intervals considering specific right extreme values of the unsafe region of the bearing capacity, respectively 250 kN/m², 200 kN/m² and 150 kN/m²

$$integrals250=[qu250(1) qu250(2) qu250(3) qu250(4)]$$

$$integrals200=[qu200(1) qu200(2) qu200(3) qu200(4)]$$

$$integrals150=[qu150(1) qu150(2) qu150(3) qu150(4)]$$

D.3 Subroutines for the definition of the integrals of the objective function

Using the following subroutines it is possible to define the integrals of the optimization function F to be estimated.

1) Subroutine for defining the integral of the failure probability P_f , where $f1=f_X(x)$. The function $f_X(x)$ is the probability density function of the shifted lognormal function:

function f1 = Q1mod(x,par)

$$f1 = (1./((2*pi)^0.5).*(par(2)).*(x-par(3))).*(exp(-0.5.*(((log(x-par(3))-par(1))./(par(2))).^2)))) ;$$

2) Subroutine for defining the integral of the mean value μ_{qfred} , where $f2=x*f_X(x)$:

function f2 = Q2mod(x,par)

$$f2 = x.*((1./((2*pi)^0.5).*(par(2)).*(x-par(3))).*(exp(-0.5.*(((log(x-par(3))-par(1))./(par(2))).^2)))));$$

3) Subroutine for defining the integral of the variance σ_{qfred}^2 , knowing the mean value μ_{qfred} from the subroutine 2). The function f3 corresponds to $(x-\mu_{qfred})^2*f_X(x)$:

function f3 = Q3mod(x,par)

$$f3 = ((x-\mu_{qfred}).^2).*((1./((2*pi)^0.5).*(par(2)).*(x-par(3))).*(exp(-0.5.*(((log(x-par(3))-par(1))./(par(2))).^2)))));$$

4) Subroutine for defining the integral of the skewness coefficient v_{qfred} , knowing the mean value μ_{qfred} and the variance σ_{qfred}^2 respectively from subroutine 2) and 3). The function f4 corresponds to $(x-\mu_{qfred})^3*f_X(x)/\sigma_{qfred}^3$:

function f4 = Q4mod(x,par)

$$f4 = (((x-\mu_{qfred})./(\sigma_{qfred})).^3).*((1./((2*pi)^0.5).*(par(2)).*(x-par(3))).*(exp(-0.5.*(((log(x-par(3))-par(1))./(par(2))).^2)))));$$

D.4 Optimisation results for the bearing capacity problem

D.4.1 Case with $\rho_{c'\tan\phi'} = 0$

The results of the optimization problem previously described considering the bearing capacity results of Table 6.19 and the failure probability as known are listed above:

- the parameters of the shifted lognormal distribution

$$m = 5.905 \text{ kN/m}^2$$

$$s = 0.233 \text{ kN/m}^2$$

$$u = -95.868 \text{ kN/m}^2$$

- the low failure probability of the bearing capacity considering as right extreme value of the unsafe region, respectively, 150 kN/m², 200 kN/m² and 250 kN/m²

$$Pf_{150} = 0.043$$

$$Pf_{200} = 0.0437$$

$$Pf_{250} = 0.0463$$

- the extreme values of the integration interval of the objective function

$$x_0 = -95.768 \text{ kN/m}^2$$

$$x_m = 140.477 \text{ kN/m}^2$$

- the statistical values of the entire shifted lognormal distribution of the bearing capacity

$$\text{mean_value} = 280.954 \text{ kN/m}^2$$

$$\text{standard_deviation} = 10.392 \text{ kN/m}^2$$

$$\text{skewness} = 0.083$$

- the minimum value of the objective function

$$F_{\text{eval}} = 0.00005$$

D.4.2 Case with $\rho_{c'\tan\phi'} = -0.6$

For the bearing capacity results of Table 6.21 the optimization problem earlier described leads to the following results, considering the failure probability as known:

- the parameters of the shifted lognormal distribution

$$m = 5.478 \text{ kN/m}^2$$

$$s = 0.251 \text{ kN/m}^2$$

$$u = 36.456 \text{ kN/m}^2$$

- the low failure probability of the bearing capacity considering as right extreme value of the unsafe region, respectively, 150 kN/m², 200 kN/m² and 250 kN/m²

$$Pf_{150} = 0.0015$$

$$Pf_{200} = 0.0016$$

$$Pf_{250} = 0.0029$$

- the extreme values of the integration interval of the objective function

$$x_0 = 36.556 \text{ kN/m}^2$$

$$x_m = 141.814 \text{ kN/m}^2$$

- the statistical values of the entire shifted lognormal distribution of the bearing capacity

$$\text{mean_value} = 283.629 \text{ kN/m}^2$$

$$\text{standard_deviation} = 7.941 \text{ kN/m}^2$$

$$\text{skewness} = 0.096$$

- the minimum value of the objective function

$$F_{\text{eval}} = 1.524$$

Bibliography

ANG, A.H.-S.; TANG, W.H. (1975): "Probability Concepts in Engineering Planning and Design, Vol. I: Basic Principles". John Wiley and Sons, New York.

ANG, A.H.-S.; TANG, W.H. (1984): "Probability Concepts in Engineering Planning and Design, Vol. II: Decision, Risk and reliability". John Wiley and Sons, New York.

ANG, A.H.-S.; TANG, W.H. (2006): "Probability Concepts in Engineering. Emphasis on Applications to Civil and Environmental Engineering". 2nd Edition, John Wiley and Sons, New York.

BAECHER, G. B. (1982): "Statistical methods in site characterization". *Updating subsurface samplings of soils and rocks and their in-situ testing*, Engineering Foundation, Santa Barbara, California, pp. 463-492.

BENJAMIN, J.R.; CORNELL, C.A. (1970): "Probability, statistics and decision making for civil engineers". McGraw Hill, London, New York.

BRINCH HANSEN, J. (1961): "A general formula for bearing capacity". Danisch Geotechnical Institute, Bulletin 11.

BÜCHTER, A.; HENN, H.-W. (2000): "Elementare Stochastik. Eine Einführung in die Mathematik der Daten und des Zufalls". *Mathematik für das Lehramt*. Springer, Berlin.

CAQUOT, A.; KERISEL, J. (1953): "Sur le terme de surface dans le calcul des fondations en milieu pulverulent". 3th ICSMFE, Rotterdam, Vol. 1: pp. 265-270.

- CHERUBINI, C. (1997): "Data and considerations on the variability of geotechnical properties of soils". Proceedings of the International Conference on Safety and Reliability (ESREL) 97, Lisbon, Vol. 2: pp. 1583-1591.
- CHERUBINI, C. (1998): "Reliability of shallow foundation bearing capacity on c' , ϕ' soils". *Canadian Geotechnical Journal*, Vol. 37: pp. 264-269.
- CHOWDHURY, R.N. (1984): "Recent developments in landslide studies: Probabilistic methods, State-of-the-art-report – Session VII(a)". *International Symposium on Landslide*, pp. 209-228.
- CHRISTIAN, J.T. (2004): "Geotechnical Engineering Reliability: How Well do we know what we are doing?". *Journal of Geotechnical and Geoenvironmental Engineering*, Vol. 130(10): pp. 985-1003.
- CHRISTIAN, J.T.; LADD, C.C.; BAECHER, G.B. (1992): "Reliability Applied to Slope Stability Analysis". *Journal of Geotechnical Engineering*, Vol. 120: pp. 2180-2207.
- CHRISTIAN, J.T.; LADD, C.C.; BAECHER, G.B. (1994): "Reliability and Probability in Stability Analysis". *Stability and Performance of Slopes and Embankments II (Geotechnical Special Publication)*: pp. 1071-1111.
- CHRISTIAN, J.T.; BAECHER, G.B. (1999): "Point Estimate Method as Numerical Quadrature". *Journal of Geotechnical and Geoenvironmental Engineering*: pp. 779-786.
- CHRISTIAN, J.T.; BAECHER, G.B. (2002): "The point estimate method with large numbers of variables". *International Journal for Numerical and Analytical Methods in Geomechanics*, Vol. 26: pp. 1515-1529.
- CORNELL, C.A. (1969): "A probability-based structural code". *Journal of the American Concrete Institute*, Vol. 66: pp. 974-985.
- DAS, B.J. (1996): "Principles of Geotechnical Engineering". California State University, Sacramento.

- DITLEVSEN, O.; MADSEN, H. O. (1996): “Structural reliability methods“. Chichester: John Wiley & Sons.
- DUNCAN, J.M. (2000): “Factors of Safety and reliability in geotechnical engineering”. *Journal of Geotechnical and Geoenvironmental Engineering*, Vol. 126: pp. 307-316.
- EINSTEIN, H. H.; BAECHER, G. B.(1982): “Probabilistic and statistical methods in engineering geology. I. Problem statement and introduction to solution”. *Rock Mechanics*, Supp. 12, pp. 47-61.
- EL-RAMLY, H.; MORGENSTERN, N.R.; CRUDEN, D.M. (2001): “Probabilistic Slope Stability Analysis for Practice”. *Canadian Geotechnical Journal*, Vol. 40: pp. 851-855.
- EL-RAMLY, H.; MORGENSTERN, N.R.; CRUDEN, D.M. (2003): Reply to the discussion by J.M. Duncan, M. Navin, and T.F. Wolff on “Probabilistic Slope Stability Anaylsis for Practice”. *Canadian Geotechnical Journal*, Vol. 39: pp. 665-683.
- EL-RAMLY, H.; MORGENSTERN, N.R.; CRUDEN, D.M. (2005): “Probabilistic assessment of stability of a cut slope in residual soil”. *Géotechnique*, 55: 77-84.
- EUROCODE 7 (1994): “ENV 1997-1 Geotechnical design, general rules”. Delft: CEN European Committee for Standardisation.
- EVANS, M.; HASTINGS, N.; PEACOCK, B. (1993): “Statistical distributions”. Wiley, New York.
- FENTON, G.A. (2006): “Basics of Simulation”. Proceedings of the CISM-Meeting “Probabilistic Methods in Geotechnical Engineering”, Udine.
- FENTON, G.A.; GRIFFITHS, D.V. (2003): “Bearing Capacity Prediction of Spatially Random $c-\phi$ soils”. *Canadian Geotechnical Journal*, Vol. 40: pp. 54-65.

- FENTON, G.A.; GRIFFITHS, D.V. (2004): "Reply to the discussion by R. Popescu on "Bearing Capacity Prediction of Spatially Random $c-\phi$ soils"". *Canadian Geotechnical Journal*, Vol. 41: pp. 368-369.
- GRIFFITHS, D.V.; FENTON, G.A.; TVETEN, D.E. (2002): "Probabilistic Geotechnical Analysis: how difficult does it need to be?". International Conference on Probabilistics in Geotechnics, pp. 3-20.
- GRIFFITHS, D.V.; FENTON, G.A.; MANOHARAN, N. (2002): "Bearing Capacity of Rough Rigid Strip Footing on Cohesive Soil: Probabilistic study". *Journal of Geotechnical and Geoenvironmental Engineering*, Vol. 128: pp. 743-755.
- HARR, M. T. (1989): "Probabilistic estimates for multivariate analyses". *Appl. Math. Modelling*, Vol. 13(5): pp. 313-318.
- HARR, M. E. (1996): "Reliability-based design in civil engineering". *Dover publications, Inc., Mineola, New York*.
- HASOFER, A. M.; LIND, N. (1974): "Exact and Invariant Second-Moment Code Format". *Journal of Engineering Mechanics*, Vol. 100(1): pp. 111-121.
- HONG, H. P. (1998): "An efficient point estimate method for probabilistic analysis". *Reliability Engineering and System Safety*, Vol. 59(3): pp. 261-267.
- HONJO, Y.; AMATYA, S. (2005): "Partial factors calibration based on reliability analyses for square footings on granular soils". *Géotechnique*, Vol. 6: pp. 479-491.
- KATZENBACH, R.; MOORMANN, C. (2003): "Überlegungen zu stochastischen Methoden in der Bodenmechanik am Beispiel des Frankfurter Tons". *Beiträge anlässlich des 60. Geburtstages von Herrn Prof. Dr. S. Semprich, Heft 16 der Gruppe Geotechnik, Technische Universität Graz*: pp. 255-282.
- KENNEY, J. F.; KEEPING, E. S. (1951): "Mathematics of Statistics". Pt. 2, 2nd Ed., Princeton, NJ: Van Nostrand.

- KOTTEGODA, N. T.; ROSSO, R. (1997): "Statistics, Probability and Reliability for Civil and Environmental Engineers". The McGraw-Hill Companies, Inc, USA.
- KULHAWY; F. H. (1992): "On evaluation of static soil properties". In Stability and performance of slopes and embankments II (GPS 31), American Society of Civil Engineers, Seed, R. B., Boulanger, R. W., eds, pp. 95-115.
- LACASSE, S.; NADIM, F. (1996): "Uncertainties in Characterizing Soil Properties". In *Uncertainty in the Geologic Environment: from Theory to Practice*, Proceedings of Uncertainty '96, ASCE Geotechnical Special publication No. 58, C.D. Shackelford, P.P. Nelson, M.J.S. Roth, eds., pp. 49-75.
- LADD, C. C.; DASCAL; O.; LAW, K.T.; LEFEBRVE, G.; LESSARD, G.; MESRI, G.; TAVENAS, F. (1983): Report of the subcommittee on embankment stability – annex II. Committee of Specialists on Sensitive Clays on the NBR Complex, Société d'Énergie de la Baie James, Montréal, Quebec.
- LANCELLOTTA, R. (1993): "Geotechnical Engineering". Mc Graw-Hill.
- LANCELLOTTA, R.; CALAVERA, J. (1999): "Fondazioni". McGraw-Hill.
- LI, K.S. (1992): "Point-estimate method for calculating statistical moments". *Journal of Engineering Mechanics*, ASCE 118(7): pp. 1506-1511.
- LI, K.S.; LUMB, P. (1987): "Probabilistic design of slopes". *Canadian Geotechnical Journal*, Vol. 24: pp. 520-535.
- LI, K.S.; WHITE, W. (1987): "Probabilistic Approaches to Slope Design". Research Report No. 20, Civil Engineering Department, Australian Defence Force Academy, Canberra, Australia, pp. 54.
- LIND, N.C. (1983): "Modelling uncertainty in discrete dynamical systems". *Applied Mathematical Modelling*, Vol. 7(3): pp. 146-152.
- LUMB, P. (1969): "Safety factors and the probability distribution of soil strength". *Canadian Geotechnical Journal*, Vol. 7(3): pp. 225-242.

Bibliography

- MEYERHOF, G. G. (1963): "Some recent research on the bearing capacity of foundations". *Canadian Geotechnical Journal*, Vol. 1: pp. 16-26.
- MOSTYN, G.R.; LI, K.S. (1993): "Probabilistic Slope Analysis-State of Play". *Probabilistic Methods in geotechnical Engineering*, eds Li & Lo, pp. 89-109.
- NATIONAL RESEARCH COUNCIL REPORT (1995): "Appendix A: Basic Concepts of Probability and Reliability". *Probabilistic Methods in Geotechnical Engineering*.
- NADIM, F. (2006): "First Order Second Moment (FOSM), First and Second Order Reliability Methods (FORM & SORM), Monte Carlo Simulation, System Reliability". Proceedings of the CISM Course "Probabilistic methods in geotechnical engineering", Udine.
- PESCHL, G. M. (2004): "Reliability analysis in geotechnics with the random set finite element method". Heft 25 des Institutes für Bodenmechanik und Grundbau, Technische Universität Graz.
- PHOON, K.-K.; KULHAWY, F.H. (1994): "Characterization of Geotechnical Variability". *Canadian Geotechnical Journal*, Vol. 36: pp. 612-624.
- PHOON, K.-K.; KULHAWY, F.H. (1999): "Evaluation of geotechnical property variability". *Canadian Geotechnical Journal*, Vol. 36: pp. 625-639.
- POPESCU, R. (2004): "Discussion of Bearing Capacity Prediction of Spatially Random c - ϕ soils". *Canadian Geotechnical Journal*, Vol. 41: pp. 366-367.
- PÖTTLER, R.; KLAPPERICH, H.; SCHWEIGER, H.F. (2002): "International Conference on Probabilistics in Geotechnics. Technical and Economic Risk estimation".
- PRANDTL, L. (1921): "Eindringungsfestigkeit und Festigkeit von Schneiden". *Zeitung für angewendete Mathematik und Mechanik*, Vol. 1:15.
- PULA, W. (2006): "FORM/SORM applications in bearing capacity problems". Proceedings of the CISM Course "Probabilistic methods in geotechnical engineering", Udine.
- RÉTHÁTI, L. (1987): "Probabilistic Solutions in Geotechnics".

- ROSENBLATT, M. (1952): "Remarks on a Multivariate Transformation". *Annals of Math. Stat.*, Vol. 23(3): pp.470-472.
- ROSENBLUETH, E. (1975): "Point estimates for probability moments". *Proc. Nat. Acad. Sci. USA*, Vol. 72 (10): pp. 3812-3814.
- ROSENBLUETH, E. (1981): "Two-point estimates in probabilities". *Appl. Math. Modelling*, Vol. 5(2): pp. 329-335.
- ROSSI, F.; SALVI, F. (2001): "Manuale di Ingegneria Civile. Vol. I: Matematica, Idraulica, Ingegneria Geotecnica, Costruzioni idrauliche". Zanichelli, ESAC.
- ROSS, S. M. (1995): "A course in simulation". Macmillan, New York.
- RUSSELLI, C.; VERMEER, P. A. (2005): "Probabilistic Methods applied to Geotechnical Engineering". *Proceedings of the 2nd International Workshop of Young Doctors in Geomechanics (WHYDOC)*, Ecole Nationale des Ponts et Chaussées (ENPC), Champs-sur-Marne, France, pp. 361-366.
- RUSSELLI, C.; VERMEER, P. A. (2006): "Wahrscheinlichkeitsmethoden angewendet auf geotechnische Probleme". *Tagungshandbuch des 5. Kolloquiums "Bauen in Boden und Fels"*, Technische Akademie Esslingen (TAE), Esslingen, pp. 183-186.
- SCHAD, H.; WALLRAUCH, E. (1985): "Rutschungen im Keuper". Otto-Graf Institut (MPA), Universität Stuttgart.
- SCHNEIDER, J.; SCHLATTER, H.P. (1996): "Sicherheit und Zuverlässigkeit im Bauwesen. Grundwissen für Ingenieure". Hochschulverlag AG an der ETH Zürich & B.G. Teubner Stuttgart.
- SCHWEIGER; H.F.; THURNER, R.; PÖTTLER, R. (2001): "Reliability Analysis in Geotechnics with Deterministic Finite Elements. Theoretical Concepts and Practical Application". *The International Journal of Geomechanics*, Vol. 1: 389-413.

- SHOOMAN; M.L. (1968): "Probabilistic Reliability: An Engineering Approach". McGraw-Hill Book Co., New York.
- SPEEDIE, M. G. (1956): "Selection of Design Value from Shear Test Results". *Proceedings of the 2nd Australia-New Zealand Conference on Soil Mechanics and Foundation Engineering*, Wellington, pp. 107-109.
- TERZAGHI, K. (1943): "Theoretical Soil Mechanics". Wiley, New York.
- THURNER, R. (2000): "Probabilistische Untersuchungen in der Geotechnik mittels deterministischer Finite Elemente-Methode". Dissertation eingereicht an der Fakultät für Bauingenieurwesen der Technischen Universität Graz.
- TOBUTT, D. C. (1981): "Monte Carlo Simulation Methods for Slope Stability". *Computers & Geosciences*, Vol. 8(2): pp. 199-208.
- TUNG, Y-K. (1998): "Uncertainty and Reliability Analysis in Water Resources Engineering". Department of Civil & Structural Engineering, Hong Kong University of Science & Technology.
- U.S. Army Corps of Engineers (1995): "Introduction to Probability and Reliability in Geotechnical Engineering". Appendix B to ETL 1110-2-547.
- VANMARCKE, E.H. (1980): "Probabilistic stability analysis of earth slopes". *Engineering Geology*, Vol. 16: pp. 29-50.
- VaP (Variables Processor) 2.2 - User manual (2006). PSP-Petschacher Software und Entwicklungs GmbH.
- VRIJLING, J.K. (1997): "Probabilities in civil engineering, Part 1: Probabilistic design in theory". *CUR-Publicatie 190*, Delft University of Technology, Stichting CUR, Gouda.
- WHITMAN, R.V. (1984): "Evaluating the calculated risk in geotechnical engineering". *Journal of Geotechnical Engineering*, ASCE, Vol. 110(2): pp. 145-188.

WOLFF, T.F.; SHANNON; WILSON (1999): “An Overview of Probabilistic Analysis for Geotechnical Engineering Problems”. Appendix A to *U.S. Army Corps of Engineers: Circular Risk-Based Analysis in Geotechnical Engineering for Support of Planning Studies*, ETL 1110-2-556.

WOLFF, T.F. (1994): “Evaluating the Reliability of Existing Levees”. Research report prepared for *U.S. Army Waterways Experiment Station*, Michigan State University.

ZHOU, J.; NOWAK, A.S. (1988): “Integration formulas to evaluate functions of random variables”. *Structural safety*, Vol. 5: pp. 267-284.

Curriculum Vitae

09.01.1977

Born in Venaria Reale, Turin, Italy

1996 – 2000

Study in Civil Engineering at the Polytechnic University of Turin

2000 – 2001

Study in Civil Engineering at the “Institut National des Sciences Appliquées” (INSA), Lyon

08. – 11.2001

Internship at the TNO Building and Construction Research, Delft

19.03.2002

Diploma graduation at the Polytechnic University of Turin

07. – 09.2002

Research Associate at the Institute of Automotive Engineering and Vehicle Engines (FKFS), University of Stuttgart

10.2002 – 09.2003

Research Associate at the MPA Otto-Graf-Institute, University of Stuttgart

10.2003 – 10.2006

Doctoral study; Research and Teaching Assistant at the Institute of Geotechnical Engineering, University of Stuttgart

since 02.2007

Research Assistant at the MPA Otto-Graf-Institute, University of Stuttgart

14.02.2008

Doctoral exam

Mitteilungen des Instituts für Geotechnik

- Nr. 01 Thamm, B. R. (1974) Anfangssetzungen und Anfangsporenwasserüberdrücke eines normalverdichteten wassergesättigten Tones
€ 5,11
- Nr. 02 Gußmann, P. (1975) Einheitliche Berechnung von Grundbruch und Böschungsbruch
€ 2,56
- Nr. 03 Feeser, V. (1975) Die Bedeutung des Kalziumkarbonats für die bodenphysikalischen Eigenschaften vom Löß
vergriffen
- Nr. 04 Du Thin, K. (1976) Standsicherheit von Böschungen: Programm-Dokumentation
vergriffen
- Nr. 05 Smolczyk, U./ Pertschi, O./ Hilmer, K. (1976) Messungen an Schleusen in der UDSSR. Schleusennorm der UDSSR (SN 30365)
vergriffen
- Nr. 06 Hilmer, K. (1976) Erddruck auf Schleusenkammerwände
€ 9,20
- Nr. 07 Laumans, Q. (1977) Verhalten einer ebenen, in Sand eingespannten Wand bei nichtlinearen Stoffeigenschaften des Bodens
€ 9,20
- Nr. 08 Lächler, W. (1977) Beitrag zum Problem der Teilflächenpressung bei Beton am Beispiel der Pfahlkopfanschlüsse
vergriffen
- Nr. 09 Spotka, H. (1977) Einfluß der Bodenverdichtung mittels Oberflächenrüttelgeräten auf den Erddruck einer Stützwand bei Sand
vergriffen
- Nr. 10 Schad, H. (1979) Nichtlineare Stoffgleichungen für Böden und ihre Verwendung bei der numerischen Analyse von Grundbauaufgaben
vergriffen

- Nr. 11 Ulrich, G. (1980) Verschiebungs- und kraftgesteuerte Plattendruckversuche auf konsolidierenden Böden
Gußmann, P. Zum Modellgesetz der Konsolidation
€ 10,23
- Nr. 12 Salden, D. (1980) Der Einfluß der Sohlenform auf die Traglast von Fundamenten
€ 12,78
- Nr. 13 Seeger, H. (1980) Beitrag zur Ermittlung des horizontalen Bettungsmoduls von Böden durch Seitendruck-versuche im Bohrloch
€ 12,78
- Nr. 14 Schmidt, H.H. (1981) Beitrag zur Ermittlung des Erddrucks auf Stützwände bei nachgiebigem Baugrund
€ 12,78
- Nr. 15 Smolczyk, U./ (1981) Vorstudie über bauliche Alternativen für Schweikert, O. Durch-gangsstraßen in Siedlungen
€ 6,14
- Nr. 16 Malcharek, K./ (1981) Vergleich nationaler Richtlinien für die Smolczyk, U. Berechnung von Fundamenten
€ 7,67
- Nr. 17 Gruhle, H.D. (1981) Das Verhalten des Baugrundes unter Einwirkung vertikal gezogener Ankerplatten als räumliches Problem des Erdwiderstandes
vergriffen
- Nr. 18 Kobler, W. (1982) Untersuchungen über Böschungs- und Grundbruch bei begrenzten Lastflächen
€ 12,78
- Nr. 19 Lutz, W. (1983) Tragfähigkeit des geschlitzten Baugrunds neben Linienlasten
€ 12,78
- Nr. 20 Smolczyk, U. (1983) Studienunterlagen "Bodenmechanik und Grundbau"; überarbeitete Ausgabe 1993
€ 20,45

- Nr. 21 Schweikert, O. (1984) Der Einfluß des Böschungswinkels auf die Berechnung des aktiven Erddrucks
€ 10,23
- Nr. 22 Vogt, N. (1984) Erdwiderstandsermittlung bei monotonen und wiederholten Wandbewegungen in Sand
vergriffen
- Nr. 23 Buchmaier, R. (1985) Zur Berechnung von Konsolidationsproblemen bei nichtlinearem Stoffverhalten
€ 12,78
- Nr. 24 Schad, H. (1985) Möglichkeiten der Böschungssicherung bei kleinen Baugruben
Smolczyk, U./
Schad, H./
Zoller, P. Sonderkonstruktionen der Böschungssicherung
€ 17,90
- Nr. 25 Gußmann, P. (1986) Die Methode der Kinematischen Elemente
€ 10,23
- Nr. 26 Steinmann, B. (1985) Zum Verhalten bindiger Böden bei monotoner einaxialer Beanspruchung
vergriffen
- Nr. 27 Lee, S.D. (1987) Untersuchungen zur Standsicherheit von Schlitz-zen im Sand neben Einzelfundamenten
vergriffen
- Nr. 28 Kolb, H. (1988) Ermittlung der Sohlreibung von Gründungskör-pern unter horizontalem kinematischen Zwang
€ 12,78
- Nr. 29 Ochmann, H. (1988) Ebene Grenzzustände von Erdböschungen im stochastischen Sicherheitskonzept
€ 12,78
- Nr. 30 Breinlinger, F. (1989) Bodenmechanische Stoffgleichungen bei großen Deformationen sowie Be- und Entlastungsvor-gängen
€ 15,34

- Nr. 31 Smoltczyk, U./ (1989) Beitrag zur Bemessung von Tunneln in offener
Breilinger, F./
Schad, H./
Wittlinger, M. € 12,78
- Nr. 32 Gußmann, P./ (1990) Beiträge zur Anwendung der KEM (Erddruck,
Schanz, T./
Smoltczyk, U./
Willand, E. **vergriffen**
- Nr. 33 Gruhle, H.D. (1990) Der räumliche Erdwiderstand vor überwiegend
horizontal belasteten Ankerplatten
vergriffen
- Nr. 34 Henne, J. (1995) Zur Bewehrung von verformten
Bodenschichten durch Einsatz zugfester
Geokunststoffe
€ 15.34
- Nr. 35 Wittlinger, M. (1994) Ebene Verformungsuntersuchungen zur We-
ckung des Erdwiderstandes bindiger Böden
€ 15,34
- Nr. 36 Schad, H. (1992) Zeit- und geschwindigkeitsabhängiges Materi-
alverhalten in der Geotechnik - Experimentelle
Erfassung und numerische Analyse
€ 15,34
- Nr. 37 Belz, I. (1992) Zur Ermittlung dynamischer Bodenkennwerte
in situ aus der Systemantwort des Erregers
€ 15,34
- Nr. 38 Ma, J. (1994) Untersuchungen zur Standsicherheit der durch
Stützscheiben stabilisierten Böschungen
€ 15.34
- Nr. 39 Smoltczyk, U. (1994) Sonderheft: 25 Jahre Lehre und Forschung in
der Geotechnik
€ 15.34
- Nr. 40 Rilling, B. (1994) Untersuchungen zur Grenztragfähigkeit bindi-
ger Schüttstoffe am Beispiel von Lößlehm
€ 17.90

- Nr. 41 Vermeer, P.A. (1996) Deponiebau und Geotechnik
€ 17,90
- Nr. 42 Vermeer, P.A. (1997) Baugruben in Locker- und Festgestein
€ 17,90
- Nr. 43 Brinkmann, C. (1998) Untersuchungen zum Verhalten von Dichtungs-übergängen im Staudammbau
€ 17,90
- Nr. 44 Fiechter-Scharr, I. (1998) Beeinflussung von Erdbaustoffen durch Beimi-schen eines organophilen Bentonits
€ 17,90
- Nr. 45 Schanz, T. (1998) Zur Modellierung des mechanischen Verhaltens von Reibungsmaterialien
€ 17,90
- Nr. 46 Akinrogunde, A.E. (1999) Propagation of Cement Grout in Rock Discontinuities Under Injection Conditions
€ 17,90
- Nr. 47 Vogt-Breyer, C. (1999) Experimentelle und numerische Untersuchungen zum Tragverhalten und zur Bemessung hori-zontaler Schraubanker
€ 17,90
- Nr. 48 Vermeer, P.A. (1999) Neue Entwicklungen in der Geotechnik
€ 17,90
- Nr. 49 Marcher, T. (2002) Resultate eines Versuchsprogramms an Beau-caire Mergel
€ 17,90
- Nr. 50 Marcher, T. (2003) Nichtlokale Modellierung der Entfestigung dichter Sande und steifer Tone
€ 17,90
- Nr. 51 Ruse, N.M. (2004) Räumliche Betrachtung der Standsicherheit der Ortsbrust beim Tunnelvortrieb
€ 17,90
- Nr. 52 Beutinger, P.H. (2005) Ein geotechnischer Beitrag zur Standsicherheit mobiler Baumaschinen
€ 17,90

- Nr. 53 Wehnert, M. (2006) Ein Beitrag zur drainierten und undrainierten Analyse in der Geotechnik
€ 17,90
- Nr. 54 Möller, S. C. (2006) Tunnel induced settlements and forces in linings
€ 17,90
- Nr. 55 Benz, T. (2007) Small-Strain Stiffness of Soils and its Numerical Consequences
€ 17,90
- Nr. 56 Abed, A. (2008) Numerical Modeling of Expansive Soil Behavior
€ 17,90
- Nr. 57 Hintner, J. (2008) Analyse der Fundamentverschiebungen infolge vertikaler und geneigter Belastung
€ 17,90
- Nr. 58 Russelli, C. (2008) Probabilistic Methods applied to the Bearing Capacity Problem
€ 17,90